INL RPT-23-71227
Revision 0

Grid-Integrated Production of Fischer-Tropsch Synfuels from Nuclear Power

May 2023

Geographic Competitiveness of Synfuel Production at Nuclear Power Plants Across the United States

Marisol Garrouste, Daniel Wendt, William D. Jenson, Qian Zhang, Maria A. Herrera Diaz, and Frederick Joseck

Idaho National Laboratory

IES
Integrated Energy Systems

INL is a U.S. Department of Energy National Laboratory operated by Battelle Energy Alliance, LLC

INL RPT-23-71227
Revision 0

Grid-Integrated Production of Fischer-Tropsch Synfuels from Nuclear Power

Geographic Competitiveness of Synfuel Production at Nuclear Power Plants Across the United States

Marisol Garrouste, Daniel Wendt, William D. Jenson, Qian Zhang, Maria A. Herrera Diaz, and Frederick Joseck
Idaho National Laboratory

May 2023

Idaho National Laboratory
Integrated Energy Systems
Idaho Falls, Idaho 83415

http://www.ies.inl.gov

Prepared for the
U.S. Department of Energy
Office of Nuclear Energy
Under DOE Idaho Operations Office
Contract DE-AC07-05ID14517

Page intentionally left blank

EXECUTIVE SUMMARY

Transportation accounts for 38% of the total U.S. carbon emissions [1]. Using a low-carbon energy source, such as nuclear power, to convert CO_2 into drop-in synthetic transportation fuels is a possible approach for reducing the transportation sector CO_2 emissions. According to the U.S. Department of Energy (DOE), aviation fuel makes up roughly 10% of all transportation fuel CO_2 emissions, which is equivalent to 205 metric tons or 2% of all U.S. CO_2 emissions. Diesel fuel contributed 471 million metric tons of CO_2 emissions in 2021, which accounts for 26% of all CO_2 emissions from the transportation sector [2, 3]. The U.S. government with the 2022 Inflation Reduction Act (IRA) is providing financial incentives to produce clean hydrogen, which can be used in the production of synfuels. As a result, major transportation sectors, such as the airline industry, are starting to invest in synfuels, investigating the use of nuclear power for their production. The reliability of nuclear power makes it a prime candidate for the source of primary energy for synfuels production using CO_2 emissions from industrial processes to produce a drop-in transportation fuel product with a very low well-to-wheel (WTW) emissions profile. The existing fleet of light water reactor (LWR) nuclear power plants (NPPs) is struggling for economic profitability on the current electricity market due to the increased penetration of variable renewable technologies. By using their thermal and electrical output to produce synfuels when it is not needed to meet grid demand, NPP revenues would no longer be solely reliant on electricity markets but also would contribute to the decarbonization of the transportation sector.

Idaho National Laboratory (INL) investigates the relative economic profitability of an integrated energy system (IES) coupling an NPP with a synfuel production process at selected case study locations across the United States. In the synfuel IES, a high-temperature steam electrolysis (HTSE) plant is thermally and electrically coupled with an NPP to produce zero-carbon hydrogen. The synthetic fuel is produced from this H_2 combined with a CO_2 supply using the reverse water gas shift process followed by the Fischer-Tropsch (FT) reaction. This analysis considers a system in which the CO_2 is sourced from regional CO_2 emitters via the construction and operation of pipeline-based CO_2 supply networks. Locating the FT plant at the same site as the NPP and HTSE plants enables the NPP to provide zero-carbon heat and power to the HTSE plant and zero-carbon power to the FT plant as well as avoid the requirement for long-distance H_2 product transport from the HTSE plant to the FT plant. Hydrogen storage is used to enable the NPP to dispatch power to the electrical grid (instead of the HTSE plant) when grid demand increases, thus enabling the FT plant to continue to operate in a steady-state production mode. The ability to cease hydrogen production for several hours within each day enables the NPP to provide power to the grid to balance the electricity market during peak periods and maximize revenues for the nuclear synfuel IES.

The FT process design considered has a 99% carbon conversion efficiency [4]. The use of nuclear energy and nuclear energy-derived hydrogen enables synfuel production to achieve this high level of carbon utilization. Additionally, the life-cycle carbon emissions of the nuclear-based synfuel production process are very low, with WTW emissions of approximately -25 gCO_2e/MJ, including steam credits (generated from FT process excess heat), and approximately 7 gCO_2e/MJ, if steam credits are excluded. This compares favorably with the WTW emissions of 90.5 gCO_2e/MJ for a compression-ignition, direct injection (CIDI) vehicle with a fuel economy of 31.6 miles per gallon gasoline equivalent (MPGGE), using low-sulfur diesel produced using conventional petroleum production and refining processes [4].

Several NPPs in various regions of the U.S. are considered as case study analyses. Supply locations and transportation via pipeline of the CO_2 feedstock to the NPP site are analyzed through the National Energy Technology Laboratory (NETL) CO_2 Transport Cost model [5]. The team finds that the amount of CO_2 generated by different sectors is sufficient for the synfuel production process at all locations considered. The CO_2 transportation costs are functions of the distance of the source to the NPP location, the CO_2 capture cost at the source, and the quantity of CO_2 transported.

Historical electricity prices for the NPP case study locations are collected and analyzed. Monthly average prices, price range, and duration of negative-price periods vary among these locations. For each location, an auto-regressive moving average (ARMA) model is trained on historical electricity price data. ARMA validation is done to ensure the synthetic price distributions represent one of historical prices with high fidelity. Synthetic time series from these ARMA models are used in a coupled dispatch and system optimization in the Holistic Energy Resource Optimization Network (HERON) to compute the differential net present value (NPV) of the IES. The team finds that this econometric is positive, ranging from $14M–1.3bn (2020) depending on the location (see Figure ES-1). The optimal synfuel IES configuration to obtain this increase in NPV often maximizes the size of the synfuel production process with regards to the size of the NPP. However, the team shows that the NPP still plays a stabilizing role for the grid: In periods of high prices and high loads, more electricity from the NPP is sent to the grid. A high variability of electricity prices and extreme maximum prices tend to drive up electricity production. While it requires significant investment, the synfuel IES could increase the economic profitability for the existing fleet of LWRs across the country while still maintaining the grid stabilizer role of NPPs.

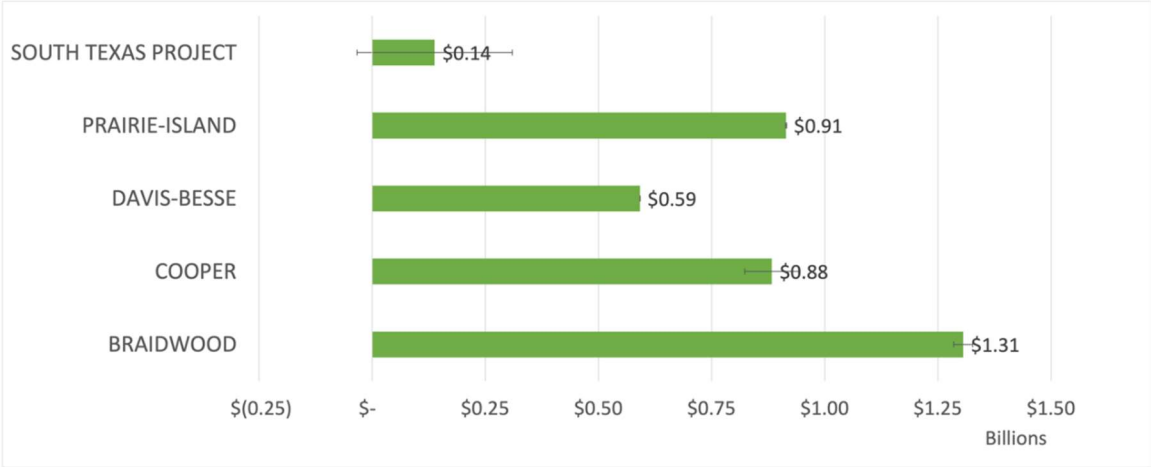

Figure ES-1. Δ(NPV) for the synfuel IES compared to the business-as-usual (BAU) case at each NPP location.

During its lifetime, the main costs for the nuclear synfuel IES are the carbon feedstock transportation costs, followed by the capital expenses (CAPEX) and operation and maintenance (O&M) costs while the revenue comes first from the IRA H_2 production tax credit (PTC) and then from the sales of synfuel products. The profitability of the synfuel IES is most sensitive to the value of the hydrogen PTC and the synfuel products as well as the cost of the carbon feedstock, highlighting the importance of governmental incentives regarding hydrogen, carbon emissions, and synfuel in driving the deployment of future nuclear synfuel IESs. When perturbing input parameters, the team finds that the value of the hydrogen PTC and an added cost for the carbon feedstock have the most influence on the profitability of the synfuel IES.

CONTENTS

FIGURES

TABLES

ACRONYMS

AEO	Annual Energy Outlook
API	Application Programming Interface
ARMA	Auto-Regressive Moving Average
BAU	Business-as-usual
BoP	Balance-of-plant
bpd	Barrels per day
BMT	Billion metric tons
CAGR	Compound annual growth rate
CAPEX	Capital expenses
CO_2	Carbon dioxide
DOE	U.S. Department of Energy
EIA	U.S. Energy Information Administration
EU	European Union
FERC	Federal Energy Regulatory Commission
FT	Fischer-Tropsch
GW	Gigawatt
GHG	Greenhouse gas
H_2	Hydrogen
HERON	Heuristic Energy Resource Optimization Network
HTSE	High-temperature steam electrolysis
IES	Integrated Energy System
INL	Idaho National Laboratory
IRA	Inflation Reduction Act
ISO	Independent system operator
LMP	Locational marginal price
LWR	Light water reactor
MMBtu	Million British Thermal Units
MMT	Million metric tons
MOU	Memorandum of understanding
MPGGE	Miles per gallon gasoline equivalent
MSTL	Multiple Seasonal-Trend decomposition using Loess
MTG	Methanol-to-gasoline
MW	Megawatt

MWe	Megawatt electrical
MWh	Megawatt hour
MWth	Megawatt thermal
NEI	Nuclear Energy Institute
NETL	National Energy Technology Laboratory
NOAK	nth-of-a-kind
NPP	Nuclear power plant
NPV	Net present value
NRC	U.S. Nuclear Regulatory Commission
NREL	National Renewable Energy Laboratory
O&M	Operation and maintenance
O_2	Oxygen
OSRM	Open Street Routing Machine
PTC	Production tax credit
RAF	Royal Air Force
RAVEN	Risk Analysis Virtual ENvironment
RT-LMP	Real-time locational marginal price
RTO	Regional Transmission Organizations
RTM	Real-time market
RTO	Regional transmission organization
SAF	Sustainable aviation fuel
SOEC	Solid oxide electrolyzer cell
TCI	Total capital investment
TDL	Thermal delivery loop
U.K.	United Kingdom
U.S.	United States
UAL	United Airlines
USAF	U.S. Air Force
VARMA	Vector Auto-Regressive Moving Average
WACC	Weighted Average Cost of Capital
WEF	World Economic Forum

Grid-Integrated Production of Fischer-Tropsch Synfuels from Nuclear Power

1. INTRODUCTION

The U.S. transportation sector accounts for 67% of the total U.S. petroleum consumption [6] and represents the largest U.S. use of petroleum products. For the U.S. transportation sector, CO_2 emissions represent about 40% of the total U.S. emissions. For 2021, 1.8 billion Metric Tons (BMT) out of the 4.9 BMT of CO_2 came from the transportation sector. Therefore, decarbonization of the transportation sector would significantly reduce the total U.S. emissions. Transportation sector decarbonization strategies often focus on vehicle electrification. While this approach may be relevant for light-duty transportation vehicles, it is not applicable for aviation, rail, marine, and heavy ground transportation. The energy density required for these kinds of transportation systems is higher than what can currently be achieved by electric batteries. However, synthetic transportation fuels, or synfuels, produced using low-carbon energy sources could be used as drop-in replacements for conventional fossil fuels. With a hydrogen feedstock from an emissions-free energy source and a CO_2 feedstock from an atmospheric source, the resulting synfuels have a low-carbon footprint. The modifications required for the use of synfuels in the current vehicles and fuel transport and delivery infrastructure are minimal. Such a transition could be made at minimal cost and with uncertainty.

While a variety of options exist for low-carbon energy sources to produce decarbonized synfuels, the reliability and availability of nuclear power in the U.S. make it a prime candidate. A nuclear power plant (NPP) could power both the hydrogen and the synfuels production plants in a sustained operational and reliable manner. Across the U.S., the existing fleet of light water reactors (LWRs) are located amongst various industrial sources of CO_2 emissions that could be used as a feedstock. The existing LWR fleet is currently used to provide electrical power to the grid. Given their operational constraints, NPPs have difficultly balancing their costs because they play the role of a baseload producer in a market where the increased penetration of wind and renewables have driven the prices down. Coupling existing LWRs with hydrogen and synfuel production facilities to form a nuclear synfuel IES could provide the nuclear sector with the opportunity to regain economic profitability while providing the U.S. with low-carbon synfuels for the transportation sector.

The present analysis builds upon a previous economic assessment of the production of synfuels from nuclear energy via the FT process [7]. In this study, hydrogen is produced via a high-temperature steam electrolysis (HTSE) process using nuclear power from the Braidwood NPP in the PJM market. An FT-based synfuel production process was also co-located with the NPP and would use power from the NPP to produce a mix of naphtha, jet fuel, and diesel. This nuclear synfuel IES has been found to have a greater economic value when compared to the current use of NPPs in which all power output is sold into the electricity market. The same IES configuration is considered in this analysis. The nuclear synfuel IES plant configuration and operating strategy is optimized and assessed for different locations and electricity markets across the country. Additionally, the ability for the nuclear synfuel IES to dynamically vary the quantity of power sent to the electrical grid and synfuel production was considered. The following NPP locations were chosen because they are in different markets and regions of the United States: Braidwood, Davis-Besse, Prairie Island, Cooper Nuclear Station, and South Texas Project. Note that these NPPs were chosen for their ability to represent different regions of the U.S. and the associated variations in energy and fuel market pricing and for their geographic proximity to potential CO_2 feedstock sources. The operators of these NPPs have not specifically expressed interest in or commitment to the production of nuclear-based synfuels.

2. SYNFUEL MARKET

A research report completed by McKinsey & Company suggests sustainable fuels could account for 37% of the transportation energy demand by 2050 [8]. These findings bode well based on incentives created through the Inflation Reduction Act (IRA), which provides a $1.25/gallon credit for sustainable aviation fuel (SAF) purchases [9]. The act also extends incentives by two years for biodiesel and renewable diesel. These incentives and credits are not factored into the financial model used in this report but are mentioned here as they will impact demand for low or zero-carbon alternative fuels. Before the adoption of the IRA, multiple airlines were already considering ways to decarbonize air travel. In 2021, Boeing made an announcement indicating they were committed to building aircrafts capable of using 100% synthetic fuel [10]. Current regulations limit synthetic blended aviation fuel to 50% but research is being conducted to understand implications for higher synthetic concentrations.

The U.S. Department of Energy (DOE), U.S. Department of Transportation (DOT), and the U.S. Department of Agriculture (USDA) combined efforts to create the "Sustainable Aviation Fuel Grand Challenge" with the goal of making aviation fuel 100% sustainable by 2050 [11]. The near-term goal is to produce 3 billion gallons of SAF per year by 2030.

Based on figures available from the U.S. Energy Information Administration (EIA), roughly 88% of U.S. transportation energy comes from gasoline, distillates, and jet fuel (Figure 1). This report analyzes these fuels with the addition of naphtha to help explore market opportunities for synthetic fuel. It should be noted that gasoline is not being evaluated for production using the FT plant. The inclusion of gasoline market statistics is used for reference and because naphtha can be used as a blendstock for gasoline production. Trends associated with these fuels were analyzed regionally to understand potential market opportunities for specific NPPs located in five unique U.S. Census Bureau regions. Each region has unique pricing for fuel products due to changes in supply and demand conditions. These prices are further diversified by state-specific fuel taxes. Details related to regional prices will be discussed in Section 4.3 of this report.

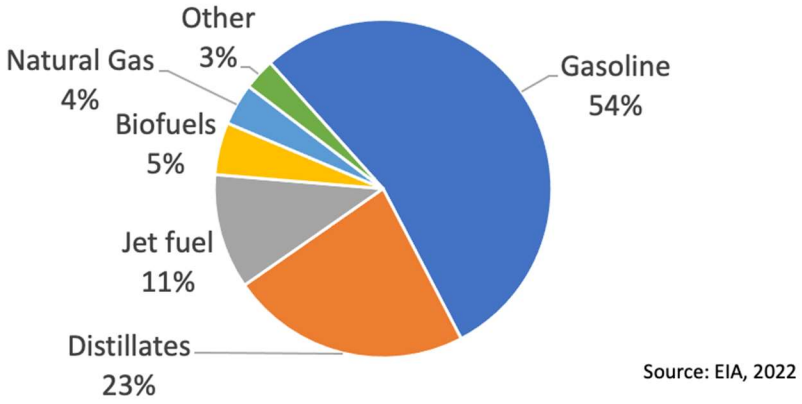

Figure 1. U.S. transportation energy sources.

2.1 Market Case Studies

Case studies for market applications of synthetic fuel are increasingly available. Military use cases for synthetic fuel can be found in the U.S. and the United Kingdom (U.K.). Both countries are exploring opportunities to utilize synthetic aviation fuel for military aircraft. The U.K. Royal Air Force (RAF) plans to transition an airbase to achieve net-zero emissions by 2025 [12]. The U.S. Air Force (USAF) indicated through an Energy Flight Plan that their entire fleet has been certified to use alternative fuels with synthetic to traditional fuel mixtures of up to 50% [13].

Applications of synthetic fuels are not limited to governments. Multiple large commercial airlines are investing in synthetic fuel producers. In one case, Royal Dutch Shell is working with Vattenfall AB and LanzaTech, Inc. to use the Forsmark NPP in Sweden [14]. This case study is of particular interest given the scope of research currently being conducted.

Private producers of SAF are partnering with major airlines. In some cases, airlines are making financial investments in these private companies. In 2015, United Airlines claimed to be the first U.S. airline to invest in an SAF company when they partnered with Fulcrum BioEnergy [15]. They quickly followed the investment in 2016 by using SAF in regularly scheduled flights. By 2021, they completed a passenger flight using 100% SAF. United Airlines has made the commitment to reduce greenhouse gas (GHG) emissions 100% by 2050. Some of the other airlines making similar investments include Alaska Airlines, JetBlue, Southwest, and Delta. Some of the SAF producers include Alder, SG Preston, Twelve, Aemetis, Fulcrum BioEnergy, and World Energy. It appears the commercial airline industry is moving together toward widespread use of SAF.

Audi has been working on producing synthetic diesel fuel with Sunfire since 2014 [16]. One report indicated that Audi was building a new e-diesel facility in Laufenber, Switzerland, in addition to their existing facility in Dresden, Germany. This time Audi is partnering with Ineratec and Energiedienst AG. The new facility has a planned capacity of more than 105,000 gallons per year. Given synthetic diesel's ability to act as a drop-in substitute for traditional diesel, the market for a synthetic version could be widely adopted.

2.2 Market Size

Comparing multiple industry reports, the global market for diesel fuel makes up 39% of the combined $2.4 trillion value outlined in Table 1 [17-19]. It should be noted that these market values are based on retail prices, which include taxes, transportation, and distribution expenses. In Section 4.3 of this report, efforts were taken to eliminate these additive costs and estimate the price of fuel at the plant gate. As indicated in Table 1, jet fuel and naphtha accounted for 13% and 10%, respectively. Fuel use statistics for diesel, gasoline, and jet fuel are available through the EIA Annual Energy Outlook. Unfortunately, there was no data available from EIA for naphtha use or prices. A process was developed to forecast naphtha prices based on historical price correlation between naphtha and gasoline. A detailed methodology for naphtha price forecasts is available in Section 4.3. Non-government data sources indicate the naphtha market size is expected to grow at a compound annual growth rate (CAGR) of 5.7%, which is higher than any of the other fuel growth rates. It should be noted that some of the CAGR growth rates from industry reports conflict with EIA forecasts for fuel use, which predict relatively flat growth rates for gasoline and diesel and higher growth rates for jet fuel, as seen in Figure 2.

Table 1. Global fuel market size.

Product	Global Market Size ($ Billions)	Percent of Total	CAGR*
Diesel	$935.2	39%	4.9%
Gasoline	$928.0	38%	4.4%
Jet Fuel	$312.7	13%	2.1%
Naphtha	$248.5	10%	5.7%
Total	$2,424.4	—	—
*Compound Annual Growth Rate			

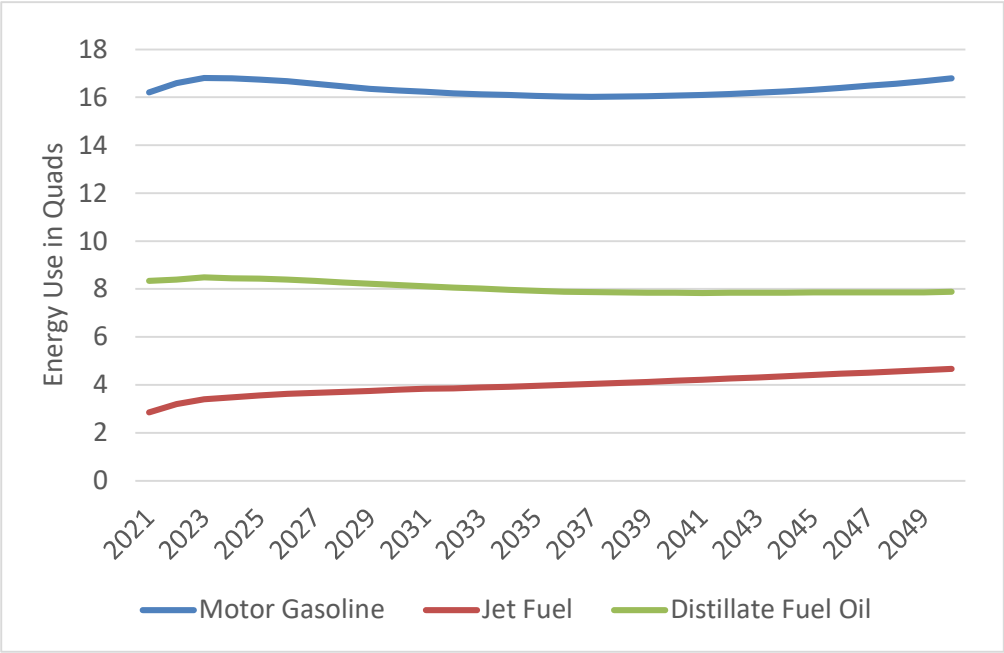

Figure 2. Total energy use by fuel [20].

In the U.S., fuel use volumes help uncover market characteristics. According to EIA forecasts, 60.4 billion gallons of distillate fuel oil (diesel) was used during 2022. These statistics account for all fuel use, not just for transportation. According to EIA, the transportation sector uses 128 million gallons of diesel fuel each day. Diesel is the preferred source of fuel for many applications because of its greater energy density and reduced flammability and because it is less likely to stall [21]. By comparison, nearly 133 billion gallons of gasoline were used in 2022, and nearly 24 billion gallons of jet fuel was used.

Regional fuel use and market size fluctuate based on the mix of industries in the region and population size. Figure 3 provides a map of the U.S. Census regions used by EIA to organize price and energy use statistics. These data became valuable tools for modeling production scenarios, which will be addressed later in this report.

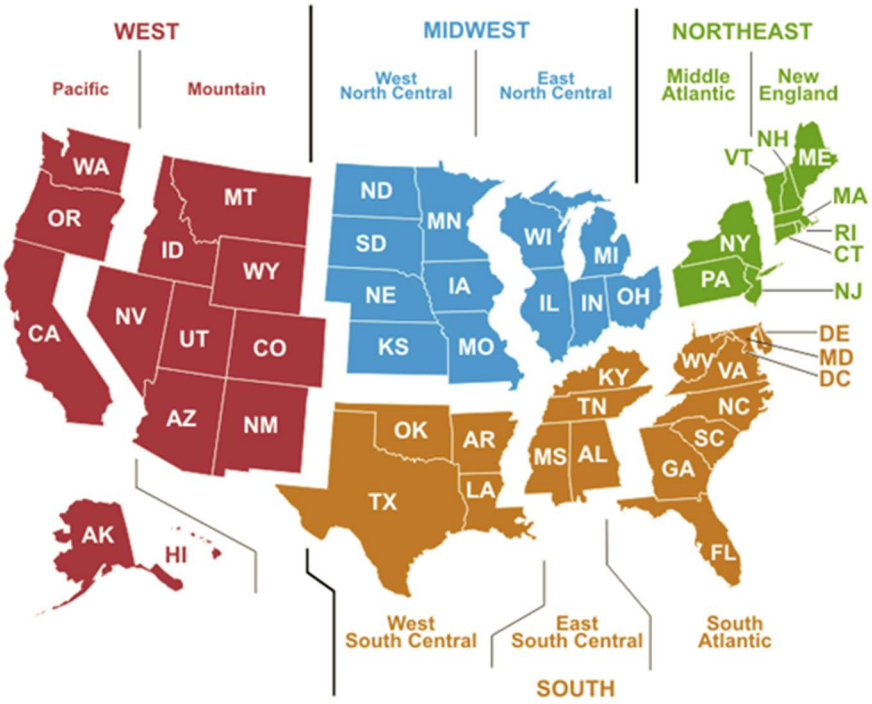

Figure 3. Map of U.S. census regions [22].

Table 2 indicates the volume of fuel used in the U.S. in 2022. This table also provides an understanding of how various regions in the country use these fuels. Of the regions analyzed in this study, the West South Central region used the most distillate fuel oil, or diesel, and was followed by East North Central. The Pacific region was by far the largest user of jet fuel. Gasoline consumption was included in the results for reference purposes only. Unfortunately, EIA does not provide energy use statistics for naphtha.

Table 2. U.S. fuel market by region and volume.

United States Fuel Market by Region and Volume (Billions of Gallons, 2022)			
Region	Distillate Fuel Oil	Jet Fuel	Motor Gasoline
United States	60.4	23.8	132.8
West North Central	6.5	0.7	9.6
Pacific	6.3	6.1	19.0
East North Central	8.1	2.1	18.7
West South Central	11.4	2.6	18.9
Source: EIA, Annual Energy Outlook, 2022			

EIA provides long-term energy use forecasts under multiple scenarios. For this report, the scenarios of most interest included forecasts under conditions of high oil and gas supply, low oil and gas supply, and a standard reference case. Section 4.3 of this report provides a summary of how a fluctuation in oil and gas supply conditions could impact fuel prices over time, according to EIA projections. A summary analysis of these energy use changes can be found in Table 3. Reference case forecasts for diesel use show a 5.5% decrease in use between 2021 and 2050 for the aggregated U.S. market. Interestingly, the East North Central region is forecasted to decrease diesel use by more than 12%. The only scenario where diesel fuel use is expected to increase is under high oil and gas supply conditions. Forecasted diesel use is greatly diminished under low oil and gas supply scenarios. This is likely the result of elevated prices that follow tight supplies.

In contrast, jet fuel use is expected to make large gains across the U.S. in all three supply scenarios. The largest gains were observed in the West South Central region. Lowest gains are expected in the East North Central region. Under the reference case, U.S. jet fuel use is expected to increase by nearly 64%. Jet fuel use is expected to increase by over 70% under a high oil and gas supply scenario and increase by 57% under the low oil and gas supply scenario.

For reference, gasoline use is expected to decrease by 1% if low oil and gas supply conditions were present. The increase in gasoline use in the other two scenarios was very modest compared to jet fuel.

Table 3. Forecasted percent change in energy use by source.

Forecasted Percent Change in Energy Use by Source (2021–2050)				
	Region	High oil and gas supply	Low oil and gas supply	Reference case
Distillate Fuel Oil	United States	0.2%	-10.8%	-5.5%
	Pacific	4.5%	-4.7%	-0.7%
	East North Central	-7.9%	-16.0%	-12.1%
	West North Central	3.0%	-5.8%	-1.4%
	West South Central	6.6%	-8.4%	-1.0%
Jet Fuel	United States	70.5%	57.2%	63.6%
	Pacific	65.6%	52.8%	59.0%
	East North Central	48.9%	37.0%	42.8%
	West North Central	60.2%	48.8%	54.3%
	West South Central	94.7%	80.0%	87.1%
Motor Gasoline	United States	9.4%	-1.0%	3.6%
	Pacific	6.1%	-3.1%	0.8%
	East North Central	0.9%	-8.2%	-4.3%
	West North Central	5.8%	-4.3%	0.3%
	West South Central	20.8%	8.6%	14.0%
Source: EIA, 2022 Annual Energy Outlook				

3. SYNFUEL PRODUCTION PROCESS FROM NUCLEAR ENERGY

This analysis evaluated synthetic fuel production via the Fischer-Tropsch synthetic fuel production process, which requires hydrogen and carbon dioxide feedstock. The hydrogen feedstock is specified to be supplied by a high temperature steam electrolysis process. The performance and costs of the FT and HTSE processes are summarized in the following sections.

3.1 Fischer-Tropsch Synthetic Fuel Production Process

The FT process is a chemical process that converts a syngas mixture of CO and H_2 into liquid hydrocarbons via catalyzed chemical reactions that take place in the temperature range of 150–300°C. Products from the FT process may include diesel fuel, jet fuel, and lubricants as well as blendstocks for gasoline fuels.

The FT process produces long-chain hydrocarbons through a series of condensation polymerization reactions. Generic equations representing the formation of alkane and alkene products are provided in Equation (1) and Equation (2), respectively:

$$(2n+1)\,H_2 + n\,CO \rightarrow C_nH_{2n+2} + n\,H_2O \quad (1)$$

$$2n\,H_2 + n\,CO \rightarrow C_nH_{2n} + n\,H_2O \quad (2)$$

This reaction mechanism results in primarily straight-chain hydrocarbon formation. The use of a cobalt-based catalyst favors alkane production, while the use of an iron-based catalyst favors alkene production [4]. The chain length of the products tends to range from 1 to 20, with the yield of longer chain hydrocarbons favored at lower temperatures (e.g., 220–240°C). The FT naphtha products have a chain length of $5 \leq n \leq 9$, the jet products have a chain length of $10 \leq n \leq 14$, and the diesel products have a chain length of $15 \leq n \leq 18$. FT wax products ($n>18$) can be cracked to reduce the chain length into the range of the desired fuel products listed above.

The FT process was commercialized in 1936, when Germany used it during World War II to produce liquid fuels from coal. Since then, the FT process has been used in numerous other locations for liquid fuel production from coal and natural gas. The largest FT plant in the world is the Sasol Secunda plant located in South Africa, which produces 160,000 bpd of FT liquids from a coal feedstock. As of 2020, this plant was listed as the world's largest single GHG emitter.

However, when CO_2 is used as the carbon source instead of natural gas or coal,[a] and hydrogen is sourced from a process with low-carbon emissions, such as nuclear- or renewable-based electrolysis, the net CO_2 emissions from producing and then using the resulting drop-in liquid hydrocarbon fuel could be significantly lower than from the production and use of conventional petroleum fuels. If biogenic CO_2 (or CO_2 from the atmosphere), zero-carbon hydrogen, and zero-carbon energy are used in the production of the synthetic liquid hydrocarbon fuels, the resulting synfuels may be carbon neutral.

The current analysis evaluates the economics of FT fuel production using hydrogen produced from nuclear-based electrolysis and a CO_2 feedstock sourced from corn ethanol biorefineries located around the synfuel production plant site, which is co-located with the NPP. The analysis was performed in collaboration with Argonne National Laboratory (ANL), which developed detailed Aspen Plus process models of the nuclear-integrated FT synthetic fuel production process [4, 23, 24]. A block flow diagram of the synfuel production process, including the reverse water gas shift reactor to produce synfuel from the H_2 and CO_2 feedstock, FT synthesis reactor, and product purification and recycle, are shown in Figure 4 [4].

a. The reverse water gas shift reaction may be used to convert CO_2 and H_2 to CO and H_2O, which may be further processed to yield a syngas mixture of CO and H_2 that can be converted to a wide range of potential products including synthetic fuels.

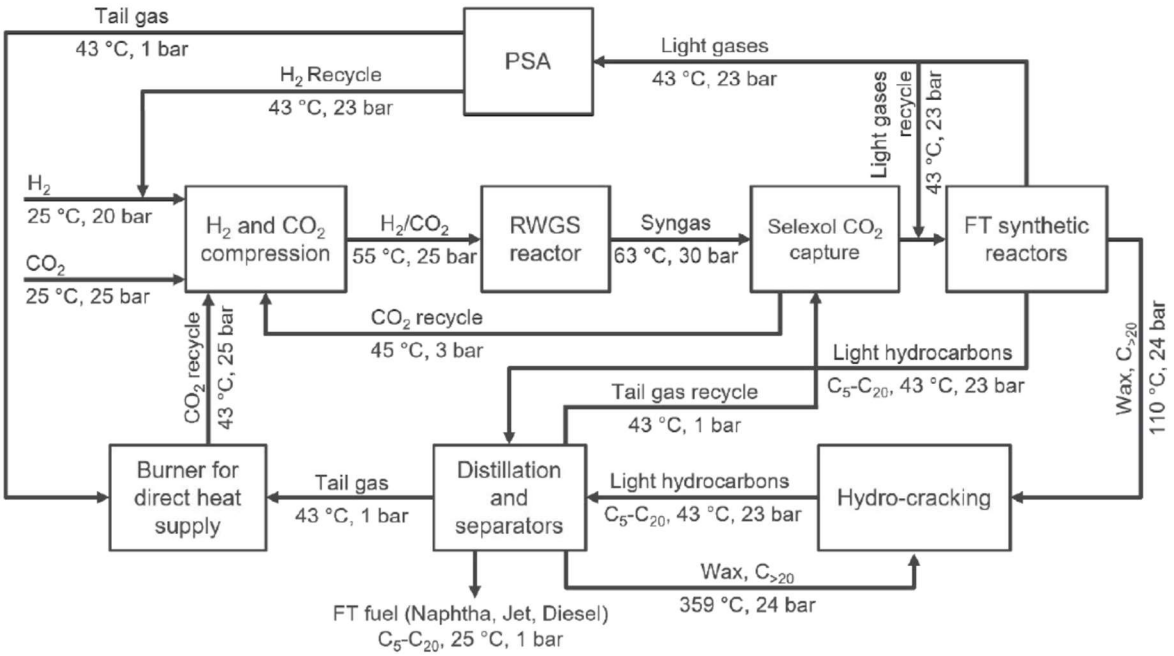

Figure 4. An FT fuel process flow diagram with temperature and pressure values of main streams. The diagram is reproduced from the "The Modeling of the Synfuel Production Process: Techno-Economic Analysis and Life Cycle Assessment of FT Fuel Production Plants Integrated with Nuclear Power" report [4].

Several FT process capacities are considered in the process and economic analyses, ranging from 100 MWe to 1000 MWe combined power requirement for the electrolysis and FT plants. As the existing fleet of LWR NPPs generally have unit capacities on the order of approximately 1000 MWe, the scale of synfuel plant capacities selected for this analysis corresponds to operating scenarios that would involve approximately 10–100% of the power produced by a LWR unit used for FT synfuel production. The analysis considers steady-state operation of the electrolysis and FT plants. It is assumed that the balance of NPP power generation continues to be sold to the electric grid. The feedstock input requirements and synfuel product flow rates for each of the production capacities considered are detailed in Table 4.

Table 4. Feedstock demand and product capacity for different plant scales. Reproduced from the "The Modeling of the Synfuel Production Process: Techno-Economic Analysis and Life Cycle Assessment of FT Fuel Production Plants Integrated with Nuclear Power" report [4].

		FT-100	FT-400	FT-1000
Feedstock	H_2 (MT/d)	56	255	601
	CO_2 (MT/d)	348	1,580	3,724
Products	Naphtha (MT/d)	39	176	414
	Jet fuel (MT/d)	47	213	502
	Diesel (MT/d)	26	118	278
	Total FT fuel (gal/d)	40,430	183,030	431,050
Carbon conversion		99%	99%	99%

The FT process capacity impacts the economics of synfuel production in several ways. First, as the capacity of the FT plant increases, the required feedstock flow rates also increase. Since water is the primary material feedstock for hydrogen production and water is assumed to be readily available at the designated synfuel production plant location, the synfuel plant capacity does not have a direct impact on water feedstock cost. However, since the CO_2 feedstock must be obtained from distributed ethanol biofuel production plants in the area surrounding the synfuel production plant, the capacity of the synfuel plant impacts the distance over which the CO_2 feedstock must be transported. As the synfuel production capacity increases, CO_2 must be obtained from a greater number of distributed biofuel plants located at further distances from the centralized synfuel plant. As the length of the CO_2 pipelines, which must be constructed to connect additional biofuel plants to the synfuel plant, increases, the average CO_2 feedstock cost increases accordingly. The relationship between CO_2 feedstock cost and synfuel plant capacity are addressed in additional detail in Section 4.2.

Second, the synfuel production process capacity impacts the capital costs of the FT plant and the electrolysis plant. The unit capital costs on a $/kW basis of each of these processes are expected to decrease as plant capacity increases due to economies of scale. FT process capital costs are detailed in Table 5, and the electrolysis process capital costs are described in Section 3.2.

Table 5. Detailed CAPEX for each of the three designed FT plant scales. Reproduced from the "The Modeling of the Synfuel Production Process: Techno-Economic Analysis and Life Cycle Assessment of FT Fuel Production Plants Integrated with Nuclear Power" report [4].

	FT-100 (10^3 USD)	FT-400 (10^3 USD)	FT-1000 (10^3 USD)
Direct depreciable capital cost			
H_2 compression	$4,977	$7,761	$14,983
RWGS reaction	$8,487	$19,627	$40,990
CO_2 capture	$6,289	$12,136	$23,428
FT synthesis	$4,759	$11,139	$23,378
Hydroprocessing	$18,739	$47,351	$81,533
Utilities	$4,600	$9,636	$19,619
Total direct depreciable capital cost	$47,851	$107,650	$203,931
Indirect depreciable capital cost			
Site preparation	$957	$2,153	$4,079
Engineering and design	$4,785	$10,765	$20,393
Project contingency	$7,178	$16,147	$30,590
Up-front permitting costs	$7,178	$16,147	$30,590
Total indirect depreciable capital cost	$20,098	$45,213	$85,651
Non-depreciable capital cost			
Land cost	$1,019	$2,293	$4,344
Total capital costs	$68,968	$155,155	$293,926

Finally, synfuel production energy requirements change with plant capacity. Table 6 provides process energy input requirements and product output energy content for each of the selected synfuel production capacities. If the energy price varies with the quantity required (e.g., greater energy demand is correlated with increased price in a similar manner to basic economic theory), then increases in the plant capacity may impact the energy costs incurred by the synfuel process. However, this Holistic Energy Resource Optimization Network (HERON) analysis, described further in Section 4.2, assumes a price taker model such that the operation of the synfuel production process does not affect electricity market pricing. Table 6 also reports the calculated process efficiency based on the lower heating value of the product slate. The calculated process efficiency depends primarily on the conversion pathway and process configuration. Since the same conversion pathway and process configuration are utilized for each of the plant capacities evaluated, the process efficiency is equal for each of the plant capacities in this analysis.

Table 6. Energy balance and overall efficiency for the combined FT plant-NPP system. The energy values were calculated with respect to the lower heating value. Reproduced from the "The Modeling of the Synfuel Production Process: Techno-Economic Analysis and Life Cycle Assessment of FT Fuel Production Plants Integrated with Nuclear Power" report [4].

		FT-100	FT-400	FT-1000
Input	Electric power (H_2 prod.)	86.2	390.9	922.2
	Thermal power (H_2 prod.)	15.0	68.0	160.4
	Electric power	3.4	15.5	36.6
Output	Naphtha	19.7	89.6	210.4
	Jet fuel	24.0	108.7	256.4
	Diesel	13.2	59.9	141.3
	Steam	16.1	73.0	174.6
Total energy efficiency		69.8%	69.8%	69.8%

3.2 High-Temperature Steam Electrolysis

This analysis considers the use of a nuclear-integrated HTSE process to produce the hydrogen feedstock necessary for synfuel production. Hydrogen production in the HTSE process occurs in a stack of solid oxide electrolyzer cells (SOECs), which operate at high temperatures (e.g., 700–800°C) to increase the efficiency of the HTSE process. In addition to electric power, the HTSE process requires thermal energy input to vaporize the feedwater stream and achieve the required stack operating temperature. The SOEC electrolyte is a solid oxide ceramic material that conducts oxygen ions within a specified operating temperature range. Electric current flows into the cathode where water is split into H_2 (gaseous) and O2- ions. The O2- ions are transported across the electrolyte to the anode where the electric current exits the cell and the O2- ions combine to form O2 (gaseous) [25]. The SOEC configuration is illustrated in Figure 5. Equations (3) and (4) show the formulas for the cathode and anode, respectively.

Cathode: $H_2O(g) + 2e^- \rightarrow H_2(g) + O^{2-}$ (3)

Anode: $O^{2-} \rightarrow \frac{1}{2}O_2(g) + 2e^-$ (4)

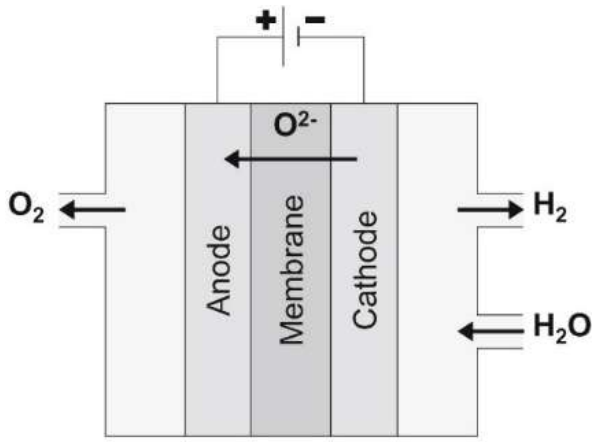

Figure 5. SOEC configuration adapted from "Future cost and performance of water electrolysis: An expert elicitation study" report [26].

To operate the SOEC stack at elevated temperatures, the process requires a balance-of-plant (BoP) configuration with a feedwater steam generator, recuperating heat exchangers (HXs), and topping heaters. The process also requires compressors and blowers to pressurize and circulate the vapor phase reactants and products and the sweep gas used to balance the pressure between the cathode and anode sides of the cells. Additionally, since the H_2 product gas exiting the SOEC stack includes a quantity of unreacted steam, additional process operations are required to remove the water vapor from the H_2 product (e.g., typical water removal steps include cooling/compression and/or pressure swing adsorption).

The NPP provides electrical power to the HTSE process to operate the SOEC stacks and to the BoP pumps, compressors, topping heaters, instrumentation, etc. A thermal delivery loop (TDL) is used to transport heat from the NPP to the HTSE plant to provide the thermal energy needed to vaporize the HTSE process feedwater. The TDL is a pipe network that circulates a heat transfer fluid that indirectly transfers heat from the NPP steam to the HTSE feedwater. The TDL enables the NPP and HTSE plant to be located a safe distance apart (e.g., ~1 km) and provides physical isolation of the nuclear and non-nuclear systems.

This analysis specifies the use of an Nth-of-a-kind (NOAK), modular construction, nuclear-integrated HTSE plant (Figure 6). Since nuclear-based synfuel production at several capacities is considered, the HTSE plant must be scaled accordingly. The design basis for the NOAK HTSE plant specifications utilized in this analysis are detailed in the Idaho National Laboratory (INL) report INL/RPT-22-66117 [27]. Table 7 provides a summary of the HTSE process operating condition specifications. Figure 6 provides a summary of the NOAK modular HTSE plant type total capital investment (TCI) as a function of plant capacity based on a SOEC stack cost of $78/kW-dc, which corresponds to an analysis by James and Murphy [28]. This stack cost is estimated for a SOEC stack manufacturing rate of 1,000 megawatt (MW)/yr. Although SOEC stack manufacturers are currently constructing factories with up to a 500 MW/yr capacity [29], additional time is required to achieve the 1,000 MW/yr target.

Table 7. HTSE and related subsystem process operating condition specifications.

Parameter	Value	Reference or note
Stack operating temperature	800°C	O'Brien et al. 2020 [30].
Stack operating pressure	5 bars	See Section 2.2.1 of INL/RPT-22-66117 [27].
Operating mode	Constant voltage (V)	—
Cell voltage	1.29 V/cell	Thermoneutral stack operating point.
Current density	1.5 A/cm²	James and Murphy 2021 [28].
Stack inlet H_2O composition	90 mol%	O'Brien et al. 2020 [30].
Steam utilization	80%	See Section 2.2.1 of INL/RPT-22-66117 [27].
HTSE modular block capacity	25 MW-dc	1000× capacity increase [30].
Sweep gas	Air	O'Brien et al. 2020 [30].
Sweep gas inlet flow rate	Flow set to achieve 40 mol% O2 in anode outlet stream	—
Stack service life	4 years	HFTO Hydrogen Production Record 20006 [31].
Stack degradation rate	0.856%/1000 hr.	HFTO Hydrogen Production Record 20006 [31].
Stack replacement schedule	Annual stack replacements completed to restore design production capacity	Based on H2A model stack replacement cost calculations.

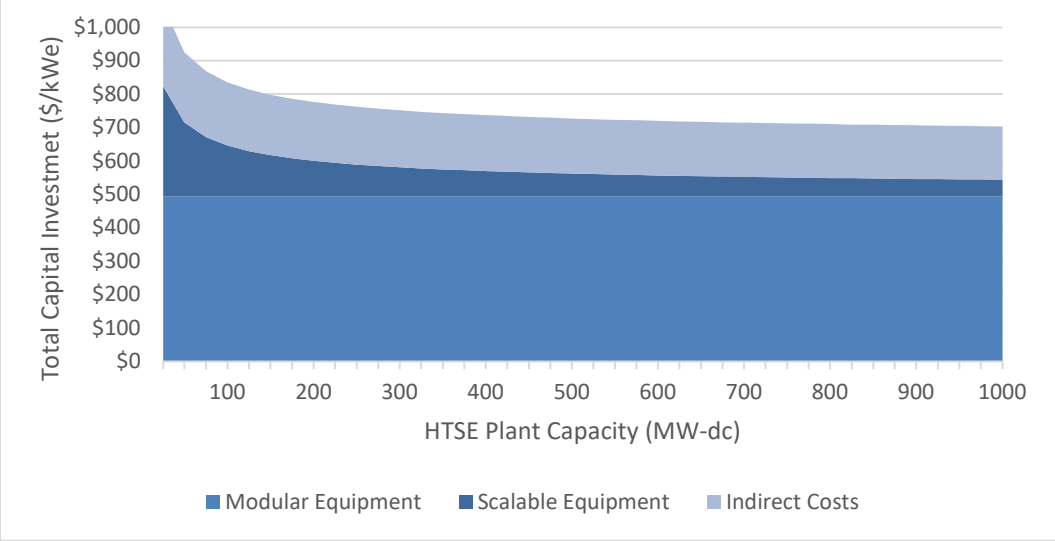

Figure 6. TCI as a function of plant capacity for an NOAK HTSE plant with a stack capital cost specification of $78/kW-dc [28].

Table 8 provides a summary of the NOAK, nuclear-integrated, modular HTSE performance and cost parameters at the capacities considered in the synfuel production analysis. Additional details regarding the HTSE process design can be found in INL/RPT-22-66117 [27].

Table 8. HTSE performance and cost parameters at selected capacities.

	FT-100	FT-400	FT-1000
HTSE Plant Design Capacity (ton-H_2/day)	56	255	601
Energy Consumption Electric (MWe) Thermal (MWth)	 86.2 15.0	 390.9 68.0	 922.2 160.4
Direct Capital Cost ($/kW-dc)	665	573	547
Total Capital Investment ($/kW-dc)	861	742	708
Fixed Operating Cost ($/kW-dc-yr)	52.6	37.0	33.2
Variable Operating Cost, excluding energy costs ($/MW-dc-hr)	3.51	3.43	3.41

4. LIGHT WATER REACTOR CASE STUDIES

Several existing fleet light water reactor nuclear power plants were selected as the basis for case study analysis of nuclear-based synfuel production. The following NPPs were chosen because they are in different markets and regions of the United States: Braidwood, Davis-Besse, Prairie Island, Cooper Nuclear Station, and South Texas Project. Each of these NPPs is in a region of the U.S. associated with different electricity market pricing, CO_2 feedstock availability, and hydrocarbon fuel pricing. Each of these factors impacts the potential economic viability of synfuel production using existing LWR fleet NPPs. The following sections describe the approach used to specify the electricity pricing, CO_2 feedstock pricing, and liquid hydrocarbon fuel product pricing used as the basis for economic evaluation of synfuel production from existing LWR fleet NPPs.

4.1 Electricity Markets

The main revenue stream for LWR NPPs has historically been the sale of power into electricity markets. While production of synfuels could provide an alternative revenue stream of NPPs, there could be benefits associated with having the NPP continue to provide power to the grid during periods of peak electricity demand. The following section describes the approach for estimating the value of electrical power that could be sold to the grid in a nuclear-synfuel IES at each of the selected case study locations.

4.1.1 Overview of Electricity Markets

As electricity markets have changed with increases in variable renewable energy within the last few decades, NPP owners have evaluated potential ways to increase profitability, flexibility, and efficiency. One of the potential solutions that researchers have considered is selling electricity to produce commodities, such as heat, potable water, hydrogen, or chemical products, in addition to selling electricity to the grid. Thus, co-generation systems, including a nuclear reactor, electricity generation turbomachinery, and an industrial process for the production and storage of a secondary commodity have been proposed for currently operating NPPs and next-generation reactors.

In this project, the NPPs considered are the following: Davis-Besse in Ohio, Braidwood in Illinois, South Texas Project in Texas, Cooper in Nebraska, and Prairie Island in Minnesota (labeled by the rectangle boxes in Figure 7[a]). Some of these power plants are integrated with their individual local

wholesale electricity markets operated by independent system operators (ISOs) and regional transmission organizations (RTOs) (see Figure 7[b]). An ISO operates the region's electricity grid, administers the region's wholesale electricity markets, and provides reliability planning for the region's bulk electricity system. RTOs perform the same functions as the ISOs but have greater responsibility for the transmission network as established by the Federal Energy Regulatory Commission (FERC). In addition, as shown in Figure 7(b), there are large sections of the U.S., particularly in the Southeast and the West, where there is not an ISO or RTO.

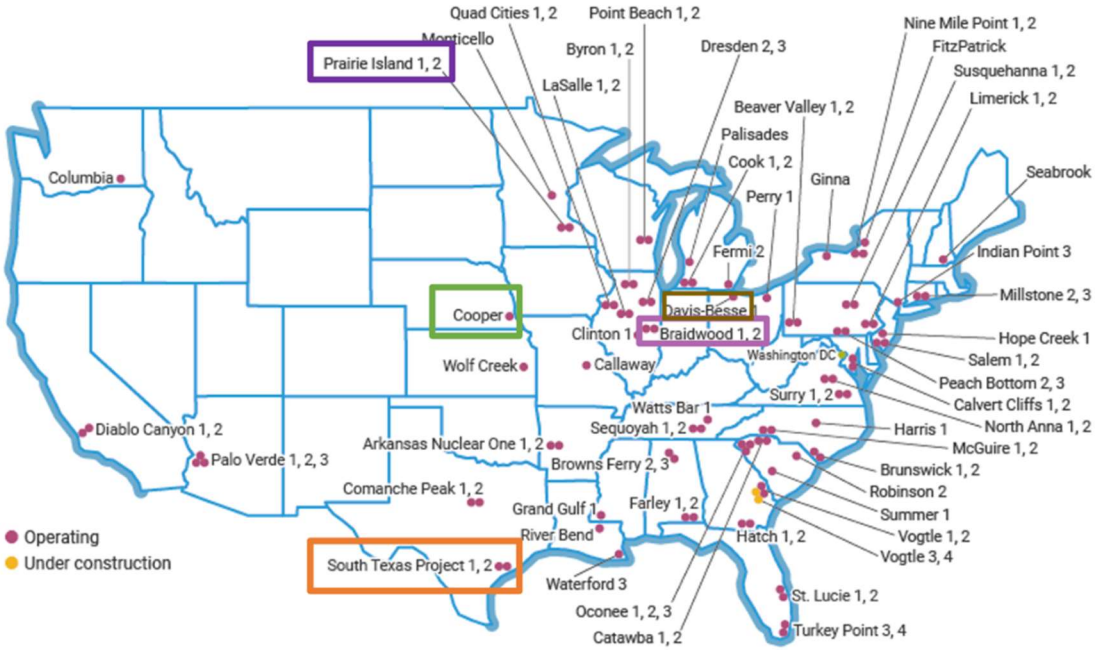

(a)

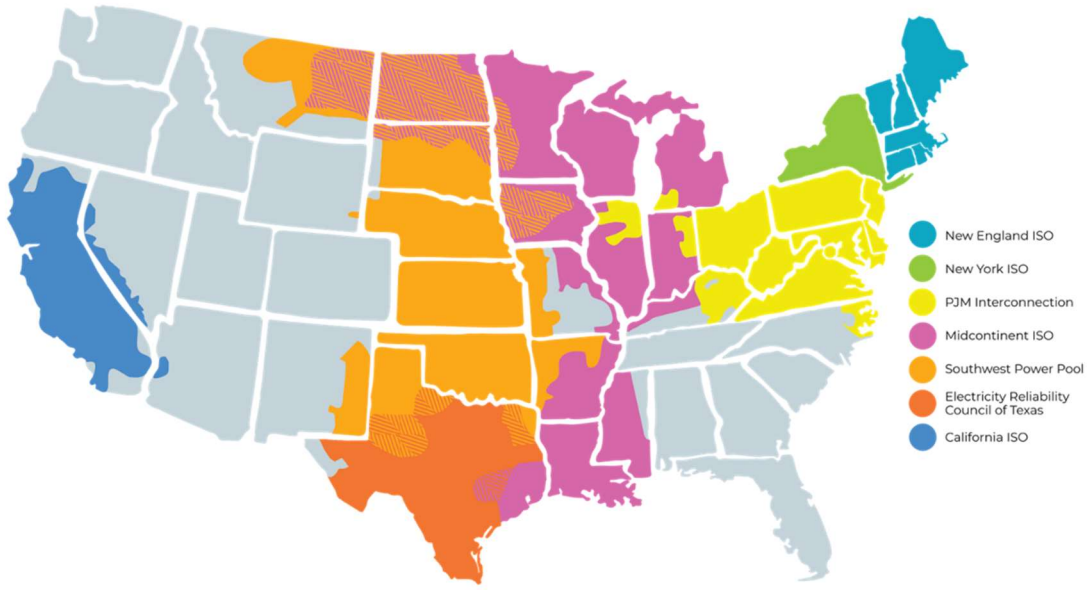

(b)

Figure 7 (a) NPPs operating in the United States. (b) ISO/RTO operating power markets in U.S.

4.1.2 Historical Data Analysis

For this analysis, 7–11 years of hourly day-ahead locational marginal price data were collected for the five locations indicated in Figure 7(a) in four ISOs (see Figure 7[b] and Table 9). The Day-Ahead Energy Market (day-ahead market) is a type of financial market that enables individuals and companies to buy and sell electric energy at prices that are fixed for the following day. This helps both buyers and sellers protect themselves against fluctuation and volatility in the real-time energy market as they are able to secure a predetermined price prior to the next operating day. Essentially, the day-ahead market operates as a means of hedging against potential price changes [32]. The locational marginal prices (LMP) in the day-ahead market offer critical information that aids decision making related to infrastructure investment, promotes greater grid stability, and facilitates the creation of competitive markets for reliable power sources [33]. In this report, the hourly day-ahead market clearing price or LMPs at the nodes where each reactor is connected to the transmission system is taken as a proxy outcome variable.

Figure 8 shows the monthly average electricity prices in the Braidwood, Davis-Besse, Cooper, STP, and Prairie Island markets, respectively. The average monthly prices before the COVID-19 pandemic for these locations are compared and indicate higher prices for Braidwood and Davis-Besse in PJM interconnection (PJM) and STP in Electric Reliability Council of Texas (ERCOT). For the average day-ahead electricity price between 2011 and 2021, the price for the STP ($41.4/MWh) market is higher than that for Braidwood ($33.9/MWh). Meanwhile, the data indicate the trend of decreasing monthly average prices in Braidwood, Davis-Besse, and STP from 2011 to 2019, which implies co-generation systems—including a nuclear reactor, electricity generation turbomachinery, and an industrial process—can potentially bring more benefits to the NPPs in these locations.

Additionally, monthly average prices in the Prairie Island (both Unit 1 and Unit 2) market are the lowest among these five locations from 2013 to 2019 (Figure 8). The low price at this node comes from a significant number of negative-price events (prices are negative in 36.9% of the hourly data points considered as shown in Table 9) existing through these years. This is because the LMP value is a calculated combination of the electricity price, congestion on the transmission grid, and line losses. For the nuclear plants, it can be time consuming and expensive to ramp up or down, meaning NPP owners may choose to keep NPPs online all day regardless of the price of electricity. Therefore, it is possible for electricity supply to exceed consumer demand in wholesale electricity markets; in these conditions, prices can go negative. Negative prices are worth further consideration because they represent a strange phenomenon: generators paying, rather than getting paid, to provide electricity. At the Prairie Island node, the frequency of negative-price events is very high. Therefore, a specific consideration for these negative-price events in the electricity market at Prairie Island is needed. Similarly, prices in the Cooper market are the second lowest from 2014 to 2019. This is also because there is a significant amount of negative prices (prices are negative in 3.6% of the hourly data points considered, see Table 9) during these years, which is worth specific consideration as well.

The team identifies peak monthly average prices each year in both STP and Braidwood (and Davis-Besse) (see Figure 8). These peak monthly average prices are associated with the local weather conditions in these locations. In STP, most of the highest monthly average prices are in the summer (e.g., 2011, 2012, 2013, 2015, 2018, and 2019), while most of the highest monthly average prices in Braidwood are in the winter (e.g., 2014, 2015, and 2018). Considering the two years (2020 and 2021) during the COVID-19 pandemic, the electricity prices decrease in 2020 compared to 2019 (Figure 10) in all the locations considered in this report, which seems to be related to the unpredictable economic scope brought by the sudden burst of the pandemic. It shows a significant increase in electricity prices in 2021. A very high price is observed in February of 2021 in STP, Cooper, Braidwood, and Davis-Besse (Figure 9), which is probably associated with the extreme cold weather in the corresponding areas and high inflation rate during the pandemic.

Finally, it is worth noting that there are two electricity market configurations in the U.S.: regulated and deregulated. In a regulated electricity market, vertically integrated monopoly utilities are responsible for overseeing the complete value chain under the supervision of a public regulator. In such a market, consumers do not have the option to select their power providers and must rely on the utility company operating within their geographical area. Regulated markets are particularly prevalent in the Southeast, Northwest, and a significant portion of the West (except for California).

A deregulated electricity market operates with power plants and transmission lines owned by entities other than utility companies. This requires that companies generating electricity, known as generators, sell their output into a wholesale market, and retail energy suppliers purchase it for distribution to customers. In this context, transmission companies or utilities own and manage the transmission grid. Customers benefit from more competitive rates and generation options, including renewable energy. This market universe is managed by an ISO or regional transmission organization RTO [34]. However, not all ISO/RTOs operate in deregulated markets; in other parts of the United States, ISO/RTOs act only as grid operators based on fixed purchase and selling prices. Among the ISO/RTO considered in this report, PJM and ERCOT are deregulated markets, while Southwest Power Pool (SPP) and Midcontinent ISO (MISO) are regulated markets. Analysis reported here uses LMP data as a hypothetical case to illustrate the economic potential for hydrogen production in this report independent of the restrictions associated with the regulated market. The regulator would be required to approve the production of hydrogen using power with pricing other than the pricing at which power is sold to other customers.

The detailed data analysis using electricity prices for each location across the 7–11 years collected can be found in Appendix D, "Detailed Data Analysis for Electricity Prices for Each Location." Appendix D depicts, for each individual location, the daily, weekly, and monthly average prices, and a 365-day rolling mean. The team employs the multiple seasonal-trend decomposition (MSTL) algorithm, which is a fully automated, additive time series decomposition algorithm that can handle time series with multiple seasonal cycles to analyze the day-ahead LMP data obtained from 2011 to 2021. The team decomposes the data into trends, daily seasonal component, weekly seasonal component, monthly seasonal component, yearly seasonal component, and residuals. In Appendix D, the team presents the trend and yearly seasonality of each individual location.

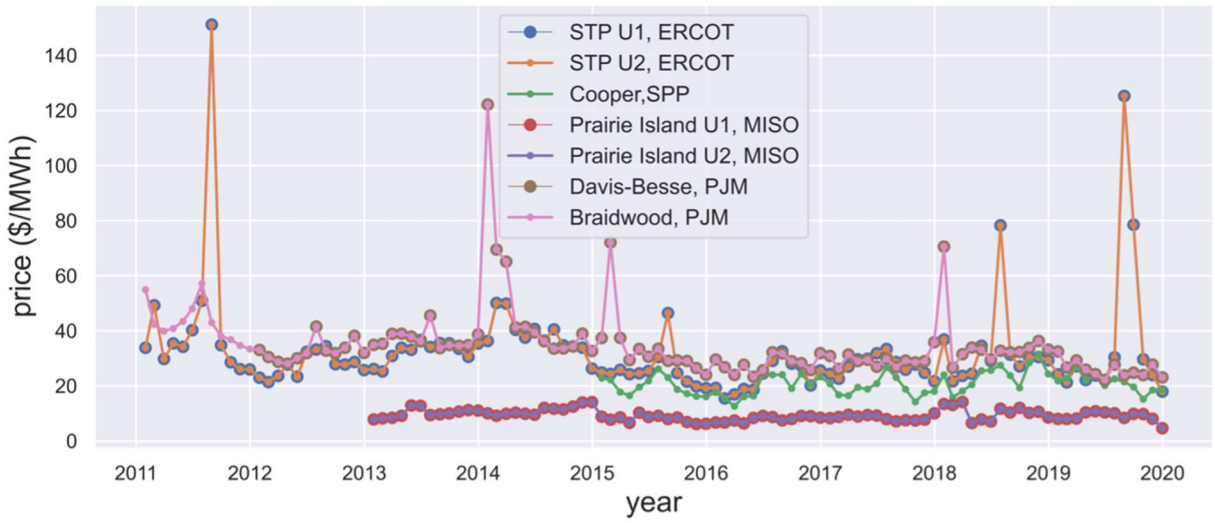

Figure 8. Monthly average day-ahead electricity prices in the years before the COVID-19 pandemic (2011–2019) for different locations. SPP stands for Southwest Power Pool. MISO stands for Midcontinent ISO. U1 and U2 stand for Unit 1 and Unit 2, respectively.

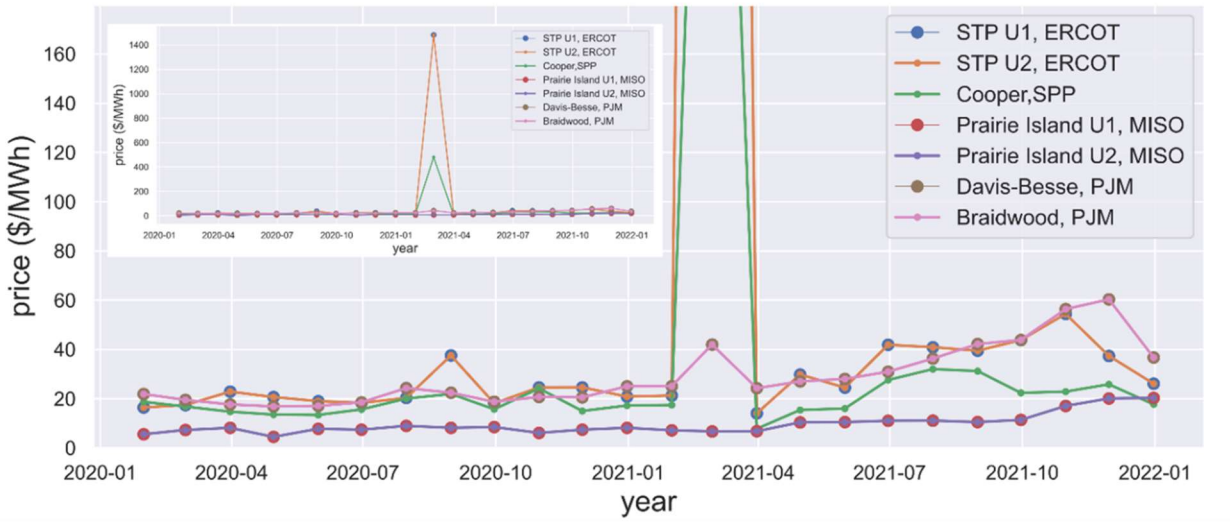

Figure 9. Monthly average day-ahead electricity prices in the years during the COVID-19 pandemic (2020–2021) for different locations. The embedded figure shows the peak value of electricity prices during the pandemic.

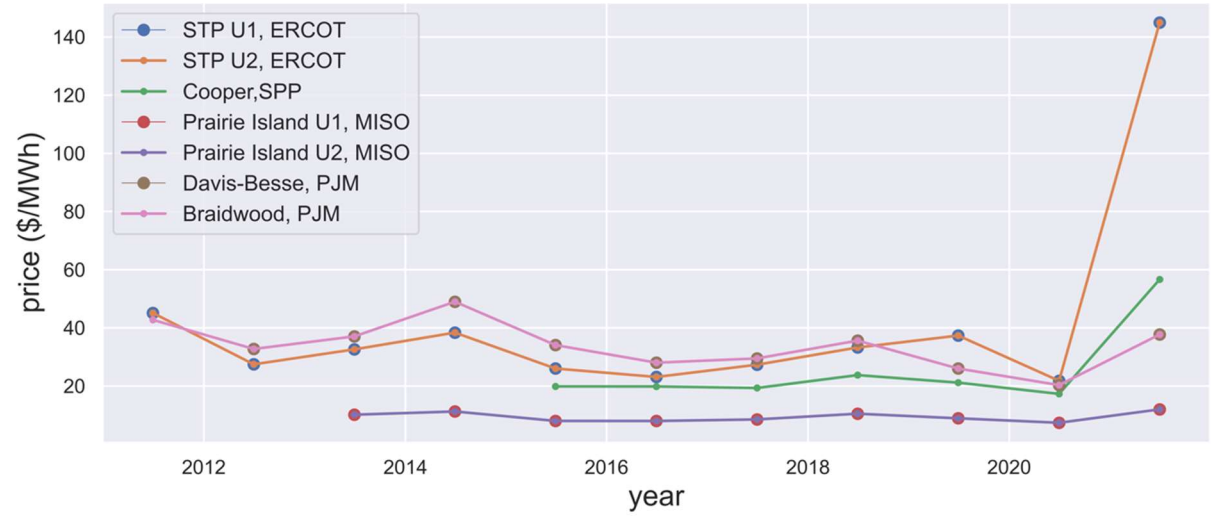

Figure 10. Yearly average day-ahead electricity prices from 2011 to 2021 for different locations.

Table 9. The average day-ahead electricity price over years for different locations in different markets.

Locations (NPP)	ISO/RTO	Years (hourly data)	Mean price ($/MWh)	Negative prices (%)
Braidwood (Unit 1)	PJM	2011–2021	33.86	0.0%
Davis-Besse	PJM	2012–2021	32.97	0.0%
Cooper	SPP	2015–2021	25.38	3.6%
Prairie Island (Unit 1)	MISO	2013–2021	9.37	36.9%
Prairie Island (Unit 2)	MISO	2013–2021	9.37	36.9%
South Texas Project (Unit 1)	ERCOT	2011–2021	41.53	0.1%
South Texas Project (Unit 2)	ERCOT	2011–2021	41.53	0.1%

4.2 CO_2 Feedstock Cost

CO_2 feedstock can be obtained from several different sources. The following sections identify potential industrial sources of CO_2 feedstock, describe the approach for estimating the capture and compression costs associated with each CO_2 source, and present CO_2 feedstock supply curves that present estimates of the cost of CO_2 from sources with varying flow rate and distance from the centralized synfuel production plant.

4.2.1 Upper Bound on CO_2 Demands of the Reactors.

The quantity of CO_2 feedstock required for synthetic fuel production depends on the capacity of the synfuel plant. Table 10 shows the maximum CO_2 demand for each NPP included in this analysis. Larger capacity synfuel plants would require CO_2 from more sources. As the number of different CO_2 emission sources needed to provide the demand of CO_2 feedstock increases, the average CO_2 transportation distance also increases.

Table 10. Upper bounds on CO_2 demand of the reactors.

Nuclear Power Plant	Power Generation (MW)	Upper Bound on CO_2 Demand (MT/year)
Braidwood	2,354 (from two units)	2,900,000
Prairie Island	1,041 (from two units)	1,300,000
Davis-Besse	894 (from one unit)	1,100,000
Cooper	769 (from one unit)	1,000,000
South Texas Project	1,280 (from one unit)	1,700,000
Palo Verde	1,311 (from one unit)	1,800,000

4.2.2 CO_2 Sources in the U.S.

The geographical distribution of CO_2 sources reported by the Environmental Protection Agency (EPA) is presented in Figure 11 and Table 11 [35].

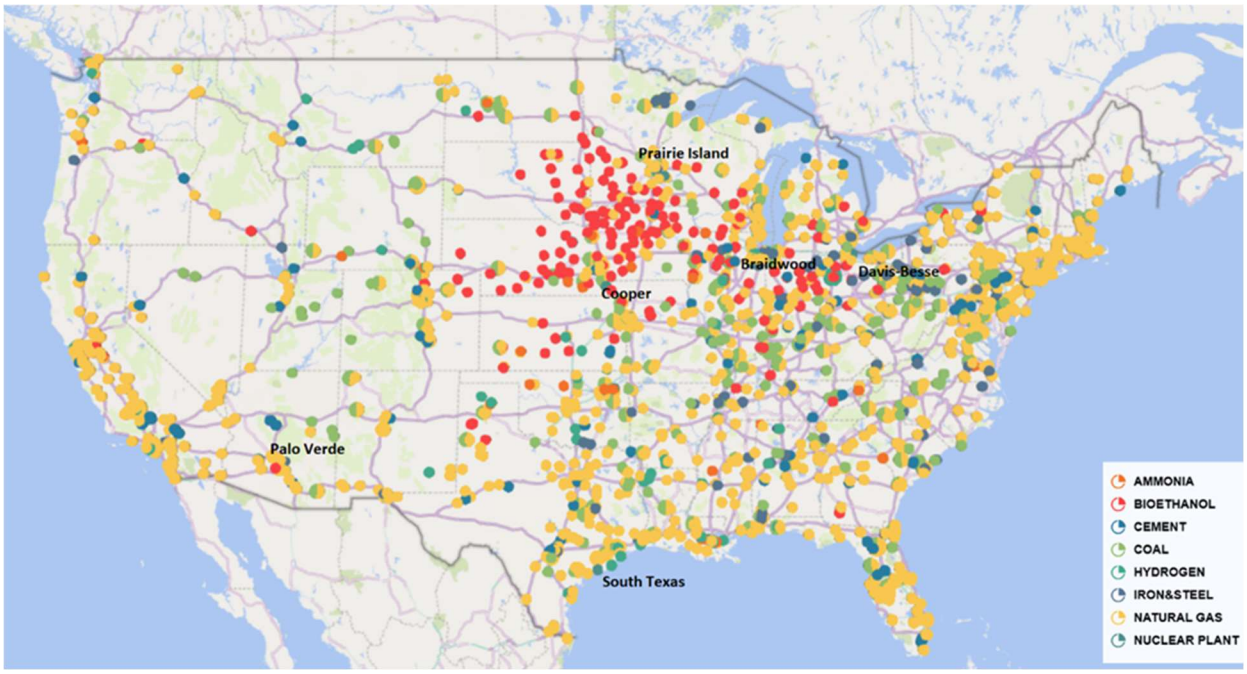

Figure 11. Geographical distribution of CO_2 sources and NPPs [35].

This analysis considered CO_2 from seven different carbon sources for synfuel production. A substantial number of bioethanol, ammonia, natural gas (power plant), coal (power plant), hydrogen, iron/steel, and cement plants operate in the areas adjacent to the five nuclear plants designated for this analysis. Availability, capture cost, and characteristics from the stream of CO_2 in each source are shown in Table 11. According to the CO_2 capture cost data, ammonia and bioethanol have a high concentration of CO_2. This condition means that the capture is less expensive compared to natural gas and coal from a power plant, where purity of CO_2 is low and more expensive to capture.

Table 11. CO_2 availability by source [36].

	U.S. CO_2 Emissions (MMT/year)	Concentration CO_2 (%vol)
Bioethanol	31	99.8%
Ammonia	35	97.1%
Natural Gas (Processing)	54	99%
Hydrogen	44	44.5%
Iron/Steel	72	23.2%-26.4%
Cement	67	22.4%
Total U.S. CO_2 Emissions (MMT/year)	303	—
Total FT Fuel (Mgal/year)	35,820	—

4.2.3 Sources of CO_2 and Capture Technology

The CO_2 capture and compression cost from each individual sector were estimated by following the procedure presented in DOE/NETL-2013/1602. Sources are separated into two groups depending on the purity of the CO_2 stream. The high-purity CO_2 sources from ethanol, ammonia, and natural gas (NG) processing do not require a CO_2 capture process to meet the CO_2 pipeline specifications. On the other hand, for lower purity streams, methyl diethanolamine-acid gas removal is required. Specific pathways for each individual source are shown in Figure 12.

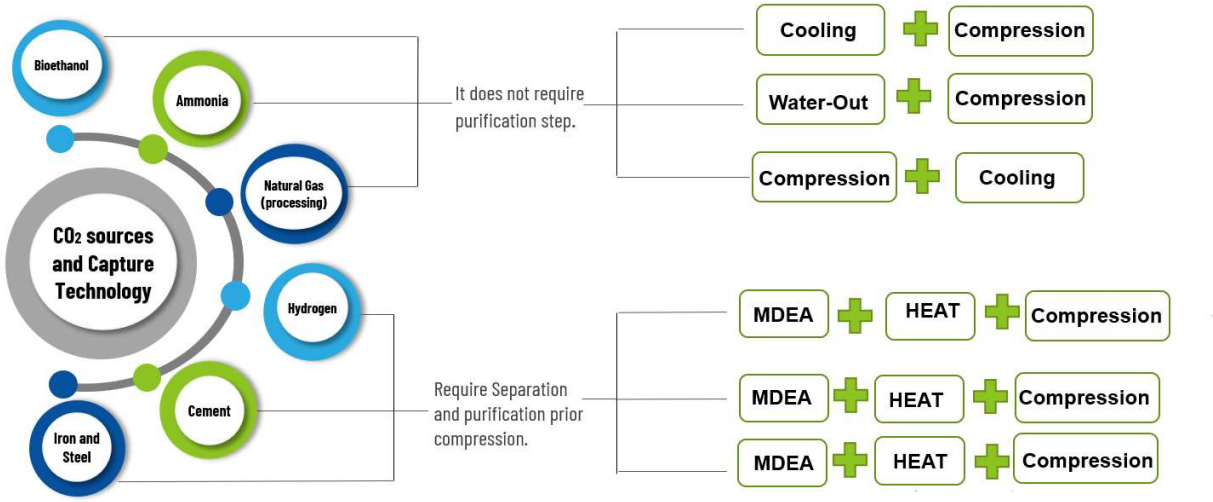

Figure 12. Sources of CO_2 and CO_2 capture and compression technology [37].

By selecting the specific technology for the different CO_2 sources, calculation of the compression cost as a function of the CO_2 flow rate is presented on Figure 13.

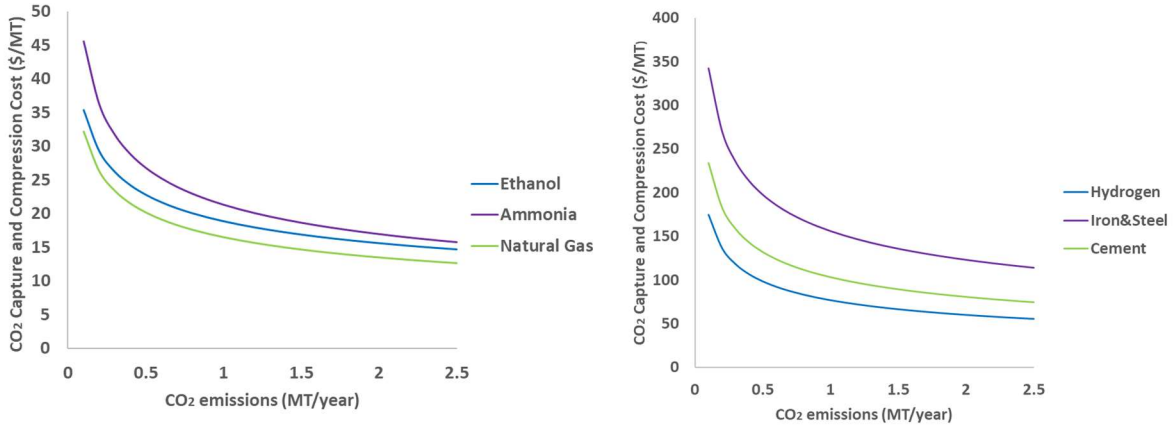

Figure 13. Capture and compression cost curve by sector [37].

4.2.4 Supply Curve by Region

CO_2 is transported from the distributed sources to the centralized synfuel plant via pipeline. A CO_2 supply chain analysis is performed using the steps presented in Figure 14. These steps include CO_2 capture and compression to liquefy the gaseous CO_2, storage in a temporary storage tank, and transport through pipelines to the conversion site at the nuclear plant.

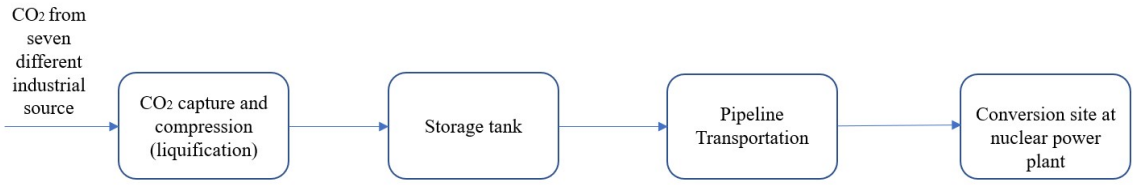

Figure 14. CO_2 supply chain.

The CO_2 feedstock supply curve was calculated by identifying the set of the closest CO_2 sources that have sufficient cumulative CO_2 production capacity to satisfy the upper bound of the CO_2 demand of the nuclear plant. Then, the National Energy Technology Laboratory (NETL) CO_2 Transport Cost model [5] was used to estimate the cost of CO_2 logistics for each plant.

The following inputs to the NETL CO_2 transport model were modified to calculate the transport costs for each pipeline segment between each ethanol biorefinery and the synfuel plant: (1) the length of the pipeline that was computed using the Open Source Routing Machine (OSRM) application programming interface (API); (2) the annual flow rate of CO_2 through the pipeline segment; (3) the region of the U.S. in which the pipeline is located, (4) the per unit electricity cost at which electricity could be purchased from the grid (i.e., $/MWhr) in the region in which the pipeline is located, and (5) CO_2 capture cost following values presented in Table 11. The NETL CO_2 Transport Cost model was then used to compute the optimal pipeline diameter and the number of booster pumps along the pipeline length that minimizes the cost of transporting CO_2 through each pipeline segment. The annualized CO_2 compression and transport costs for each pipeline segment were then used to construct the CO_2 feedstock supply curves. Finally, by sorting different plant locations in increasing order of their CO_2 logistics costs, the cumulative average logistics costs were computed using Equation (5).

$$Cumulative\ average\ logistics\ cost = \frac{\sum_{i \in N} c_i q_i}{\sum_{i \in N} q_i} \quad (5)$$

where

N = the set of ethanol plants considered in this computation indexed by i

c_i = the cost of CO2 logistics corresponding to the ethanol plant i

q_i = the amount of CO_2 transported from ethanol plant i to the NPP.

The aim of this analysis was to build supply curves that demonstrate the variation of CO_2 logistics costs with the quantity of CO_2 being transported. A summary of the results is presented in Figure 15. The difference in the results is associated with the combination of distances, CO_2 carbon capture cost by source, and the amount of the CO_2 transported.

The cost of transporting CO_2 is the lowest for the Braidwood nuclear generating station, whereas the cost is highest for transporting CO_2 to the South Texas nuclear power station. It is also observed that the CO_2 logistics cost decreases as the length of the pipeline becomes shorter and a larger amount of CO_2 is transported. The supply curves for the Prairie Island, Cooper, and Davis-Besse stations are similar as the neighboring CO_2 generation sources are at similar distances to these NPPs and the amounts of CO_2 transported are also similar.

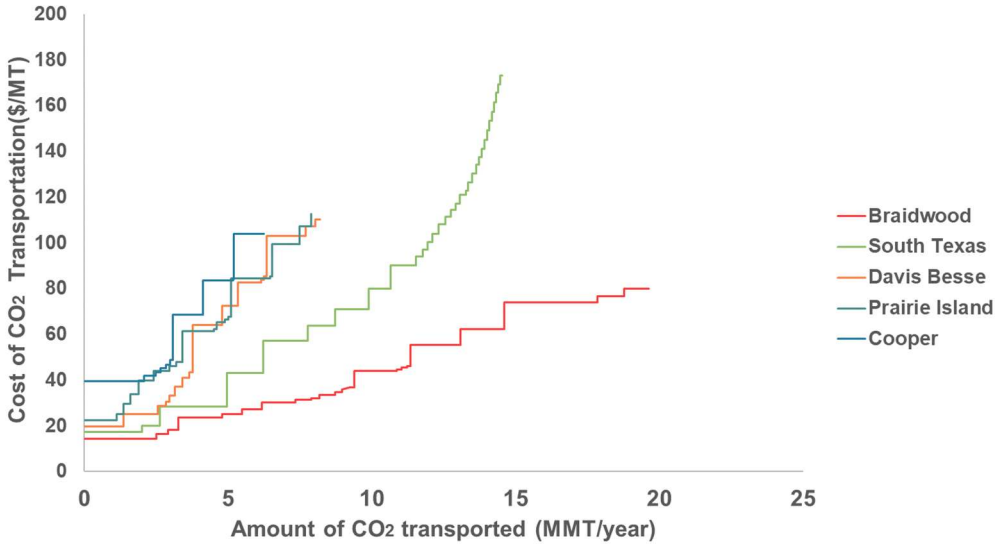

Figure 15. Supply curve for CO_2 transportation to all nuclear plant.

4.3 Fuel Price Forecasts

Each of the NPPs in the study were located in a region defined by the U.S. Census Bureau [22]. In some cases, multiple plants were in a single census region. Table 12 identifies the specific NPPs considered.

Table 12. NPP, region, and state table.

State	Illinois	Minnesota	Ohio	Texas	Nebraska	California
Region	East North Central–IL	West North Central–MN	East North Central–OH	West South Central	West North Central–NE	Pacific
Nuclear Plant	Braidwood	Prairie Island	Davis-Besse	South Texas Project	Cooper	N/A

Fuel price forecasts from EIA were adjusted by removing applicable federal and state fuel taxes. In addition, research was conducted to determine costs associated with marketing and distribution. Marketing and distribution costs were also subtracted from EIA price forecasts. These efforts were taken to reduce retail prices to levels equivalent to refinery gate prices. For illustration purposes, Figure 16 shows a graphical example of the cost factors that contribute to the retail price of jet fuel for the state of Illinois. A detailed table is available in Appendix C to show all the factors used as retail prices were adjusted down to gate or refinery prices.

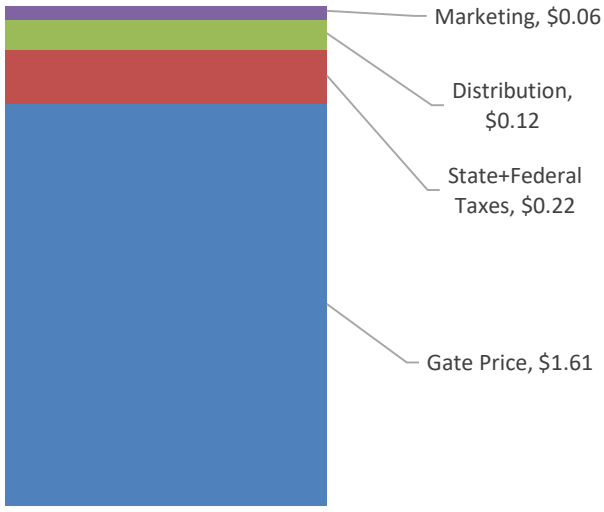

Figure 16. Jet fuel cost factors in Illinois (2022, $/gallon).

It was necessary to research each fuel type and each state's fuel tax to accurately remove applicable federal and state taxes, which are applied on a per gallon basis. Tax data used for this purpose was the most current data available at the time of the analysis, which was last updated in August 2022. A table is available in Appendix C displaying the amount of federal and state taxes per gallon that were removed. It should be noted that actual future tax policies could and most likely will impact the forecasted fuel prices. Prices used in the model for this report are based on current tax rates, which is the best available information at the time the analysis was completed. In addition, marketing and distribution costs were estimated using reports available from EIA. These EIA data reflect the average marketing and distribution costs in 2021 [38]. Retail petroleum prices from EIA also include transportation costs. Transportation costs were also removed based on specific transportation methods that would likely be used for each product and based on the geographic location of the NPP. Figure 17 illustrates how these price adjustments compare to EIA retail prices for the West South Central region. Additional figures for each region can be found in Appendix C.

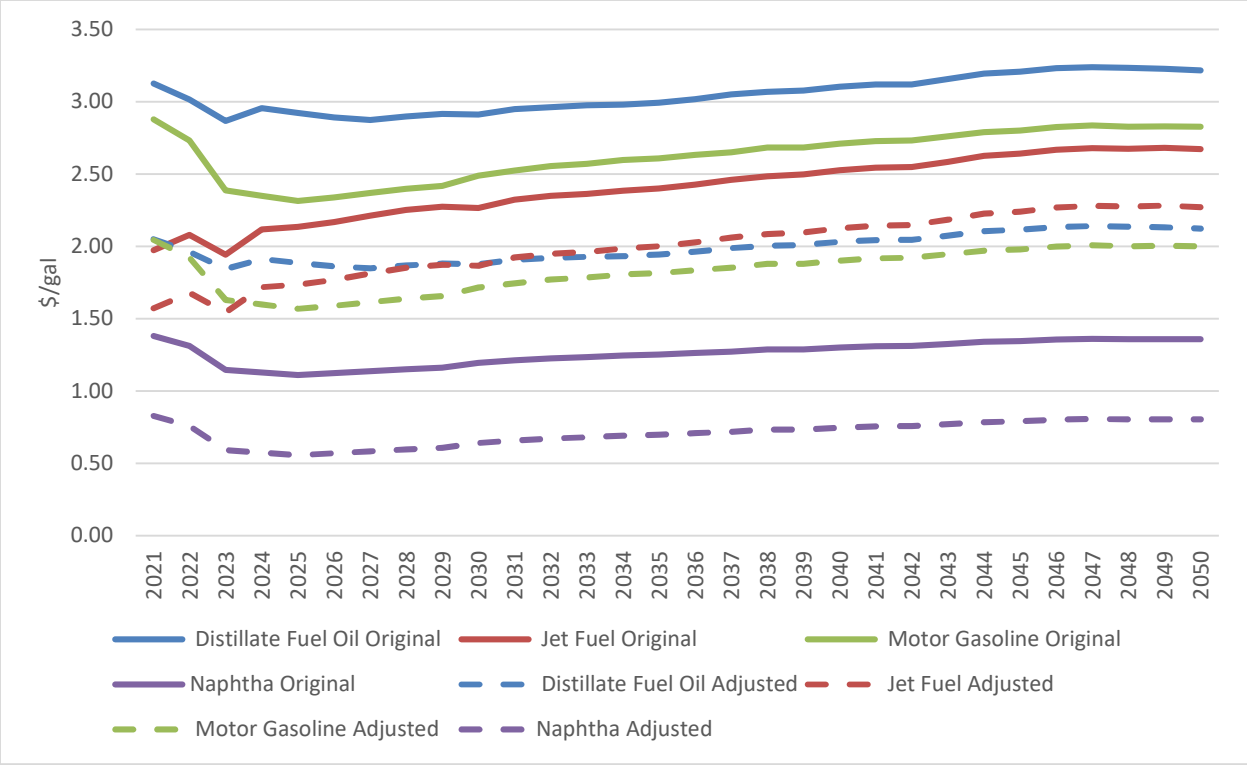

Figure 17. Original vs. adjusted fuel price forecasts for West South Central region. Adjusted prices have federal and state taxes, transportation, and marketing expense removed.

Price forecasts from EIA were not available for naphtha, but historical prices were available from other sources [39]. A process was implemented to create forecasts and include adjustments to reflect regional price variations. Naphtha and gasoline prices were highly correlated when comparing historical prices. As a result, EIA regional price forecasts for gasoline were used to provide directional changes in naphtha across the five regions in this study. Naphtha retail prices were adjusted down to refinery prices using the same approach described previously.

Prices reflected in Table 13 are the average adjusted price per gallon between 2022 and 2050 for each product and for each of the five states and four regions studied in this report. As mentioned previously, prices were adjusted by removing taxes, transportation, and marketing expenses and are based on 2022 EIA Annual Energy Outlook forecasts.

Table 13. Adjusted fuel prices.

Product	$/Gal (2022)	$/Gal (2050)	Avg. $/Gal (2022-2050)
Naphtha	$0.95	$1.06	$0.94
Diesel	$1.81	$2.04	$1.89
Gasoline	$1.93	$2.11	$1.91
Jet Fuel	$1.63	$2.17	$1.91

Oil and gas supplies will impact fuel prices over time. According to EIA projections, prices could increase by 12% under low oil and gas supply scenarios. High oil and gas supply scenarios could cause fuel prices to fall by more than 10%. Figure 18 depicts how these price variations are expected to occur

between 2021 and 2050. To provide sensitivity to the model used in this report, factors were applied to reference case prices to help account for potential changes in oil and gas supplies.

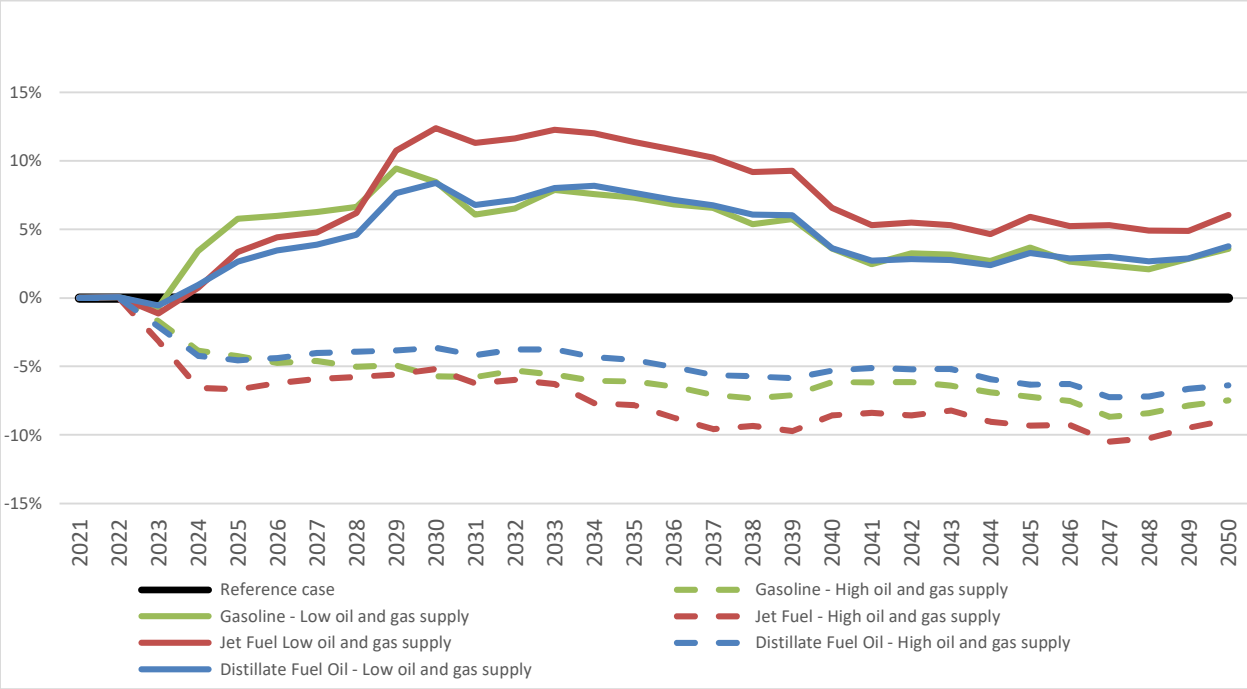

Figure 18. Oil and gas supply impact on fuel prices (EIA forecasted % difference from Reference Case).

Once regional prices were adjusted, it was possible to compare refinery prices across regions. Jet fuel prices were similar across all regions analyzed. It was also evident that EIA reference case forecasts were predicting a decrease in prices for many, but not all, regions between 2022 and 2036. In all cases, prices are expected to increase above 2022 levels by 2050. The Pacific region is expected to have the highest price for all fuel products by 2050 except for jet fuel, which is forecasted to be $0.02 more expensive in the West South Central region. In the near term, no region had consistently higher or lower prices compared to other regions.

Figure 19 provides an example of how distillate fuel oil prices are expected to fluctuate over time and across regions. Similar figures for other fuels are available in Appendix C.

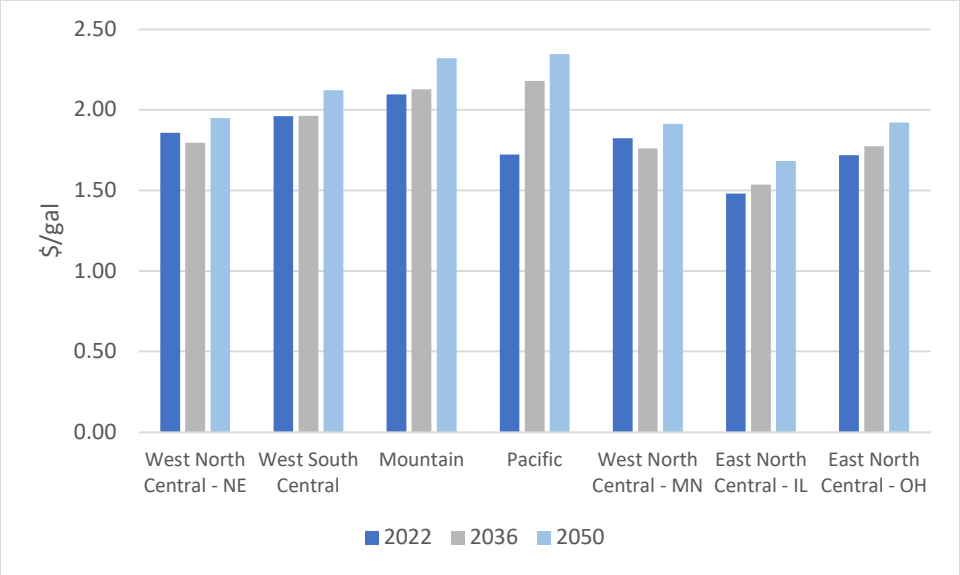

Figure 19. Adjusted distillate fuel oil prices.

5. STOCHASTIC TECHNO-ECONOMIC ANALYSIS VIA HERON

The Risk Analysis Virtual ENvironment (RAVEN) framework [40] and its dispatch optimization plugin HERON offer the capabilities necessary to evaluate the economic profitability of the synfuel IES at selected U.S. locations. The team first presents the economic metric used for this assessment, then details the modeling of the synfuel production process and the stochastic optimization in HERON.

5.1 Net Present Value Comparison

The net present value (NPV) can be computed to assess the economic profitability. The NPV corresponds to the difference between the net cash inflows and outflows over the project lifetime. For a synfuel IES, the cash inflows are the revenues from selling electricity to the grid or from selling synfuel products for the transportation sector. The outflows correspond to the CAPEX and O&M costs of the system components. The aim of the present analysis is to compare the economic benefit of using an NPP to make different products. The differential NPV is, therefore, the relevant metric that is computed to determine which uses of the nuclear plant output would be most profitable. This approach eliminates the need for data regarding the costs of the NPP and the corresponding uncertainty, as shown in Equation (6).

$$\Delta NPV = NPV\ (\text{Synfuel IES}) - NPV(B\text{AU}) \tag{6}$$

Equation (6) calculates the NPV of the studied system compared to a baseline: the business-as-usual (BAU) case, which corresponds to the current use of NPPs (all the power being produced is sold to the grid). Load-following NPP operating strategies (i.e., operation of the NPP below its rated capacity) are not considered in this analysis; therefore, cashflows, such as the O&M costs of the NPPs or credits that the NPP may benefit from by producing decarbonized power, are not included since they would later cancel out.

5.2 Synfuel Process HERON Model

Figure 20 shows the energy and material flows in the synfuel production IES, as modeled in HERON. The diagram shows the HTSE, H2 storage, and FT process technologies used as optimizing components in the present analysis. The primary source of energy is the NPP, which produces electricity for the grid and electricity and heat for the synfuel production process. The synfuel production process starts with a

HTSE plant producing hydrogen in a flexible manner (see Section 3.2). This hydrogen is either sent to a storage facility or a FT process (see Section 3.1). The FT process operates at steady-state with constant feedstock inflow and product outflow rates; the hydrogen storage facility is included to ensure this constraint is met when hydrogen production from the HTSE decreases. The FT takes in CO_2 as an inflow from surrounding sources. Three kinds of synthetic transportation fuels are produced: naphtha, jet fuel, and diesel. Section 4.3 presents the analysis performed to determine the regional prices for those products. The synfuel IES is modeled for different geographical locations corresponding to various NPPs in different electricity markets throughout the country. Table 14 presents the cases selected for the present analysis, and Table 15 shows the financial assumptions made for the HERON model and their rationale.

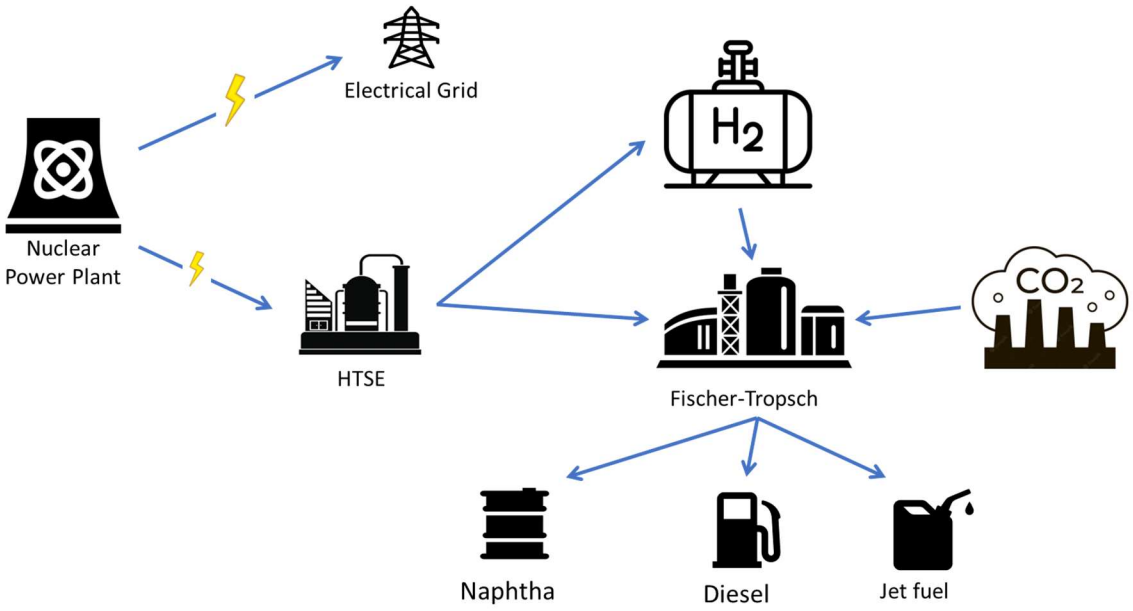

Figure 20. Grid-integrated nuclear synfuel production process, referred to as synfuel IES.

Table 14. Synfuel cases description.

NPP	Reactor Type	Capacity	Electricity Market	State	Synfuel Region
Braidwood (Unit 1)	PWR	3645 MWth 1194 MWe	PJM	Illinois	East North Central–IL
Davis-Besse	PWR	2817 MWth 894 MWe	PJM	Ohio	East North Central–OH
South Texas Project (Unit 1)	PWR	3853 MWth 1280 MWe	ERCOT	Texas	West South Central
Prairie Island (Unit 1)	PWR	1677 MWth 522 MWe	MISO	Minnesota	West North Central–MN
Cooper Nuclear Station	BWR	2419 MWth 769 MWe	SPP	Nebraska	West North Central–NE

Table 15. Financial assumptions.

Parameter	Value	Description
Project life	20 years	Representative of NRC operating license extension for existing NPPs

Parameter	Value	Description
Weighted average cost of capital (WACC)	10%	Cost of capital, minimum return to be earned on assets to satisfy investors
Inflation rate	2.18%	Average for 2000–2021
Federal corporate tax rate	21%	—
State corporate tax rate	—	Value depends on location of NPP
Depreciation schedule	15 years MACRS	—
Synthetic fuel price	—	Regional, see Section 4.3

To compute the Δ(NPV) econometric presented in the previous section, the team models the BAU case (depicted in Figure 21). The BAU case corresponds to the current use of NPPs. They only produce electricity, and their role in the electrical grid is the one of baseload power supplier. The team assumes that no load-following occurs: these NPPs operate in steady-state mode at their design capacity as price takers—they will sell their production as the day-ahead market rate whether this rate is higher or lower than their O&M costs. With the increasing penetration of renewable power generation technologies into the grid, the electricity price is more variable and frequently decreases to levels that are under many NPPs O&M costs. Since the costs of shutting down and restarting the plant are higher than the financial losses incurred during those periods NPPs continue to produce power during those periods of times, but at a net loss.

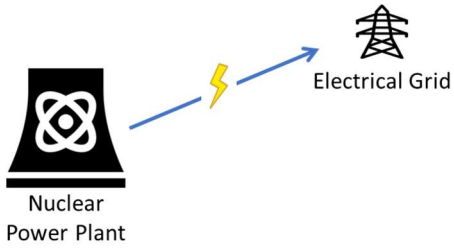

Figure 21. Baseline case representing the current use of NPPs, referred to as the BAU case.

Each case study location has a different NPP capacity, electricity price distribution, CO2 feedstock costs, and synfuels prices. Thus, HERON is used to optimize the system's components capacities to maximize NPV of the system over its lifetime. This multi-stage optimization process is presented in the following section.

5.3 HERON stochastic power system optimization

Figure 22 shows the HERON stochastic power system optimization process, which will determine the optimal configuration for an IES to maximize its NPV. The optimization of the synfuel IES corresponds to finding the optimal set of capacities for the HTSE, the H_2 storage, and the FT process. Once a point, which consists of one capacity value for the components previously mentioned, is selected for the outer loop, the system with fixed component capacities is analyzed in the inner loop. The inner loop corresponds to solving the optimal dispatch problem over the project lifetime. The inner loop is solved multiple times to account for the stochasticity of the electricity prices—more details are given in the following section. At the end of the inner loop runs, the average NPV and its standard deviation are computed and sent back to the outer loop.

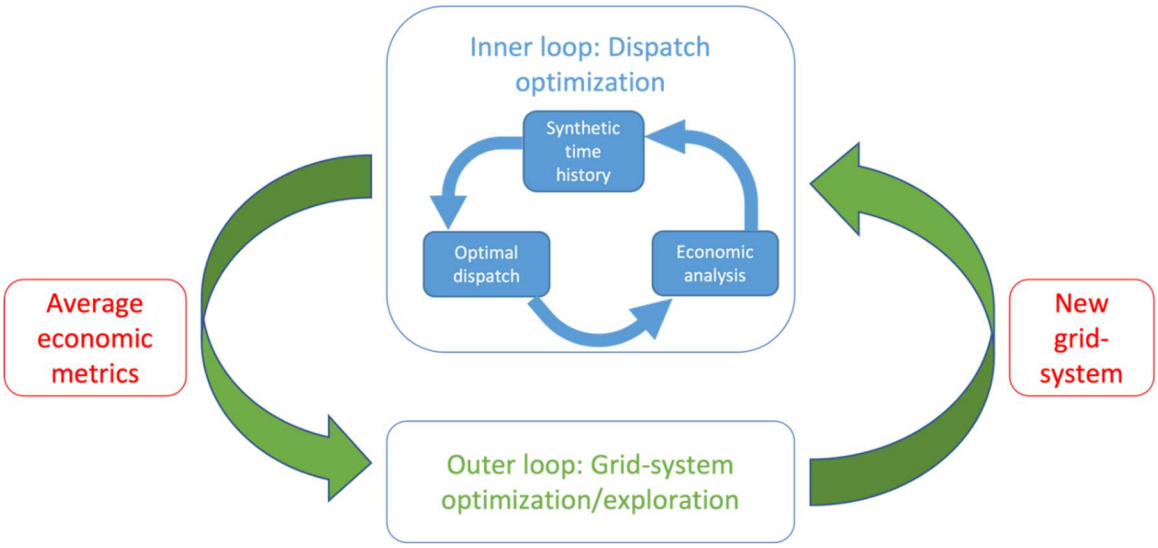

Figure 22. HERON stochastic power system optimization.

The NPV is the objective function for the outer loop. The outer loop can either be an optimization or an exploration loop. The optimization outer loop runs until convergence is achieved. For the exploration outer loop, predetermined component capacities are provided by the user for evaluation. The current analysis employs the exploration mode since the configuration presenting the maximum NPV may not be the optimal one because of uncertainties.

Figure 23 shows the results of such an exploration HERON run for the Davis-Besse location; the four configurations with the maximum NPV are shown. The top graph shows the ΔNPV for each case and the table shows the corresponding component capacities. While Case #0 may present the maximum NPV, the preferred configuration for this location is Case #2. The NPV is marginally lower for Case #2 but within Case #0's confidence interval. No hydrogen storage is required for Case #2, which reduces investment risks. Case #3 presents a lower added profitability: The synfuel production process is smaller compared to the size of the NPP; therefore, while the revenues from selling electricity to the grid increase, they do not make up for the loss from a reduced production of hydrogen and synfuels and the consequent reduction in PTC and synfuel product sales. Results of exploration runs for each location are presented in Appendix G.

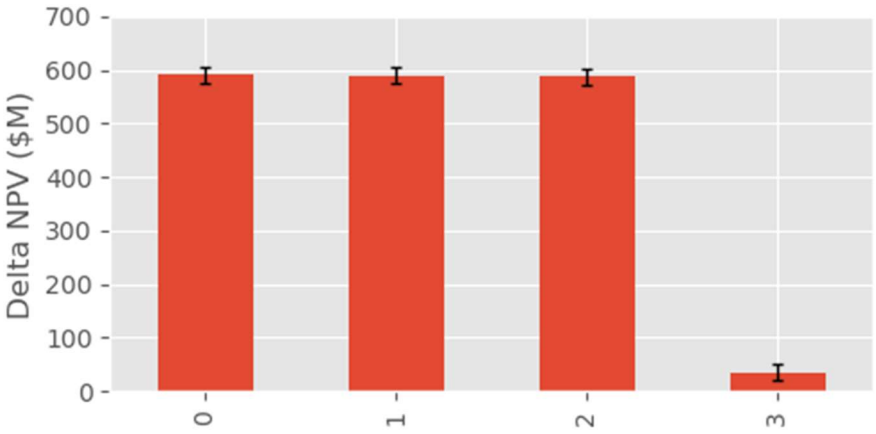

	0	1	2	3
NPP (MW)	894.0	894.0	894.0	894.0
HTSE (MW)	-879.0	-879.0	-879.0	-450.0
FT (ton-H2/h)	-22.1	-22.1	-22.1	-10.0
H2 Sto. (ton-H2)	90.0	45.0	0.0	90.0
Delta NPV ($M)	591.6	590.0	588.1	35.1
2STD Delta NPV ($M)	15.0	15.0	15.0	15.0

Figure 23. Exploration results via HERON, Davis-Besse location.

In the following section, the generation of a synthetic time series via an auto-regressive moving average (ARMA) model is detailed. Synthetic time series are used to consider the variability of electricity prices in an energy system optimization via HERON.

5.4 Stochastic Time Series

HERON enables the introduction of stochasticity in the capacity and dispatch optimization for a techno-economic analysis. Unpredictable weather and load conditions drive optimal resource utilization in any grid-energy system, thus a stochastic approach to optimizing resource utilization will result in a more robust approach. Through the ARMA methodology available in RAVEN, synthetic time series are generated to represent these stochastic signals and to use them in the HERON capacity and dispatch optimizations. The following sections detail the generation of a synthetic time series via an ARMA model for the Braidwood NPP in Illinois (PJM) and its validation.

5.4.1 Historical Electricity Pricing Data at the Braidwood Nuclear Power Plant

Figure 24 shows the historical electricity prices at the Braidwood NPP in the PJM market. From top to bottom, 10 years (2011–2021), 2 years (2015–2016), and 3 months (March–May 2016) are presented. On the top graph, outliers are present at the start of the year 2014. However, a pattern of high summer prices can be observed year after year. Examining the years 2015 and 2016 confirms that prices during the summer months—July to September—are higher than during the spring months—April and May. On the third graph, a weekly pattern of high prices during the first days of the week is visible during March 2016. There is a daily pattern that is confirmed on the last graph representing the first two weeks of March 2016: Prices are higher during daylight hours.

Through a Fourier series decomposition and an ARMA model, these periodic patterns in the electricity pricing historical data, along with the statistical randomness, can be captured. The following section presents the underlying mathematical principles of the ARMA and its capabilities.

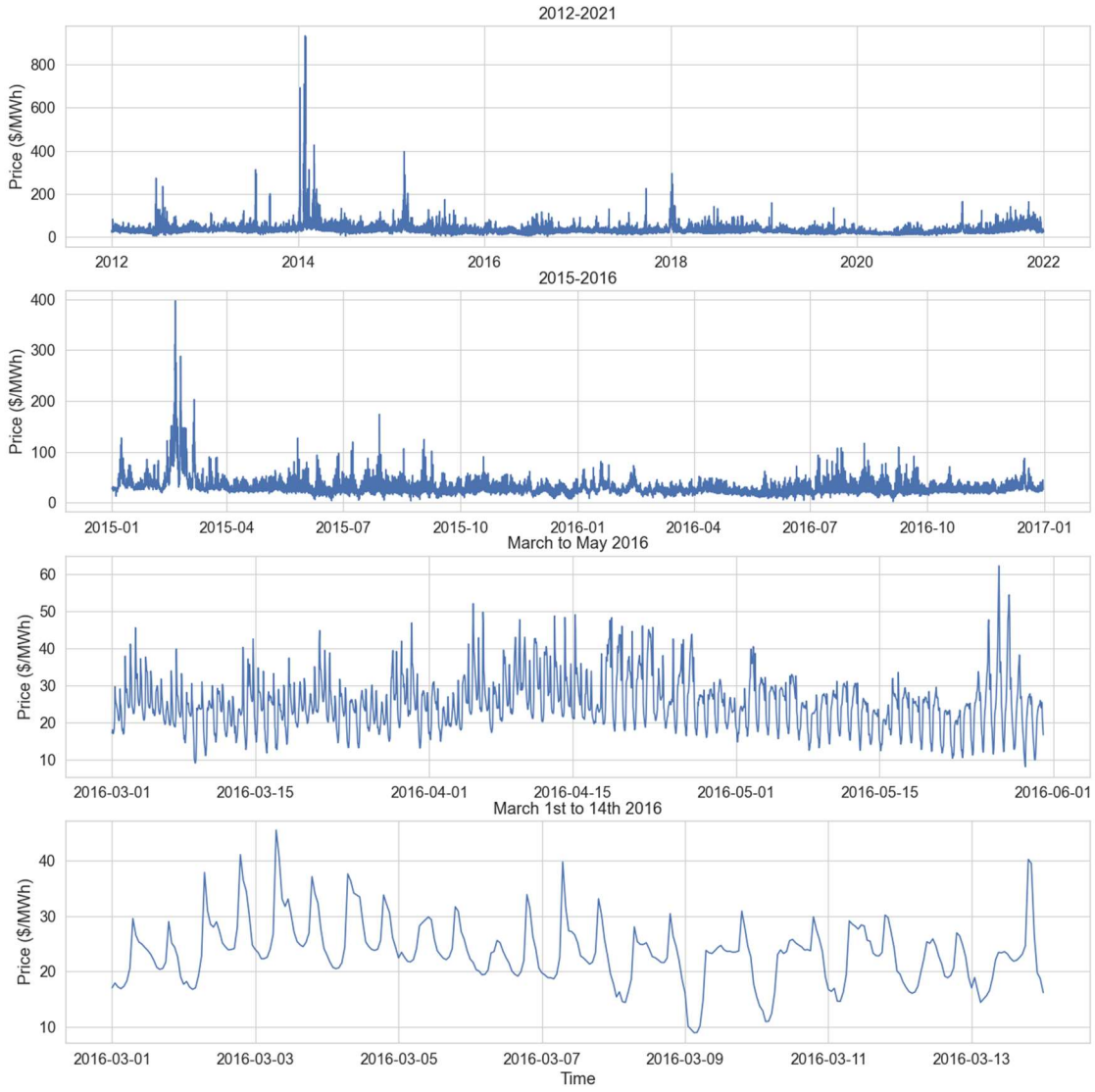

Figure 24. Historical electricity pricing data at the Braidwood NPP location in 10-year, 2-year, and 3-month timeframes.

5.4.2 Fourier Analysis and ARMA Model

Electricity prices present periodic patterns that can be described and reproduced via a Fourier series decomposition. These patterns can occur every year, season, month, or other time interval. To capture them, Fourier modes, as defined by Equation (7), are identified and subsequently removed from the price signal:

$$F = \sum_c \sum_{i=0}^{k} a_i sin\left(\frac{2\pi\ i}{c} t\right) + b_i cos\left(\frac{2\pi\ i}{c} t\right) \quad (7)$$

where $c\ is$ the set of characteristic time periods for which the original signal presents a cyclical pattern, f_i is the frequencies subdividing the characteristic time lengths, and a_i and b_i are computed to fit F to the original signal.

Once the pricing data has been detrended through Fourier analysis, the remaining noise is standardized to a standard normal distribution. This residual normalized signal is then captured via the ARMA model (Equation [8]):

$$y_t = \sum_i^P \phi_i y_{t-i} + \epsilon_t + \sum_j^Q \theta_j \epsilon_{t-j} \quad (8)$$

The first term is the auto-regressive term, where P is the maximum number of auto-regressive terms. The second term is the moving average term, where Q is the maximum number of moving average terms. ϵ is Gaussian noise; ϕ and θ are fitted to maximize likelihood.

This section provides a brief description of the mathematical foundations of the Fourier and ARMA signal processing methods; the reader is encouraged to refer to Talbot 2020 [41] for more details. The Fourier and ARMA models have been shown to produce independent, identically distributed sample time series presenting the same statistical properties as the original data. The synthetic time series obtained are used to reproduce the variability of historical electricity pricing data. The time series is then applied for future years, as predicting future electricity prices is outside the scope of this analysis.

5.4.3 Synthetic Time History Validation

Historical electricity prices have been collected for each location (see Section 4.1). Figure 25 shows the statistical distribution of these datasets for each location via a violin plot, which indicates the probability density of the data at different prices as well as potential outliers. Across all the locations, most of the prices are concentrated around their mean value. However, for the STP and the Prairie Island NPPs, the datasets include outliers. These periods of very high prices are captured by the ARMA model and may have a significant influence on the economics of the synfuel IES at these locations since high electricity prices will prompt the optimization to favor selling electricity to the grid over producing synfuel.

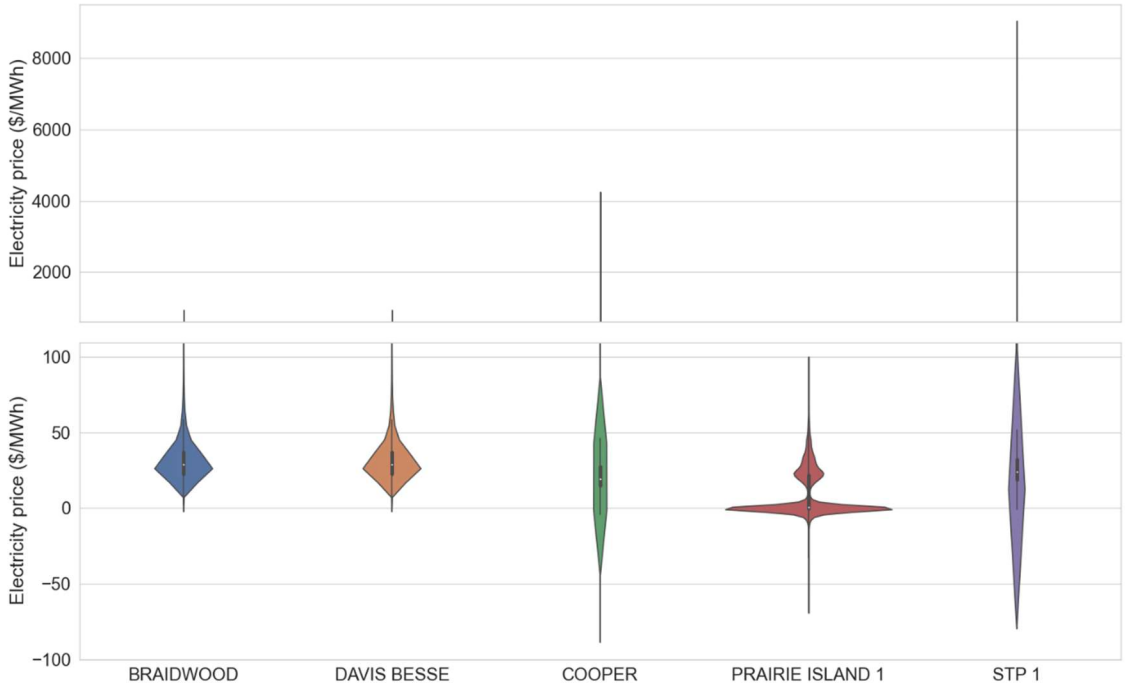

Figure 25. Electricity pricing data statistical comparison. Note that the y-axis scale is not continuous.

The Fourier detrending and ARMA modeling are applied to these historical datasets, selecting the following Fourier periods (corresponding to c in the Fourier series decomposition equation):

- 8760 hours: year
- 4380 hours: half year
- 1095 hours: 1 and a half months
- 168 hours: 1 week
- 24 hours: 1 day
- 12 hours: half a day.

To validate the quality of the Fourier periods selection and the ARMA training, the team compares the statistical distribution of the historical prices and the distribution of synthetic prices generated for the same years via the trained ARMA model. The results of this comparison for the STP NPP are provided in Figure 26. This case was selected as it presents the highest frequency of outliers as can be noted on Figure 25, which shows the distribution of electricity price data for each NPP location. The validation plots and tables for the other cases are available in Appendix B. The distribution of the synthetic and historical data matches almost perfectly. The team uses violin plots to represent the electricity pricing data, as they enable the comparison of statistical distribution by combining a box plot and a rotated kernel density. These plots indicate that the data points are mostly distributed around the mean price.

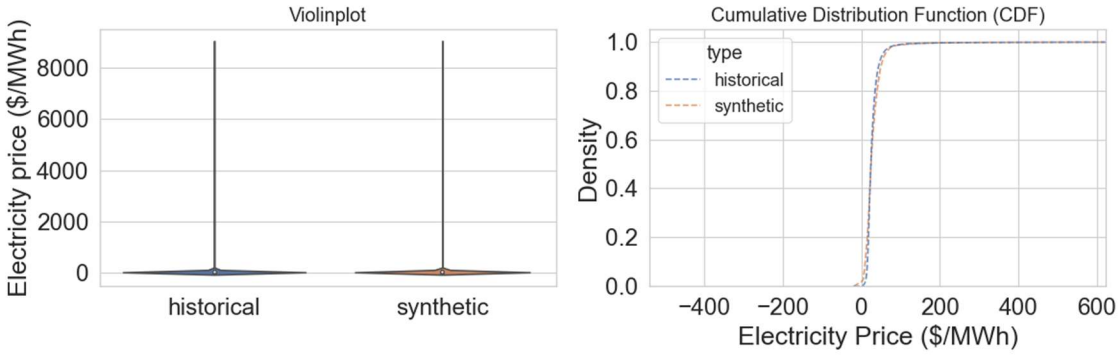

Figure 26. Comparison of synthetic and historical electricity pricing data at STP case study location.

In Table 16, the statistical moments of the synthetic data and the historical data distribution are compared. The skewness is a measure of the asymmetry of the distribution about its mean while the kurtosis is a measure of the tailedness of the distribution. The skewness and the kurtosis are very close, which indicates that the synthetic data generated via our ARMA model contains the outliers observed in the initial historical data. The ARMA model trained in this manner fulfills its role of reproducing the historical variability of electricity prices.

Table 16. STP, comparison of statistical moments.

	Historical price ($/MWh)	Synthetic price ($/MWh)
Mean	41.2	41.6
STD	290.7	290.5
Min	-20.2	-20.2
25%	18.9	16.8
50%	23.9	24.4
75%	32.0	36.4
Max	8996.8	8996.8
Kurtosis	699.6	696.9
Skewness	25.8	25.7

6. RESULTS AND DISCUSSION

6.1 The Competitiveness of the Synfuel IES Across the U.S.

The aim of the analysis is to assess the relative economic competitiveness of a nuclear-based synfuel production IES compared to the historical use of NPPs at locations across the United States. In a preliminary analysis, the synfuel IES was found to be more profitable for the Braidwood location [7] relative to electricity-only production. The analysis further investigates whether similar increased profitability could be observed in other locations and could potentially be improved by optimizing the system component capacities and operating strategy.

This section presents results of the system-level HERON optimization—the optimal component designs and the resulting additional economic value for each location. Then, the team presents the dispatch-level optimization results to illustrate how the IES responds to the variations in electricity prices on an hourly basis.

6.1.1 Synfuel IES optimal configuration

Figure 27 indicates the additional economic value of a synfuel IES compared to the existing use of NPPs at each location included in this analysis. The differential NPV is positive and ranges from $14M–$1.3bn USD (2020). With 10% rate of return on investment built into the HERON modeling, the synfuel IES revenues would enable the full repayment of investments over the lifetime of the project (20 years) and generate this added revenue for each location compared to the BAU case.

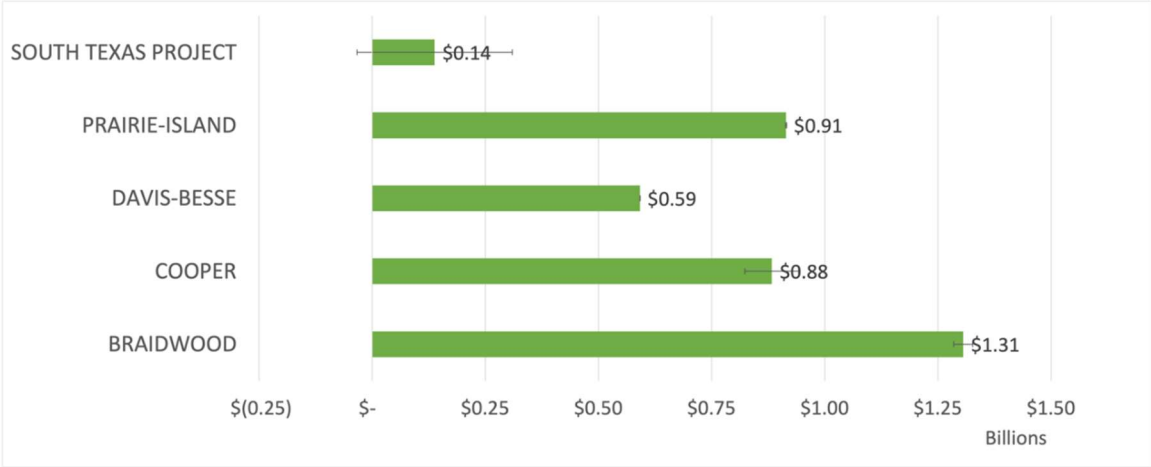

Figure 27. ΔNPV at each location.

Table 17 presents the capacities of the synfuel IES components at each location. These optimal configurations were selected using HERON in exploration mode as detailed in Section 5.3. The optimal configuration for each location consists in maximizing the capacity of the HTSE (about 15 MWe is reserved for a steady electric supply to the FT process) and of the FT process. This result aligns with expectations that the hydrogen PTC adds value to the HTSE and FT production. Namely, the PTC provides an added revenue $3/kg of hydrogen when it is produced via nuclear energy and used to produce synfuel in the FT process.

Table 17. Optimal configurations for the synfuel IES at each location.

	Component Capacities				
Location	NPP (Mwe)	HTSE (Mwe)	HTSE (ton-H2/h)	FT (ton-H2/h)	H2 storage (ton-H2/h)
Braidwood	1193	-1178	29.6	29.6	0
Cooper	769	-754	18.9	18.9	0
Davis-Besse	894	-879	22.1	22.1	0
Prairie-Island	522	-507	12.7	12.7	35
STP	1280	-1265	31.8	31.8	2,000

Figure 28 and Figure 29 show the breakdown of the cashflows for NPV of the synfuel IES at the South Texas Project and the Braidwood locations. The NPPs at these locations are similar in size: 1193 MWe and 1280 MWe. However, the profitability of the synfuel IES are drastically different, $14M with a wide confidence interval and $1.3bn, respectively. At both locations, the main source of revenue is the IRA clean hydrogen PTC which amounts to approximately $5bn. This PTC is critical to ensure the economic profitability of a synfuel production IES and the consequent production of decarbonized synfuel for the aviation and heavy transportation sector. The synfuel product sales result in $1.3bn to $1.7bn of revenues. For the South Texas Project location, the electricity prices are high enough to justify the construction of a large hydrogen storage facility equivalent to 2.5 days' worth of the FT hydrogen consumption. High electricity prices often indicate a mismatch between demand and supply (e.g., demand being higher than the online available capacities). As the NPP in the synfuel IES sells more electricity in high-load scenarios, the NPP still continues to provide grid stabilization while gaining more revenue from synfuel sales. The operational flexibility added via the hydrogen storage facility enables $235M revenue from electricity sales, but its CAPEX costs amount to $300M. The main difference in cost and the reason

the Braidwood location is much more profitable is the cost of the CO_2 feedstock transportation. As seen in Section 4.2, the CO_2 is transported via pipelines from concentrated sources to the NPP site. The further those sources are from the NPP, the more the shipping cost increases. Figure 15 shows the higher costs of this feedstock for the South Texas Project location as compared to the Braidwood location. Cashflow breakdowns for the Cooper, Davis-Besse, and Prairie Island locations are available in Appendix A, Figure A-1, Figure A-2, and Figure A-3, respectively.

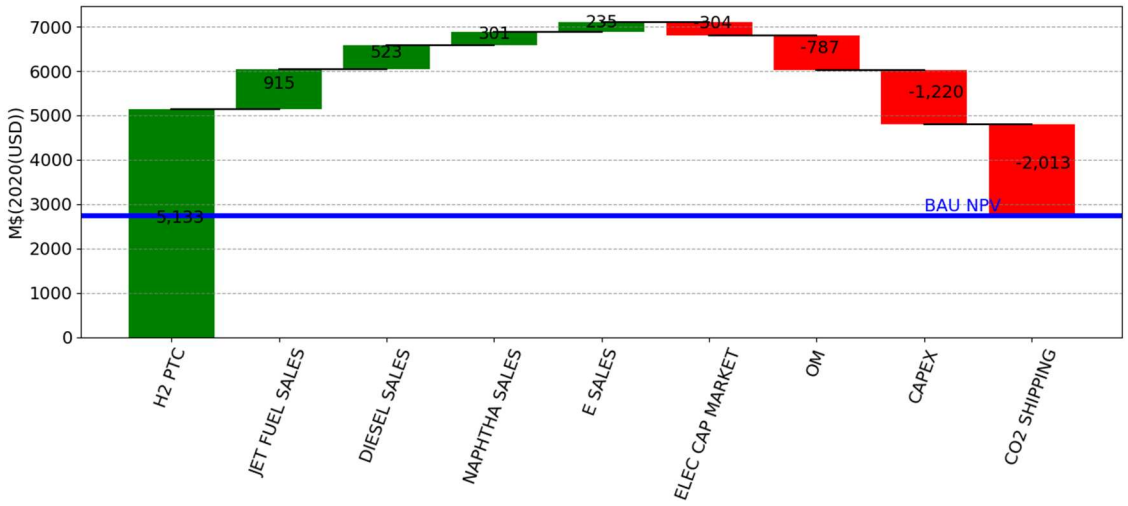

Figure 28. Lifetime cashflow breakdown, South Texas Project location.

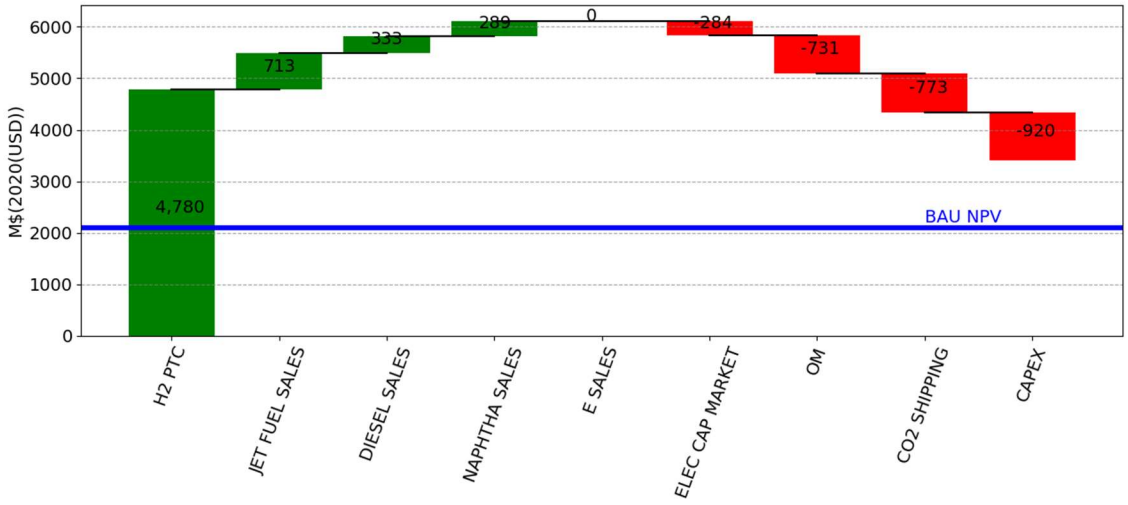

Figure 29. Lifetime cashflow breakdown, Braidwood location.

6.1.2 Dispatch Optimization

Figure 30 shows the results of one dispatch optimization via HERON for 24 hours at the Braidwood location. From top to bottom, the variations of the electricity price, the consumption and production of electricity, the consumption and production of hydrogen, and the production of synfuels are presented. Hourly electricity prices vary from $15/MWh to more than $100/MWh.

When the electricity price is lower than $100/MWh, the IES produces synfuels by sending almost the entire electricity output from the NPP to the HTSE, which then produces hydrogen for the steady-state FT process. However, between hours 14 and 16, the electricity price peaks at about $110/MWh. The synfuel IES then reduces the consumption of electricity by the HTSE to send more electricity to the grid that can be sold for a higher price. To ensure a constant flow of hydrogen to the steady-state FT process, hydrogen from the hydrogen storage is used, as shown by the decrease in the hydrogen storage level. After hour 16, the electricity price has decreased, and the synfuel IES resumes its previous type of operation. The HTSE consumption of electricity and production of hydrogen increase again, and the grid consumption decreases.

This behavior is consistent with our expectations and the maximization of the HTSE capacity seen in Section 6.1.1. Hydrogen storage facilities have high CAPEX costs. Thus, their capacities should be minimized. Producing hydrogen and synfuel products brings more revenue due to the hydrogen PTC and the higher value of synfuel products compared to electricity; therefore, to enhance profitability, their production is maximized except for periods of very high electricity prices. The optimal dispatch of the synfuel IES components still enables the NPP to support the grid in times of high load and high prices.

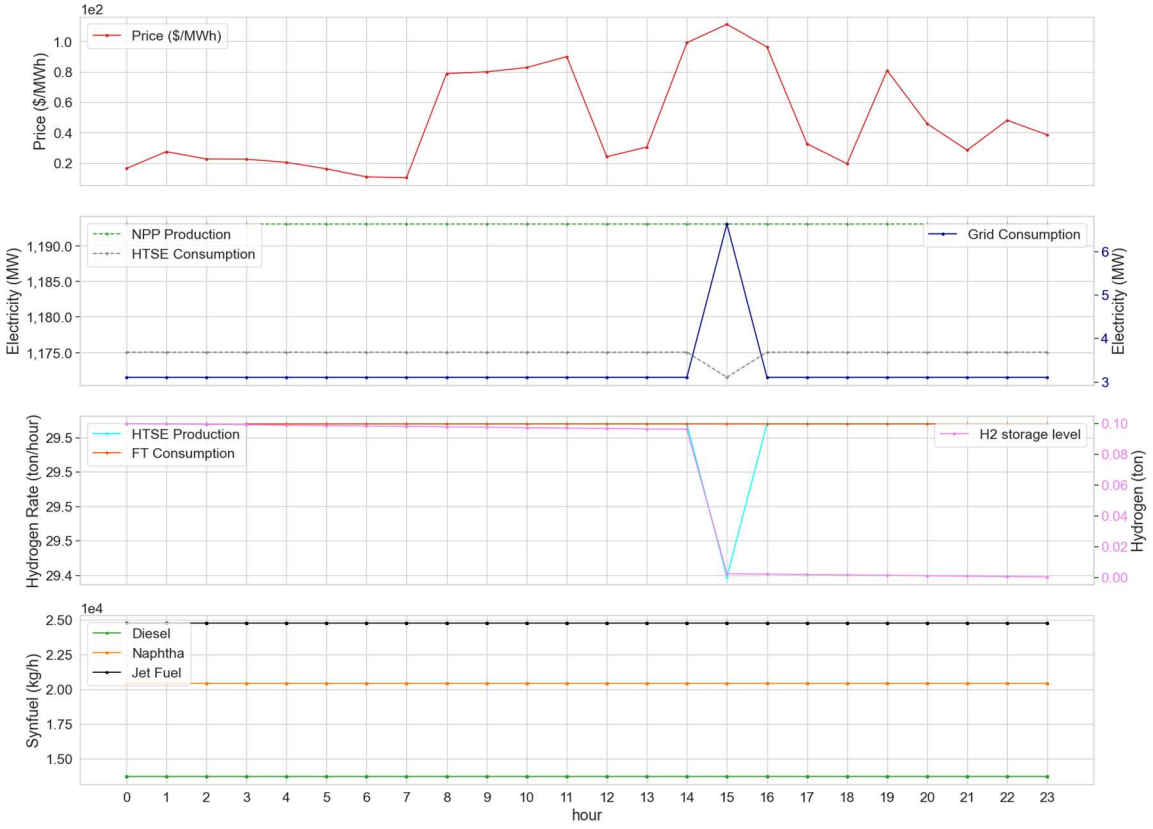

Figure 30. Braidwood NPP, dispatch optimization results, 24 hours.

6.2 Sensitivity Analysis

Examining the results at different locations shown in Figure 28 and Figure 29 (for other locations see Appendix A), the team observes that the revenues come from the hydrogen PTC and the sale of synfuel products. Regarding costs, the CO_2 feedstock cost and CAPEX costs are highest and are followed by O&M costs. Perturbed cases are run for the Braidwood location to test the robustness of the relative profitability of the synfuel IES against uncertainties and variations in those parameters. The Braidwood location distribution of electricity prices (see Figure 25) presents an intermediate mean and standard deviation as compared to the other locations; therefore, Braidwood can be considered a median case. The perturbation of these parameters is done as follows:

- H_2 PTC:
  - \$1/kg: Corresponds to the third tier of the clean hydrogen production tax credit (PTC) [42]
  - \$2.70/kg: If the utility owning the synfuel IES cannot directly benefit from the tax credit, it can be sold for 90% of its value [43]
- Synfuels prices: ±25% adjustment to the synfuel prices projected in the EIA AEO
- CAPEX costs for every component in the synfuel production process (HTSE, FT process, and H_2 storage): ±25%
- CO_2 cost: Previous cases assume that this feedstock is free and is a waste stream from other industries that must be transported to the NPP location via pipelines. Here the team considers that the CO_2 costs an additional \$30/tonne and \$60/tonne. The value of \$60/tonne represents the value that could be credited to a CO_2 emitter under Section 45Q of the U.S. Internal Revenue Code for using the CO_2 for an industrial use. It is possible that the availability of this credit could increase the market value of CO_2 emitted from the industrial sources considered in this analysis.
- O&M costs for the components of the synfuel production process: ±25%.

The sensitivity analysis results are presented in Figure 31. Each selected input parameter was perturbed by a fixed amount or percentage with every other parameter staying constant. The HERON model was then run in exploration mode, and the optimal system configuration was identified. The graph is centered at \$1.3 bn, which corresponds to the Δ(NPV) of the Braidwood location. The results correspond to our expectations from observing the breakdown of cashflows in Figure 29. The team observes that the hydrogen PTC has the most influence on the profitability of the synfuel IES. Next is the CO_2 feedstock cost; if its cost were to increase by \$30/ton, the relative profitability of the synfuel IES would decrease by 30%. The team concludes that a low-cost carbon feedstock is critical for the profitability of this IES. Optimal locations are close to large sources of concentrated and pure CO_2. The results are also sensitive to the synfuel prices. Increasing prices by 25% would increase the Δ(NPV) by 25%. Finally, the sensitivity of the results against variations in the CAPEX and O&M costs are relatively low compared to other parameters. Policies affecting the pricing of the products and feedstock of the synfuel IES have the most influence on its economic profitability. The hydrogen PTC introduced by the 2022 IRA is critical in making this system more profitable than the current use of the nuclear fleet. The implementation of tax credits or other incentives to produce decarbonized synthetic fuels and the monetization of carbon emissions via carbon taxes or carbon credits exchanged on dedicated markets would further strengthen the case for the production of synfuel using nuclear energy.

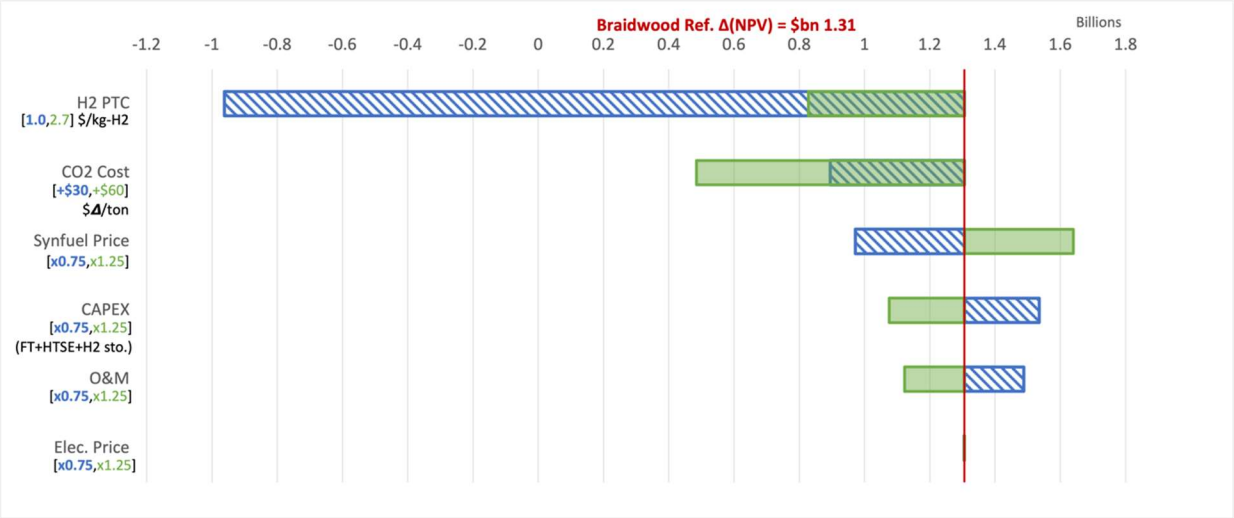

Figure 31. Sensitivity analysis results, Braidwood location, synfuel price, CAPEX, CO_2 feedstock cost, O&M costs, and H_2 PTC value.

7. CONCLUSION AND FUTURE WORK

This techno-economic analysis presented herein assessed the relative economic profitability of a synfuel IES compared to the current use of NPPs across the United States. The U.S. synfuel market potential was evaluated, and a comparison between different regions in the U.S. was made. Forecasted use of diesel and jet fuel differs across all regions in the study. Naphtha use forecasts were not available, but historical pricing suggests a strong correlation with gasoline market trends. It was evident, based on EIA forecasts, that diesel fuel use is expected to decrease by 2050 while jet fuel use is expected to increase by 64%. The historical electricity prices for the different markets for the selected NPP locations were analyzed. Periodic trends were identified and used to train ARMA models. A HERON model of the synfuel IES was constructed and run using the synthetic electricity prices from the ARMA models. The optimized synfuel IES at each location was found to add \$14M–1.3bn (2020) in NPV when compared to the BAU role of NPPs providing baseload power. A large part of this added value comes from the hydrogen PTC that the Inflation Reduction Act of 2022 put in place followed by the sales of the final synfuel products. The largest costs are attributed to the carbon feedstock transportation cost, underlining the importance of the proximity of the synfuel IES to high-purity concentrated CO_2 sources. Finally, perturbing a few selected input parameters show the sensitivity of the relative synfuel IES profitability to the value of hydrogen PTC, the prices of the synfuel products, and to the cost of the carbon feedstock, highlighting the critical role of government subsidies and incentives regarding decarbonized hydrogen and synfuel and carbon emissions.

The FT process was chosen for synfuel production given its proven technological readiness. The methanol pathway is another mature technology for synfuel production that may provide increased selectivity toward higher value synfuel products. The focus of this analysis is on mature technologies that could be deployed immediately; however, the nuclear design landscape is evolving, and with the next generation of NPPs, the size and the design of plants will drastically differ. The fourth generation of NPPs will include micro and small modular reactors that adopt novel designs. Coupling these advanced reactors with a synfuel production process may significantly increase their economic value, thus attracting more investments. However, the schedule for deployment of advanced reactors coupled with non-electrical applications is uncertain. Since the financing costs and construction timeline for nuclear power plants can significantly affect their profitability, additional analysis of these factors is recommended.

8. REFERENCES

[1] Congressional Budget Office. "Emissions of Carbon Dioxide in the Transportation Sector." 2022. Accessed February 13, 2023. https://www.cbo.gov/publication/58861

[2] U.S. Energy Information Administration. 2022. "U.S. Energy-Related Carbon Dioxide Emissions, 2021." Accessed February 13, 2023. https://www.eia.gov/environment/emissions/carbon/

[3] U.S. Energy Information Administration. "Monthly Energy Review Table 11.5. Carbon Dioxide Emissions from Energy Consumption: Transportation Sector, 2023." Accessed February 13, 2023. https://www.eia.gov/totalenergy/data/monthly/pdf/sec11_8.pdf

[4] Delgado, H., et al. 2022. "The Modeling of the Synfuel Production Process: Techno-Economic Analysis and Life Cycle Assessment of FT Fuel Production Plants Integrated with Nuclear Power." ANL-22/41, Argonne National Laboratory.

[5] Morgan, D., T. Grant, and D. Remson. 2022. "FECM/NETL CO_2 Transport Cost Model (2022)," DOE/NETL-2022/3243, National Energy Technology Laboratory. https://netl.doe.gov/projects/VueConnection/download.aspx?id=046f9b76-123d-456b-b29e-57e027a099df&filename=FECMNETLCO_2TransportCostModel2022_031422.xlsm.

[6] U.S. Energy Information Administration. 2022. "Oil and Petroleum Products Explained: Use of Oil." Accessed August 30, 2022. https://www.eia.gov/energyexplained/oil-and-petroleum-products/use-of-oil.php

[7] Wendt, D., et al. 2022. "Production of Fischer-Tropsch Synfuels at Nuclear Plants." Idaho National Laboratory. https://inldigitallibrary.inl.gov/sites/sti/sti/Sort_63673.pdf.

[8] McKinsey & Company. "Charting the Global Energy Landscape to 2050: Sustainable Fuels, 2022." Accessed September 14, 2022. https://www.mckinsey.com/industries/oil-and-gas/our-insights/charting-the-global-energy-landscape-to-2050-sustainable-fuels

[9] Congress. "H.R. 5376 - Inflation Reduction Act of 2022." Congress, 2022. https://www.congress.gov/bill/117th-congress/house-bill/5376

[10] Boeing. "Boeing Commits to Deliver Commercial Airplanes Ready to Fly on 100% Sustainable Fuels, 2021." Accessed September 14, 2022. https://boeing.mediaroom.com/2021-01-22-Boeing-Commits-to-Deliver-Commercial-Airplanes-Ready-to-Fly-on-100-Sustainable-Fuels

[11] U.S. Department of Energy. n.d. "Sustainable Aviation Fuel Grand Challenge." Accessed September 14, 2022. https://www.energy.gov/eere/bioenergy/sustainable-aviation-fuel-grand-challenge

[12] UK Ministry of Defence. 2022. "Sustainable Fuel Set to Power the Royal Air Force Reaches Landmark New Stage." Accessed September 14, 2022. https://www.gov.uk/government/news/sustainable-fuel-set-to-power-the-royal-air-force-reaches-landmark-new-stage#:~:text=The%20Royal%20Air%20Force%2C%20having,capability%20as%20a%20next%20stage

[13] U.S. Air Force. 2017. "Energy Flight Plan 2017–2036." Accessed September 14, 2022. https://www.afcec.af.mil/Portals/17/documents/Energy/AFEnergyFlightPlan2017.pdf?ver=2019-12-16-105948-090

[14] Bloomberg. 2021. "Shell Mulls Making Renewable Jet Fuel at New Swedish Facility." Accessed September 14, 2022. https://www.bloomberg.com/news/articles/2021-11-03/shell-mulls-making-renewable-jet-fuel-near-swedish-nuclear-plant

[15] United Airlines. “Our Sustainable Aviation Fuel (SAF) Program.” Accessed February 1, 2023. https://www.united.com/en/us/fly/company/responsibility/sustainable-aviation-fuel.html

[16] Audi MediaCenter. “Audi Steps Up Research into Synthetic Fuels, 2017.” Accessed January 31, 2023. https://www.audi-mediacenter.com/en/press-releases/audi-steps-up-research-into-synthetic-fuels-9546

[17] Globe Newswire. 2022. “With 4.90% CAGR, Global Naphtha Market Size Worth USD 331.1 Billion by 2028.” Accessed January 1, 2023. https://www.globenewswire.com/en/news-release/2022/08/23/2503105/0/en/With-4-90-CAGR-Global-Naphtha-Market-Size-Worth-USD-331-1-Billion-by-2028-Naphtha-Industry-Trends-Share-Price-Drivers-Outlook-Forecast-Report-by-Facts-Factors.html

[18] IBISWorld. 2023. “Gasoline and Petroleum Wholesaling in the US - Market Size 2005–2029.” Accessed January 31, 2023. https://www.ibisworld.com/industry-statistics/market-size/gasoline-petroleum-wholesaling-united-states/

[19] Globe Newswire. 2022. “Global Aviation Fuel Market to Fly High to Generate $489.2 Billion by 2028.” Accessed January 31, 2023. https://www.globenewswire.com/news-release/2022/12/13/2572711/0/en/Global-Aviation-Fuel-Market-to-Fly-High-to-Generate-489-2-Billion-by-2028-Fluctuating-Crude-Oil-Prices-Putting-Pressure-on-Airline-Operators.html

[20] U.S. Energy Information Administration. 2022. “Annual Energy Outlook 2022.” https://www.eia.gov/outlooks/aeo/.

[21] Administration, U.S.E.I. 2022. “Diesel Fuel Explained: Use of Diesel.” Accessed January 31, 2023. https://www.eia.gov/energyexplained/diesel-fuel/use-of-diesel.php

[22] U.S. Energy Information Administration. n.d. “U.S. Census Regions and Divisions.” Accessed January 31, 2023. https://www.eia.gov/consumption/commercial/maps.php#census

[23] Zang, G., P. Sun, and A. Elgowainy. 2021. “The Modeling of Synfuel Production Process: ASPEN Model of FT Production with Electricity Demand Provided at LWR scale.” ANL/ESD-22/1, Argonne National Laboratory. https://www.osti.gov/biblio/1845408.

[24] Zang, G., et al. 2022. “The Modeling of the Synfuel Production Process: Process models of Fischer-Tropsch Production with Electricity and Hydrogen Provided by Various Scales of Nuclear Plants.” ANL/EST-22/8, Argonne National Laboratory. https://www.osti.gov/biblio/1868524.

[25] Laguna-Bercero, M. A. 2012. “Recent Advances in High Temperature Electrolysis using Solid Oxide Fuel Cells: A Review.” Journal of Power Sources 203: 4–16.

[26] Schmidt, O., et al. 2017. “Future Cost and Performance of Water Electrolysis: An Expert Elicitation Study.” International Journal of Hydrogen Energy 42, no. 52: 30470–30492. https://dx.doi.org/10.1016/j.ijhydene.2017.10.045

[27] Wendt, D. S., L. T. Knighton, and R. D. Boardman. 2022. “High Temperature Steam Electrolysis Process Performance and Cost Estimates.” INL/RPT-22-66117, Idaho National Laboratory. https://doi.org/10.2172/1867883.

[28] James, B. D. and B. Murphy. 2021. “Solid Oxide Electrolysis Stack Manufacturing Cost Analysis.” Strategic Analysis, Inc., April 2021.

[29] Topsoe. 2022. “Topsoe Confirms Final Investment Decision for Construction of World’s Largest SOEC Electrolyzer Plant.” Accessed September 1, https://blog.topsoe.com/topsoe-confirms-final-investment-decision-for-construction-of-worlds-largest-electrolyzer-plant

[30] O'Brien, J. E., et al. 2020. "A 25 kW high Temperature Electrolysis Facility for Flexible Hydrogen Production and System Integration Studies." International Journal of Hydrogen Energy 45, no. 32: 15796–15804.

[31] Peterson, D., J. Vickers, and D. DeSantis. 2020. "DOE Hydrogen and Fuel Cells Program Record #20006: Hydrogen Production Cost from High Temperature Electrolysis." DOE Hydrogen and Fuel Cell Technologies Office, https://www.hydrogen.energy.gov/pdfs/20006-production-cost-high-temperature-electrolysis.pdf.

[32] ISO New England. n.d. "FAQs: Day-Ahead Energy Market—Commitment, Scheduling, and Dispatch." Accessed May 8, 2023. https://www.iso-ne.com/participate/support/faq/da-market-commitment

[33] Ozkan, S. 2022. "An Intro to Locational Marginal Pricing." Accessed May 8, 2023. https://www.enverus.com/blog/an-intro-to-locational-marginal-pricing/

[34] Customer First Renewables. n.d. "Regulated and Deregulated Energy Markets." https://infocastinc.com/market-insights/solar/regulated-deregulated-energy-markets/

[35] U.S. Environmental Protection Agency. 2022. "Greenhouse Gas Reporting Program Data Sets." Accessed January 31, 2023. https://www.epa.gov/ghgreporting/data-sets

[36] Zang, G., et al. 2021. "Synthetic Methanol/Fischer-Tropsch Fuel Production Capacity, Cost, and Carbon Intensity Utilizing CO_2 from Industrial and Power Plants in the United States." Environmental Science and Technology 55, no. 11: 7595–7604. https://www.ncbi.nlm.nih.gov/pubmed/33979128

[37] Herron, S., A. Zoelle, and W. M. Summers. 2014. "Cost of Capturing CO_2 from Industrial Sources." DOE/NETL-2013/1602, National Energy Technology Laboratory.

[38] U.S. Energy Information Administration. "Petroleum & Other Liquids: Gasoline and Diesel Fuel." Update January 30, 2023, 2023. Accessed January 31, 2023. https://www.eia.gov/petroleum/gasdiesel/dieselpump_hist.php

[39] Trading Economics. "Naphtha, 2022." Accessed September 14, 2022. https://tradingeconomics.com/commodity/naphtha

[40] Rabiti, C., et al. 2021. "RAVEN User Manual." INL/EXT-15-34123-Rev.07, Idaho National Laboratory. https://www.osti.gov/biblio/1784874.

[41] Talbot, P. W., et al. 2020. "Correlated Synthetic Time Series Generation for Energy System Simulations using Fourier and ARMA Signal Processing." International Journal of Energy Research 44, no. 10: 8144–8155.

[42] D.O.E. Hydrogen and Fuel Cell Technologies Office. n.d. "Financial Incentives for Hydrogen and Fuel Cell Projects." Accessed May 8, 2023. https://www.energy.gov/eere/fuelcells/financial-incentives-hydrogen-and-fuel-cell-projects

[43] Steinberg, D. C., et al. 2023. "Evaluating Impacts of the Inflation Reduction Act and Bipartisan Infrastructure Law on the U.S. Power System." NREL/TP-6A20-85242, National Renewable Energy Laboratory. https://www.nrel.gov/docs/fy23osti/85242.pdf.

Appendix A

Detailed Cashflow Breakdown

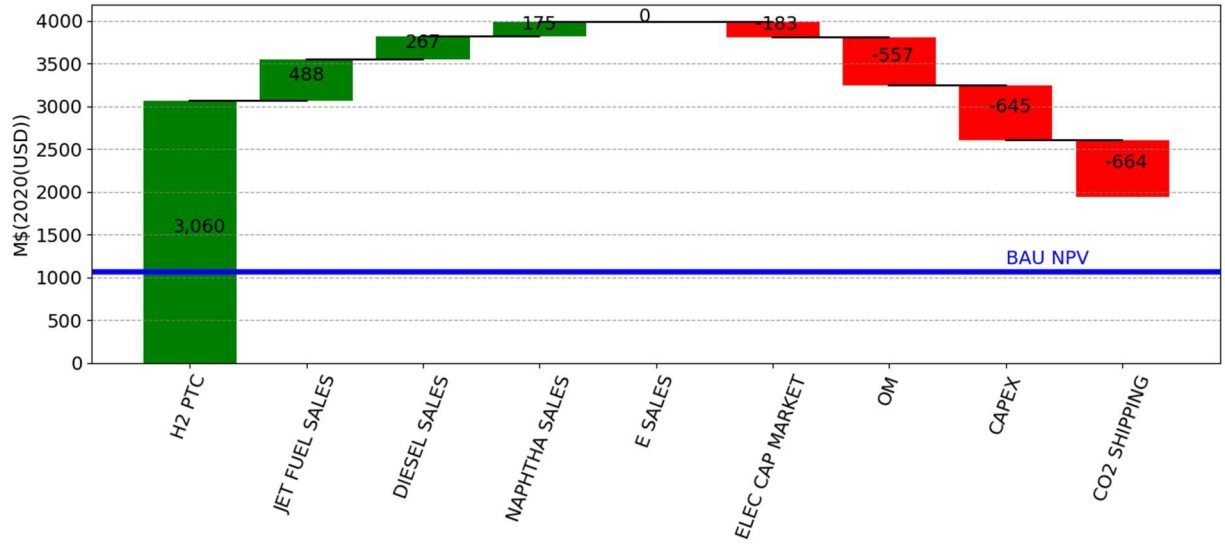

Figure A-1. Lifetime cashflow breakdown, Cooper location.

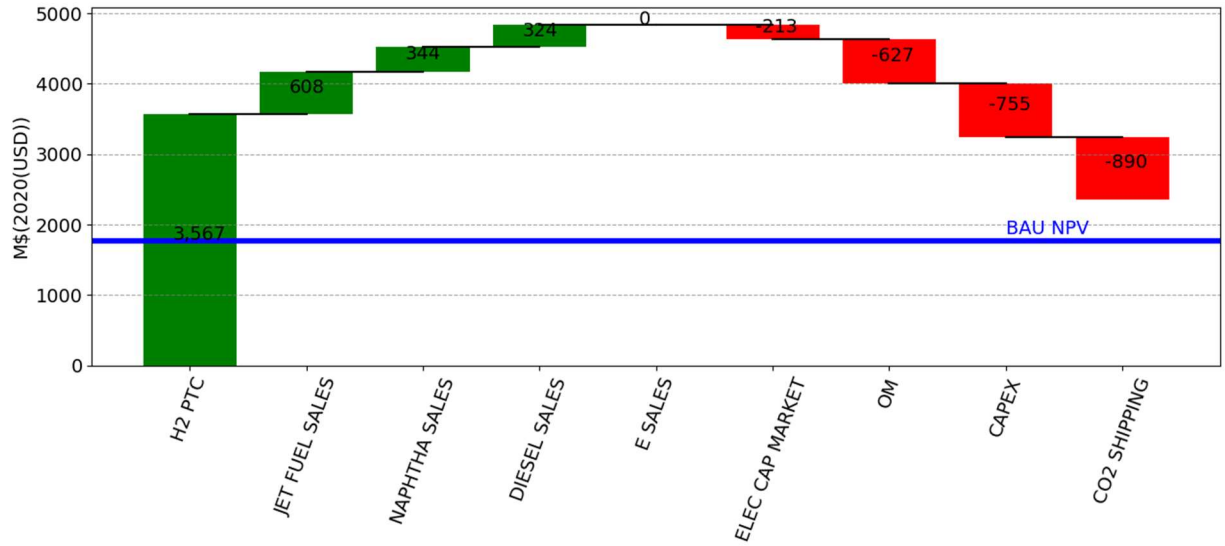

Figure A-2. Lifetime cashflow breakdown, Davis-Besse location.

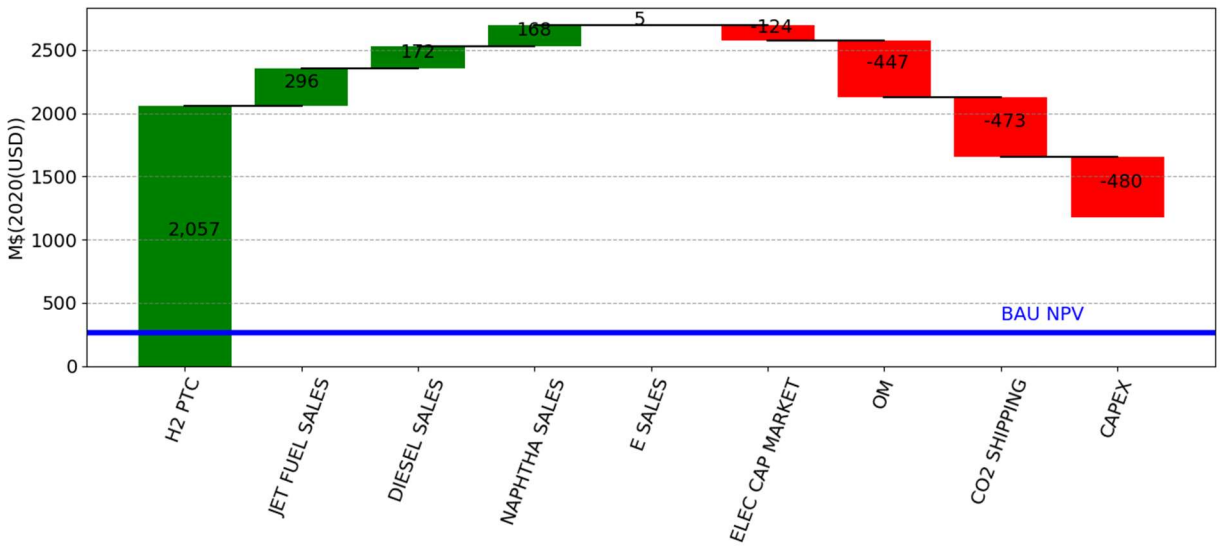

Figure A-3. Lifetime cashflow breakdown, Prairie Island location.

Appendix B

ARMA Validation for Each Location

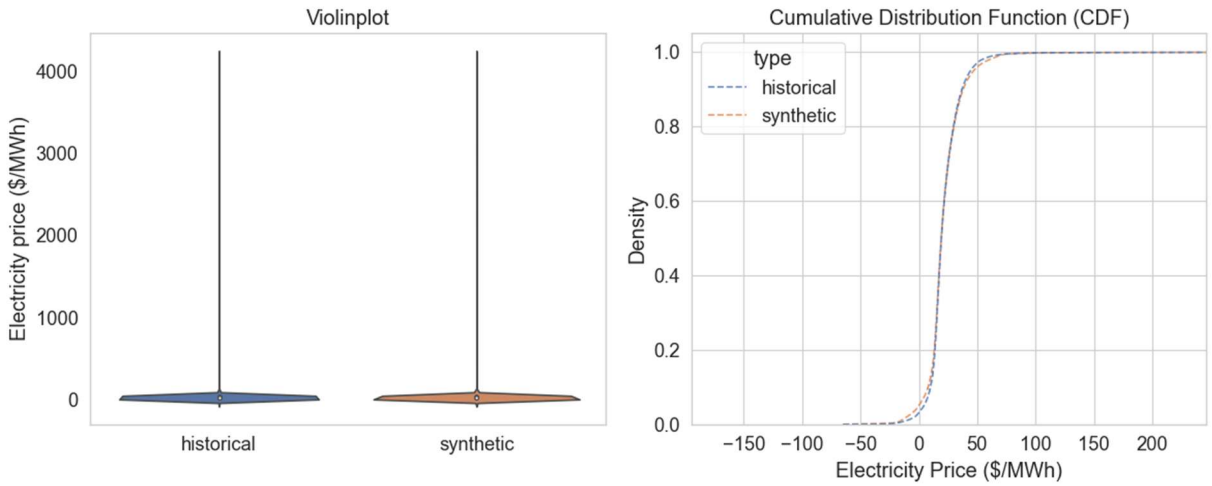

Figure B-1. Cooper Nuclear Station, comparison of synthetic and historical electricity pricing data.

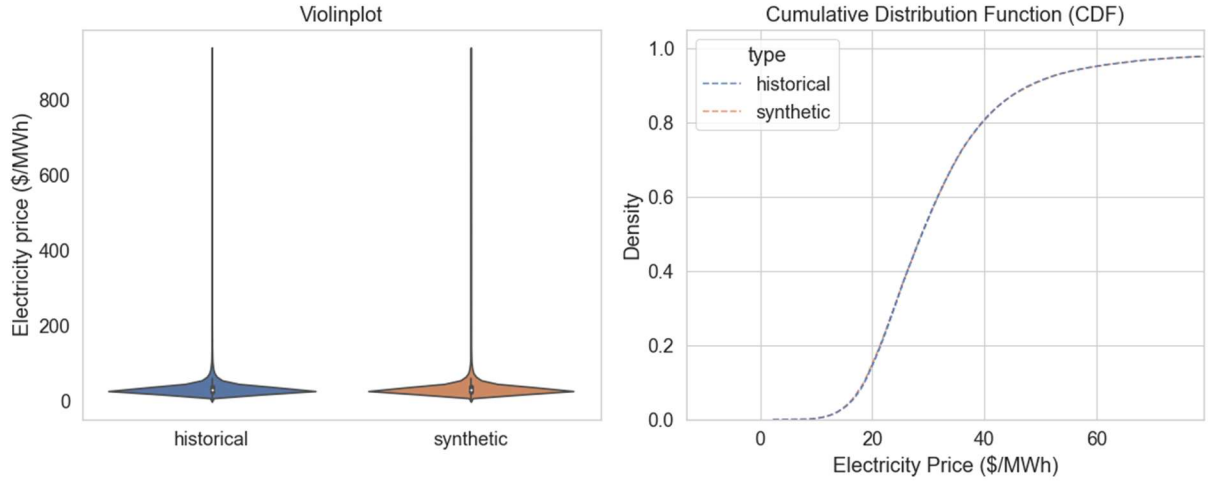

Figure B-2. Davis-Besse, comparison of synthetic and historical electricity pricing data.

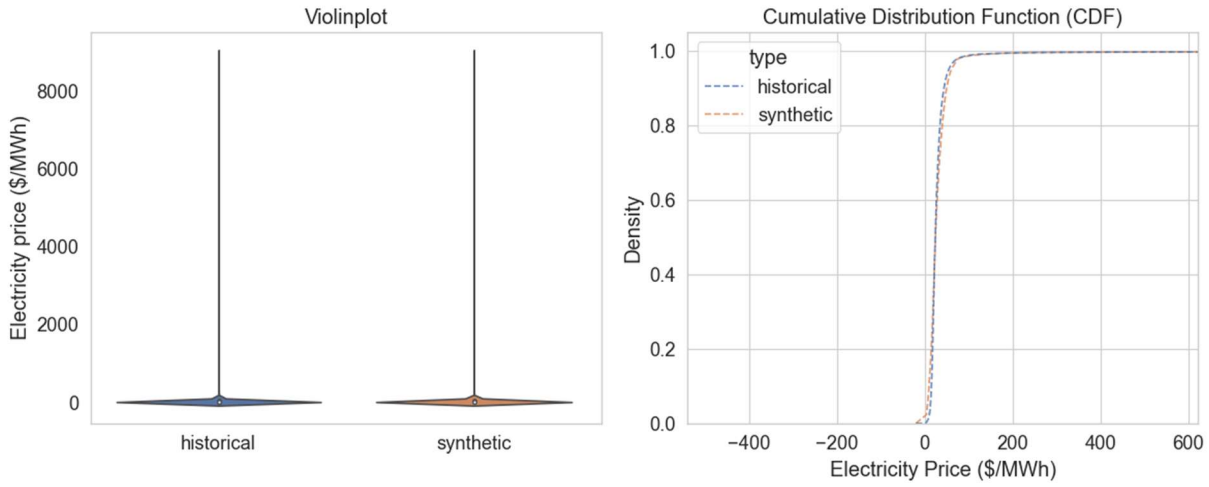

Figure B-3. STP, comparison of synthetic and historical electricity pricing data.

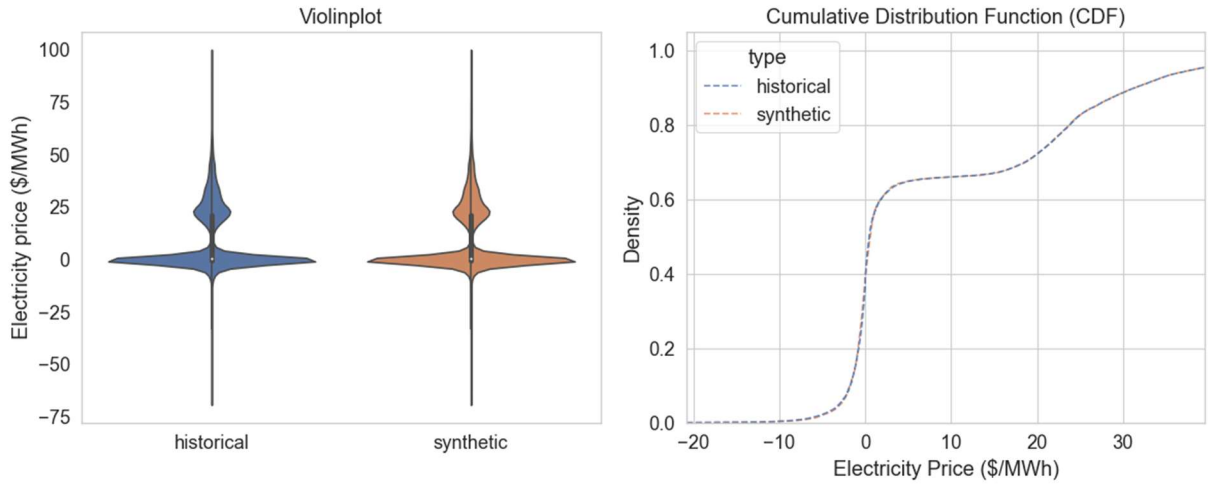

Figure B-4. Prairie Island, comparison of synthetic and historical electricity pricing data.

Appendix C

Fuel Pricing

Table C-1. Fuel price adjustment factors used to reduce retail prices down to gate or refinery price levels.

Retail Fuel Price Adjustment Table						
State	**Illinois**	**Minnesota**	**Ohio**	**Texas**	**Nebraska**	**California**
Region	**East North Central - IL**	**West North Central - MN**	**East North Central - OH**	**West South Central**	**West North Central - NE**	**Pacific**
Nuclear Plant	**Braidwood**	**Prairie Island**	**Davis-Besse**	**South Texas**	**Cooper**	
Transport Method	**Rail**	**Water**	**Water**	**Water**	**Water**	**Rail**
State+Federal Tax ($/gal) (Aug, 2022)						
Diesel Fuel	$0.952	$0.530	$0.714	$0.444	$0.495	$1.146
Jet Fuel	$0.219	$0.369	$0.219	$0.219	$0.249	$0.239
Gasoline	$0.817	$0.470	$0.569	$0.384	$0.441	$0.835
Naphtha	$0.136	$0.136	$0.136	$0.136	$0.136	$0.136
Marketing + Distribution (% of Retail Price, 2021)						
Diesel Fuel	20.2%	20.2%	20.2%	20.2%	20.2%	20.2%
Gasoline	15.6%	15.6%	15.6%	15.6%	15.6%	15.6%
Marketing ($/gal)						
Naphtha	$0.06	$0.06	$0.06	$0.06	$0.06	$0.06
Jet Fuel	$0.06	$0.06	$0.06	$0.06	$0.06	$0.06
Distribution ($/gal) (Based on Transport Method)						
Jet Fuel (Pipeline)	$0.12	$0.12	$0.12	$0.12	$0.12	$0.12
Naphtha	$0.36	$0.03	$0.03	$0.03	$0.03	$0.36
Sources: The Energy Journal, U.S. Dept. of Transportation, EIA						

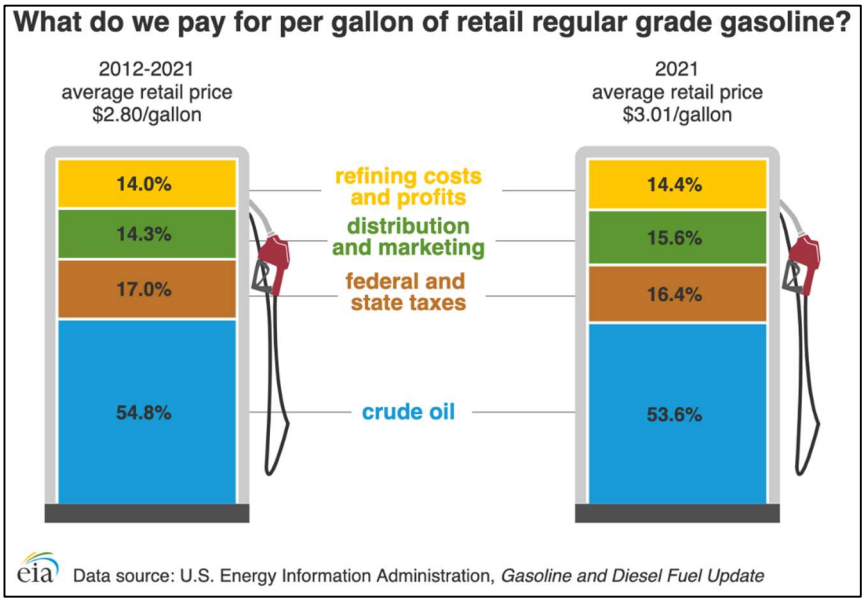

Figure C-1. EIA graphical representation of cost components for regular grade gasoline.

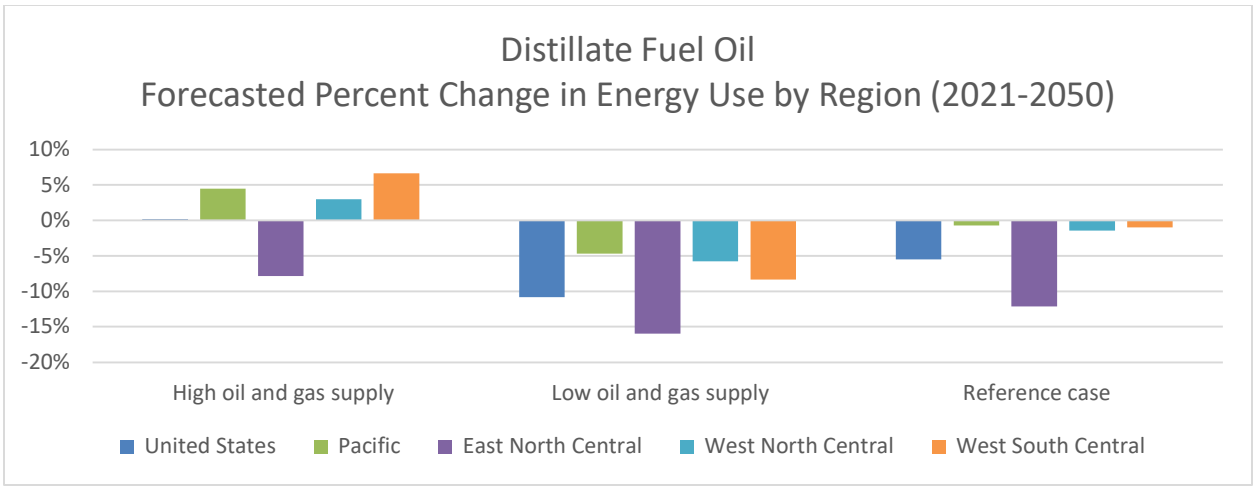

(a)

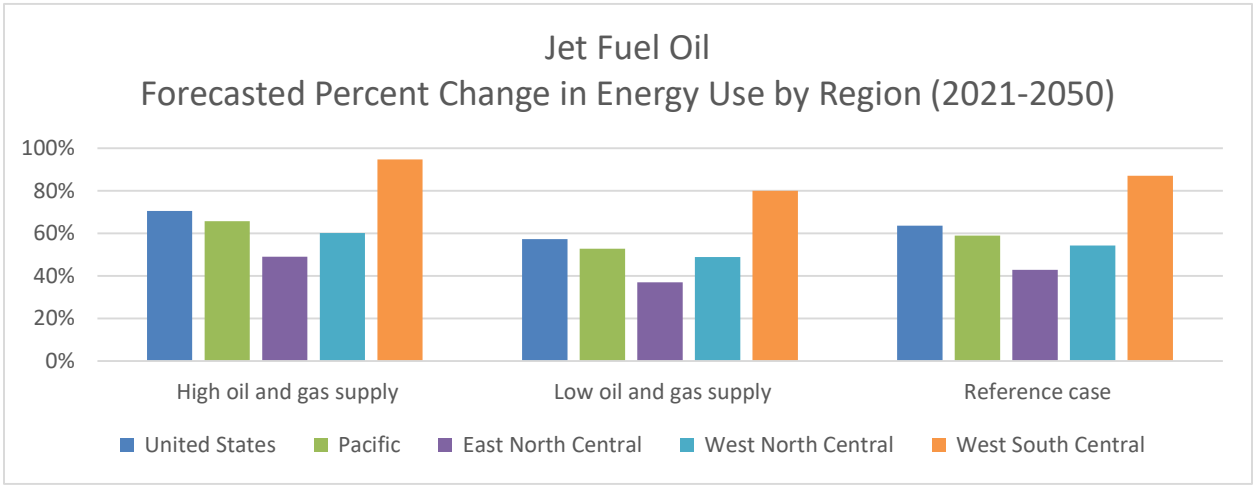

(b)

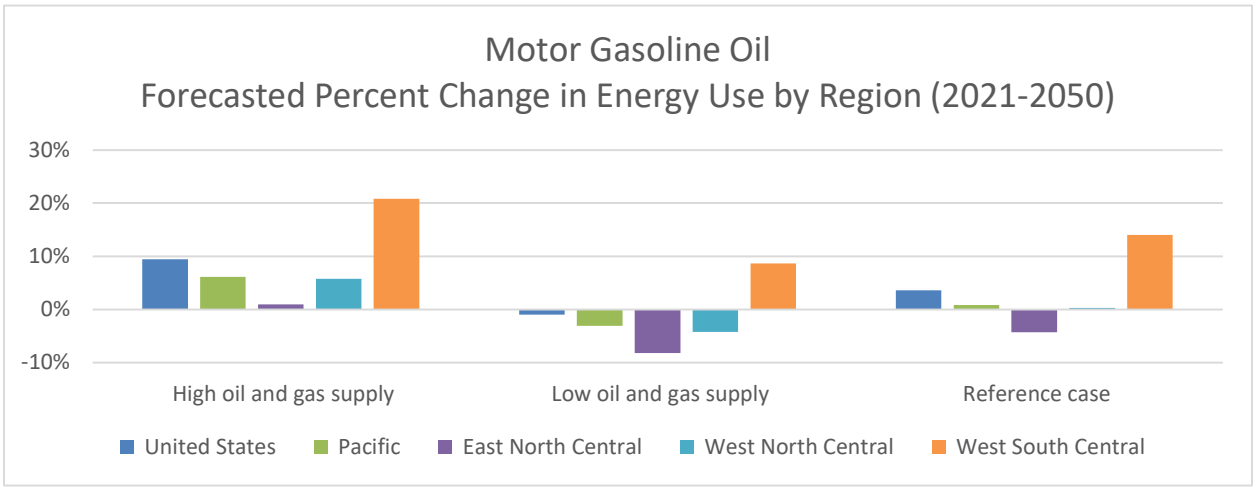

(c)

Figure C-2. Comparison of forecasted energy use by region and by type of fuel.

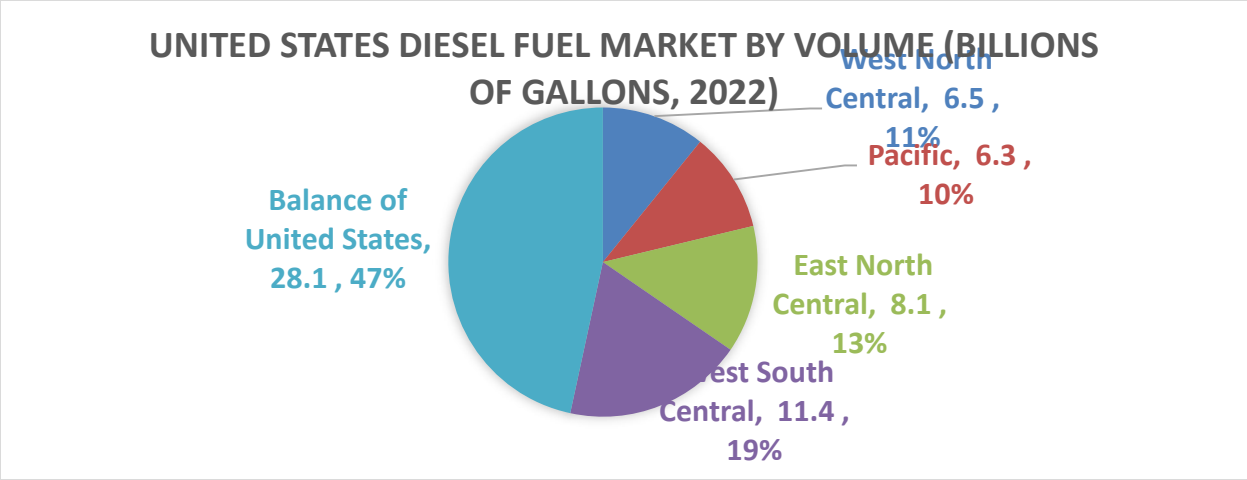

(a)

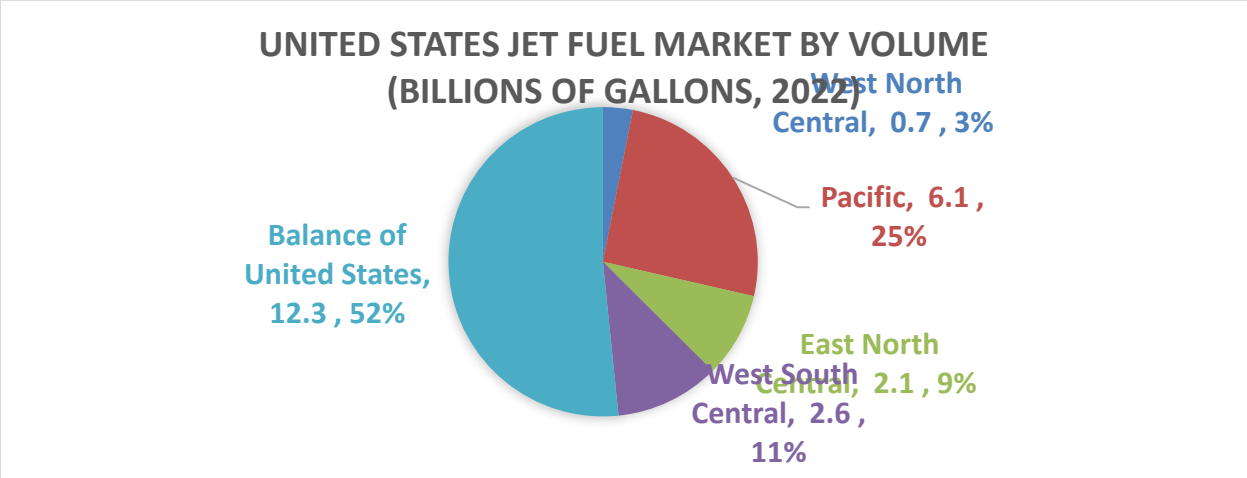

(b)

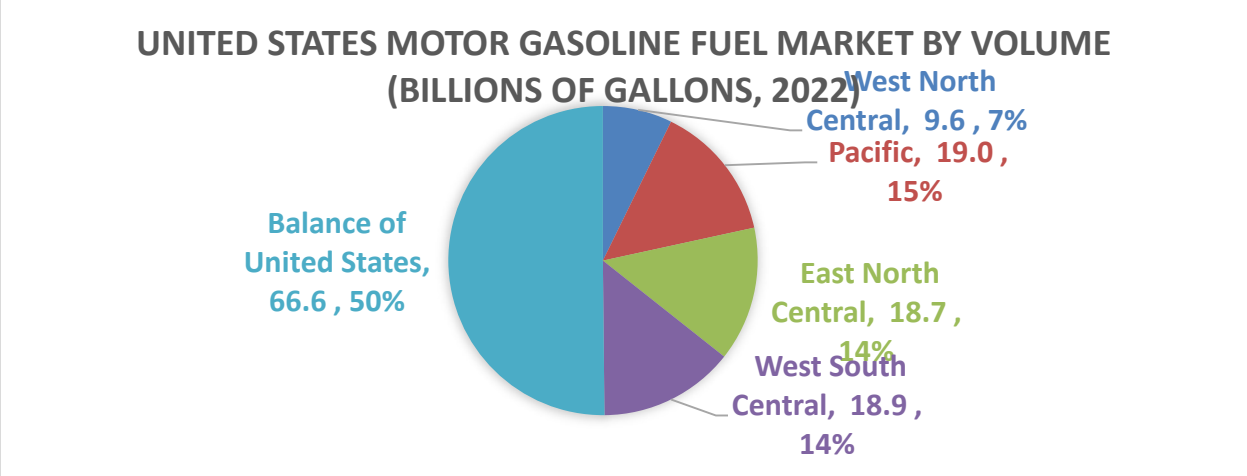

(c)

Figure C-3. Graphical representation of market volumes for specific fuels in various census regions of the United States.

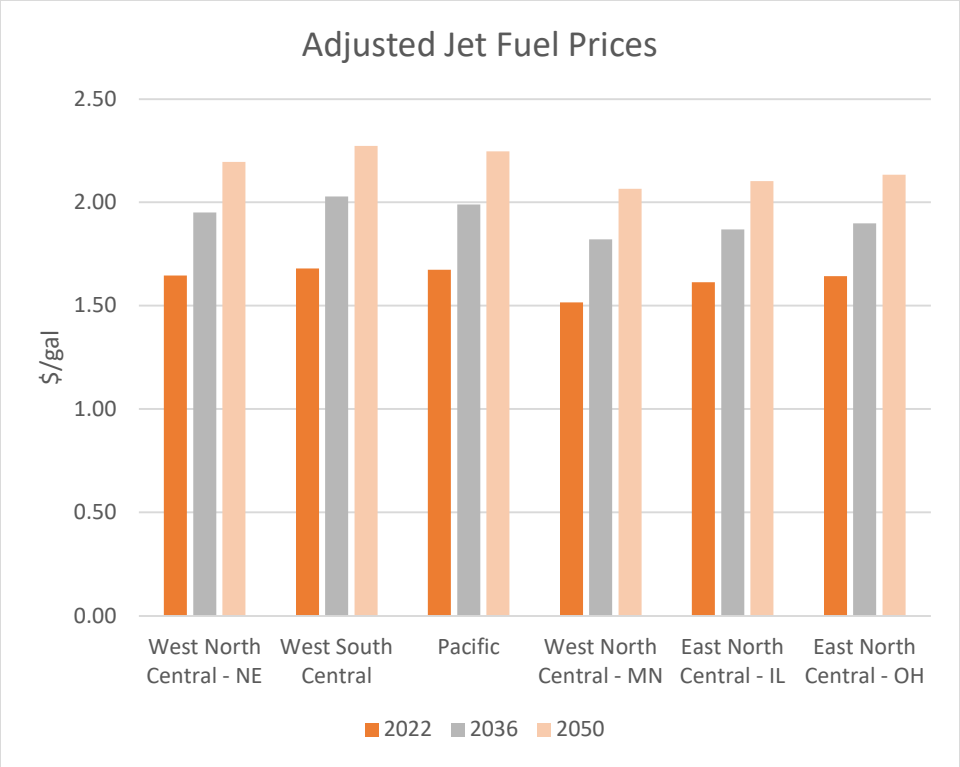
Adjusted Jet Fuel Prices
2.50
2.00
1.50
1.00
0.50
0.00
$/gal
West North Central - NE
West South Central
Pacific
West North Central - MN
East North Central - IL
East North Central - OH
2022
2036
2050

(a)

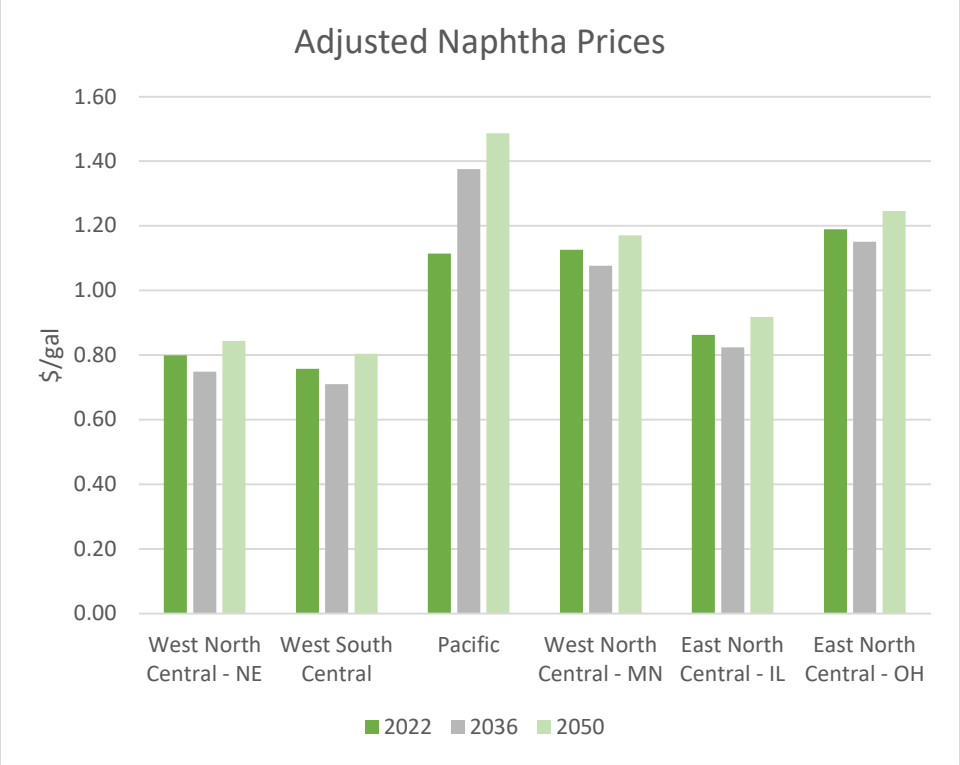
Adjusted Naphtha Prices
1.60
1.40
1.20
1.00
0.80
0.60
0.40
0.20
0.00
$/gal
West North Central - NE
West South Central
Pacific
West North Central - MN
East North Central - IL
East North Central - OH
2022
2036
2050

(b)

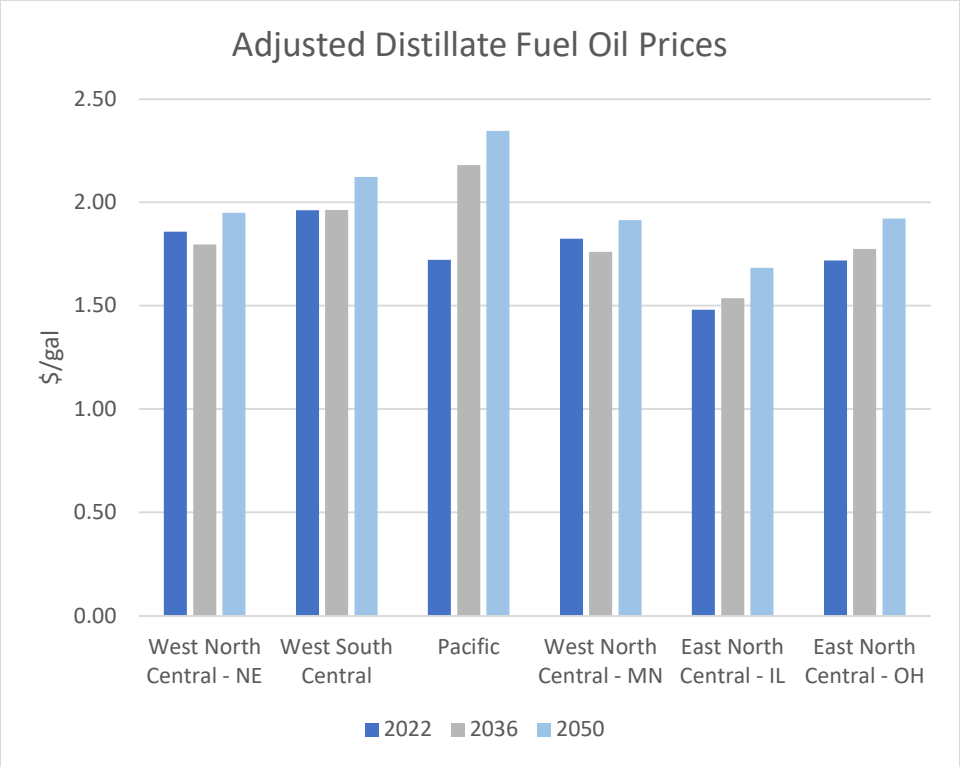

(c)

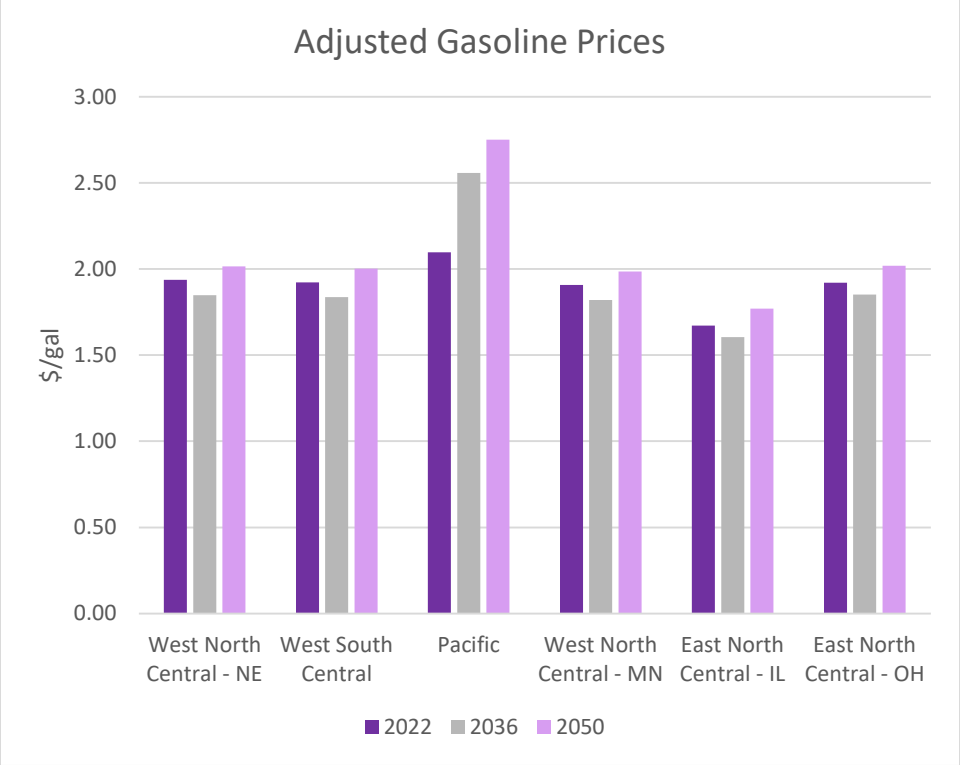

(d)

Figure C-4. Graphical representation of how adjusted fuel prices compare across time and by region.

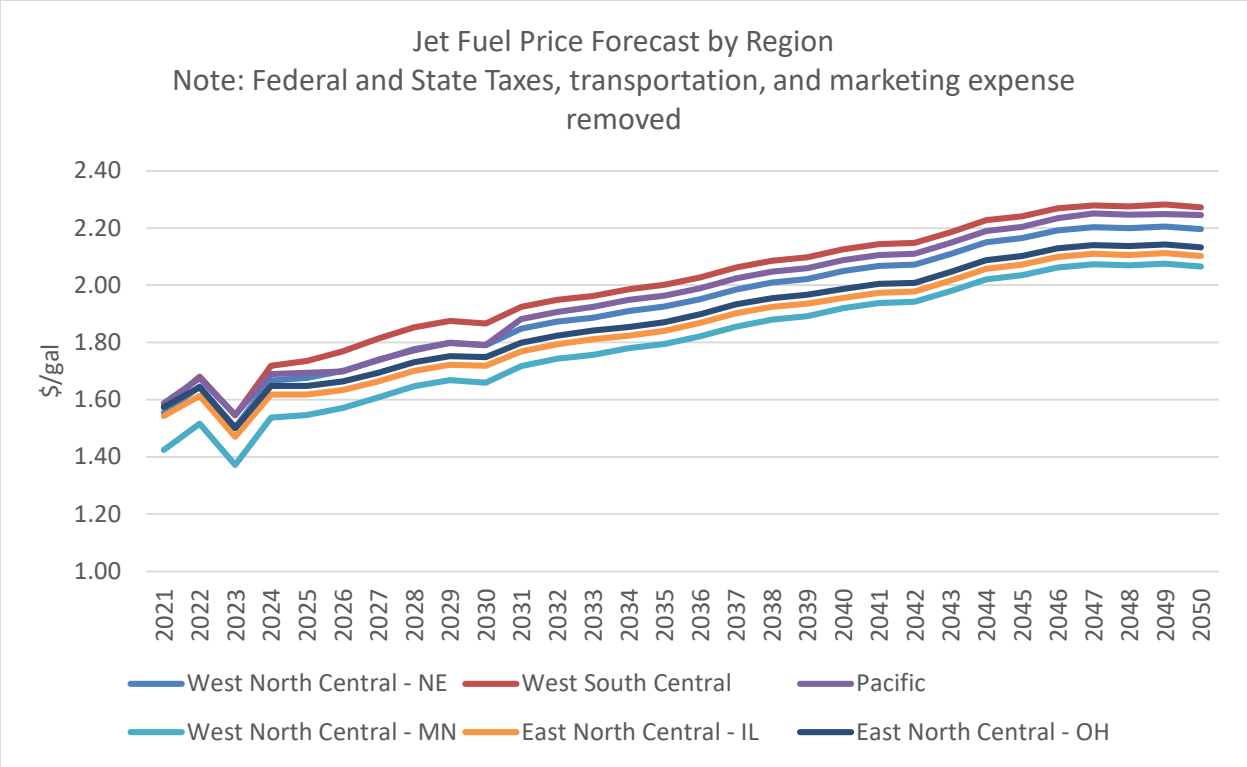
Jet Fuel Price Forecast by Region
Note: Federal and State Taxes, transportation, and marketing expense removed
$/gal
2.40
2.20
2.00
1.80
1.60
1.40
1.20
1.00
2021 2022 2023 2024 2025 2026 2027 2028 2029 2030 2031 2032 2033 2034 2035 2036 2037 2038 2039 2040 2041 2042 2043 2044 2045 2046 2047 2048 2049 2050
West North Central - NE
West South Central
Pacific
West North Central - MN
East North Central - IL
East North Central - OH

(a)

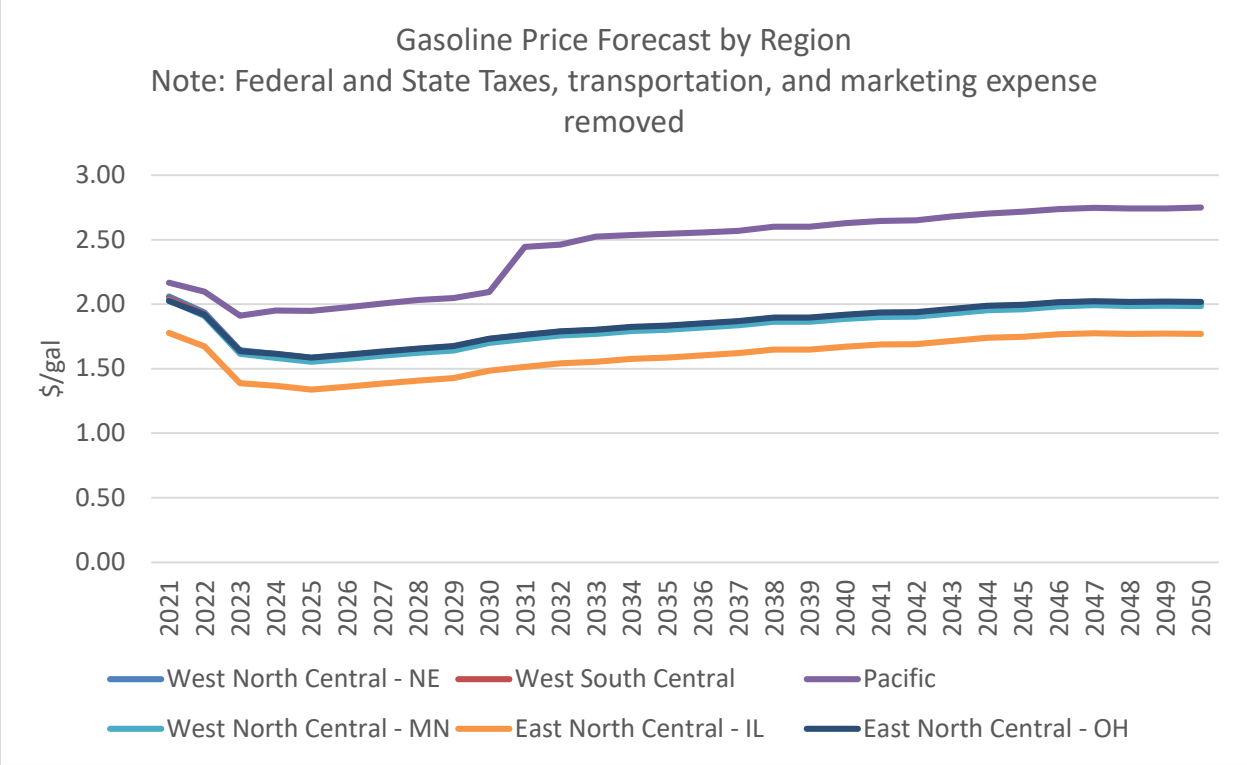
Gasoline Price Forecast by Region
Note: Federal and State Taxes, transportation, and marketing expense removed
$/gal
3.00
2.50
2.00
1.50
1.00
0.50
0.00
2021 2022 2023 2024 2025 2026 2027 2028 2029 2030 2031 2032 2033 2034 2035 2036 2037 2038 2039 2040 2041 2042 2043 2044 2045 2046 2047 2048 2049 2050
West North Central - NE
West South Central
Pacific
West North Central - MN
East North Central - IL
East North Central - OH

(b)

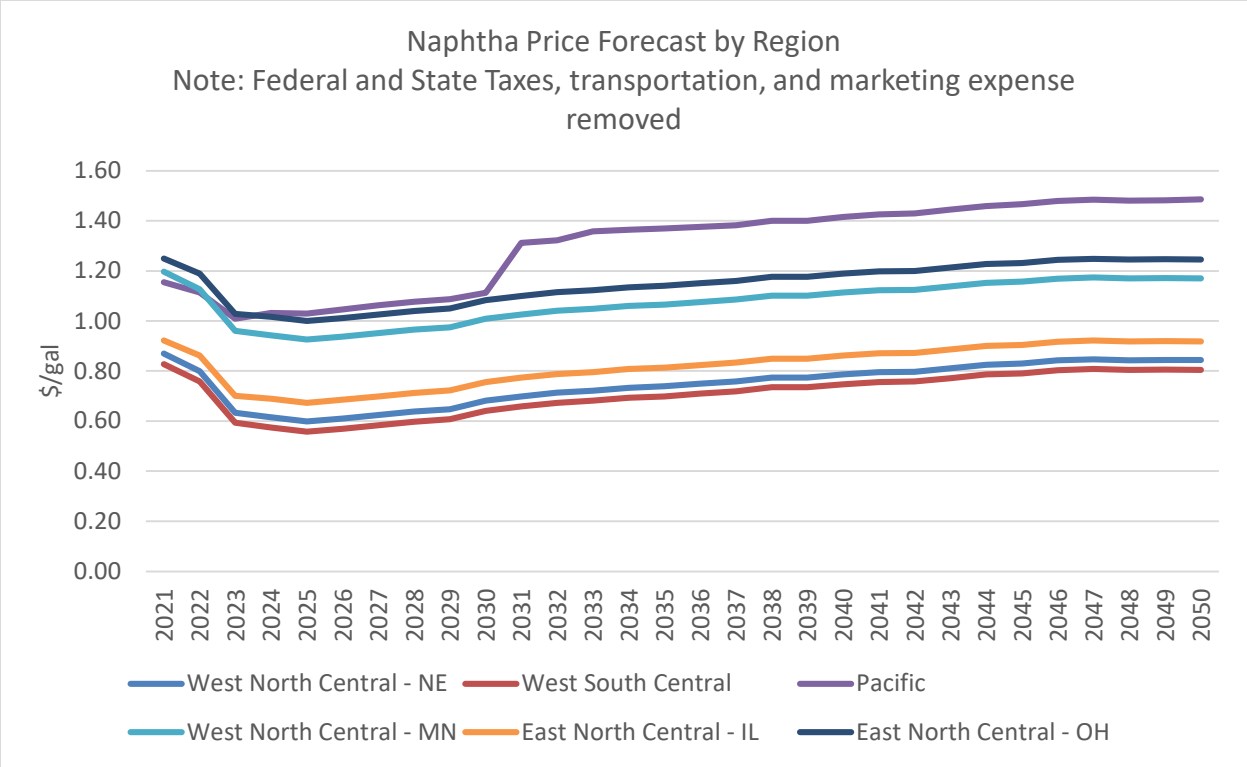

(c)

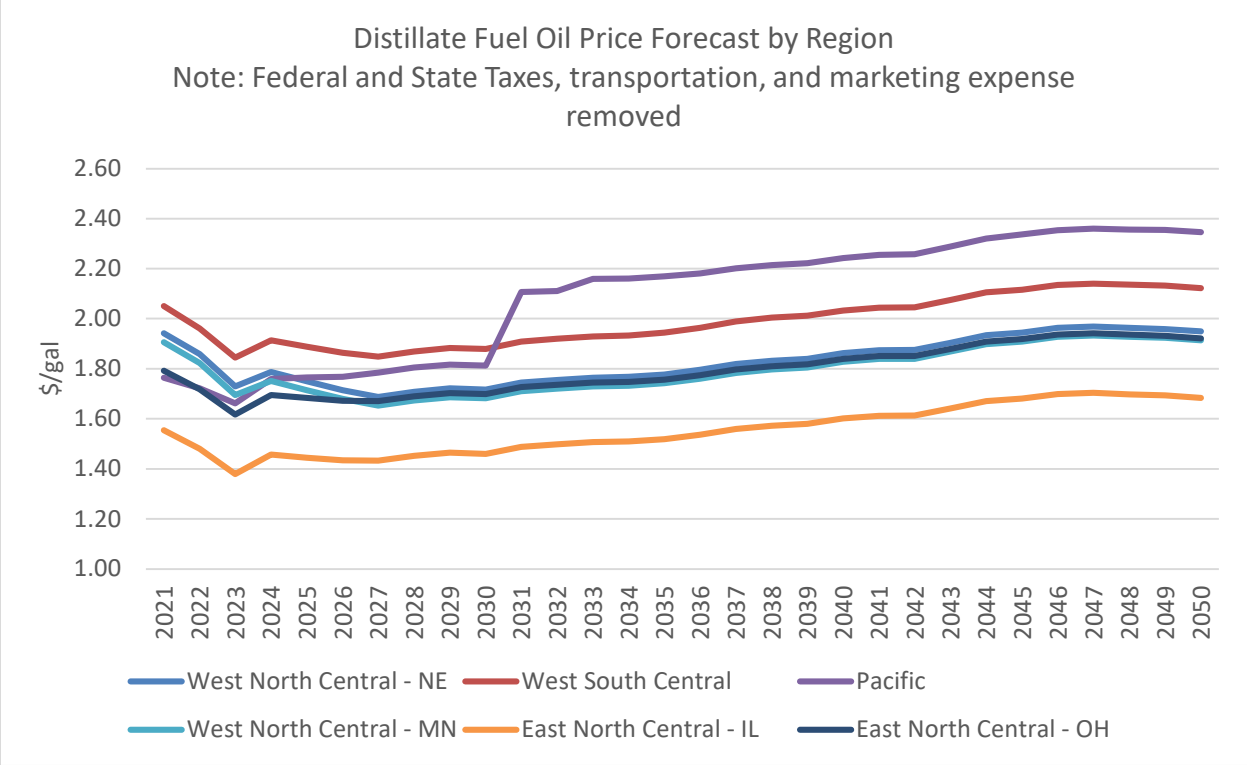

(d)

Figure C-5. Graphical representation of fuel price forecasts by region after federal and state taxes, transportation, and marketing expenses are removed.

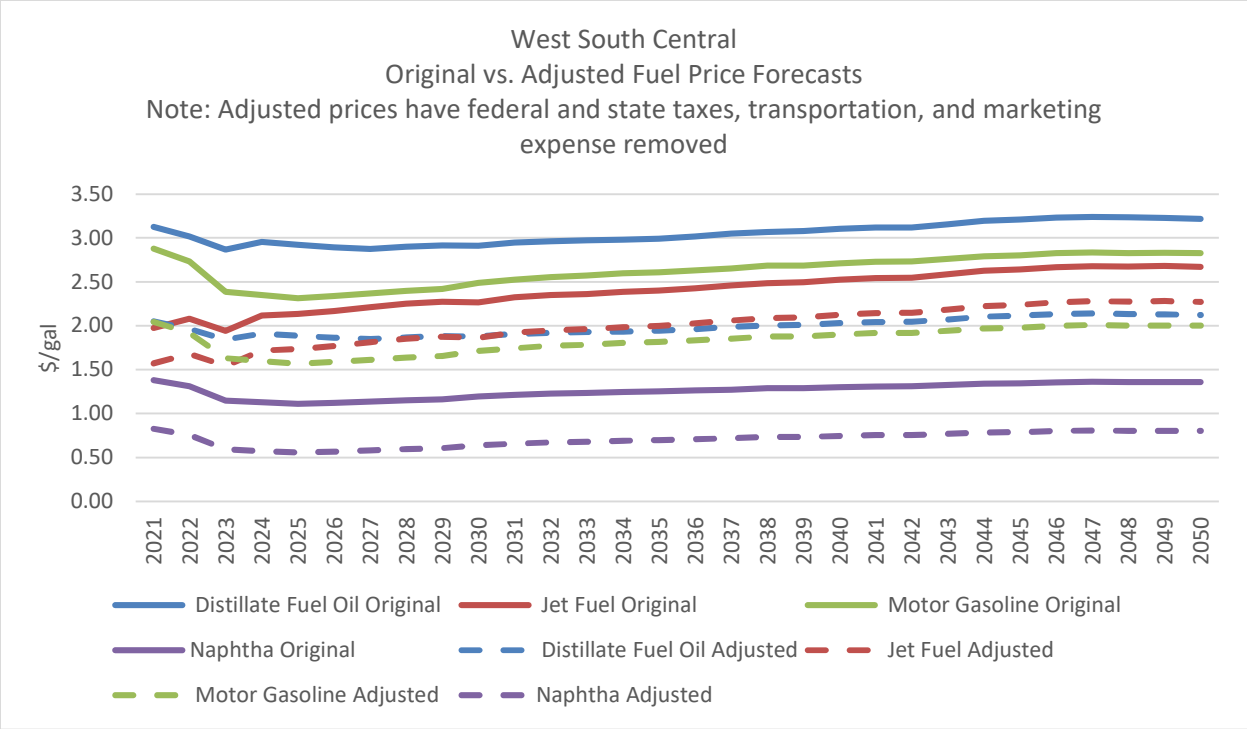
West South Central
Original vs. Adjusted Fuel Price Forecasts
Note: Adjusted prices have federal and state taxes, transportation, and marketing expense removed
$/gal
3.50
3.00
2.50
2.00
1.50
1.00
0.50
0.00
2021 2022 2023 2024 2025 2026 2027 2028 2029 2030 2031 2032 2033 2034 2035 2036 2037 2038 2039 2040 2041 2042 2043 2044 2045 2046 2047 2048 2049 2050
Distillate Fuel Oil Original
Jet Fuel Original
Motor Gasoline Original
Naphtha Original
Distillate Fuel Oil Adjusted
Jet Fuel Adjusted
Motor Gasoline Adjusted
Naphtha Adjusted

(a)

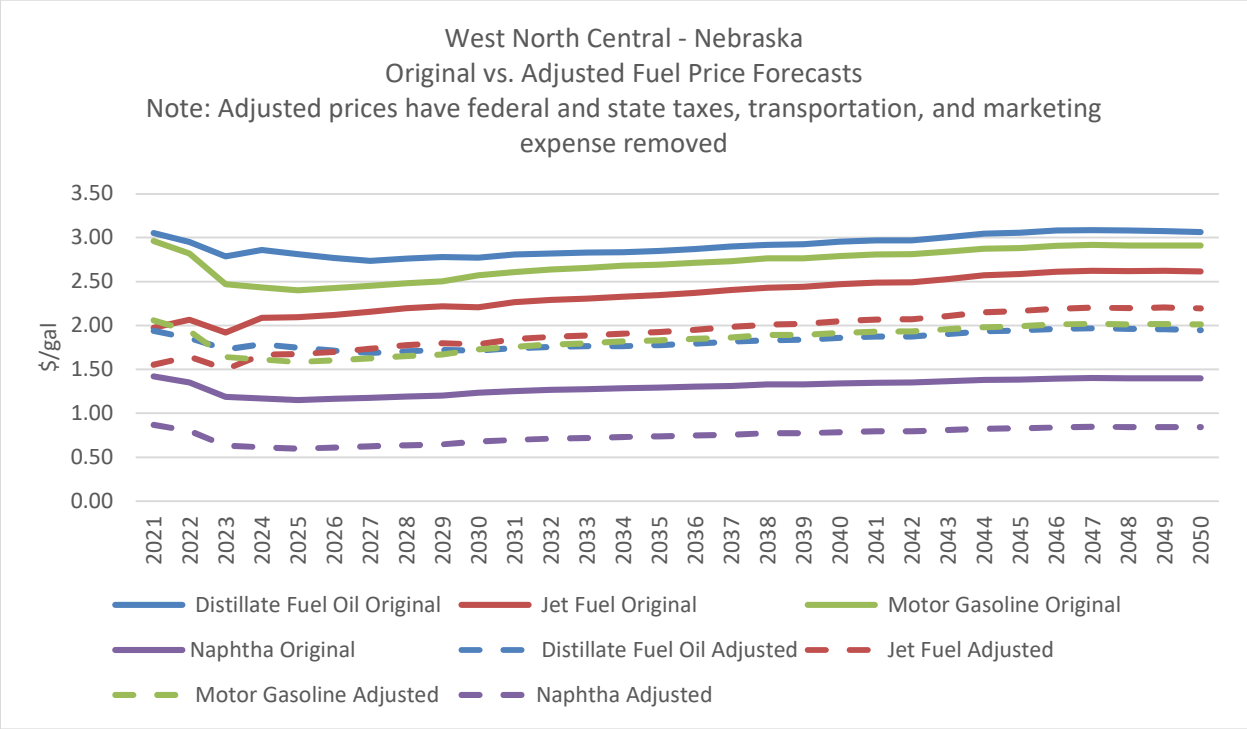
West North Central - Nebraska
Original vs. Adjusted Fuel Price Forecasts
Note: Adjusted prices have federal and state taxes, transportation, and marketing expense removed
$/gal
3.50
3.00
2.50
2.00
1.50
1.00
0.50
0.00
2021 2022 2023 2024 2025 2026 2027 2028 2029 2030 2031 2032 2033 2034 2035 2036 2037 2038 2039 2040 2041 2042 2043 2044 2045 2046 2047 2048 2049 2050
Distillate Fuel Oil Original
Jet Fuel Original
Motor Gasoline Original
Naphtha Original
Distillate Fuel Oil Adjusted
Jet Fuel Adjusted
Motor Gasoline Adjusted
Naphtha Adjusted

(b)

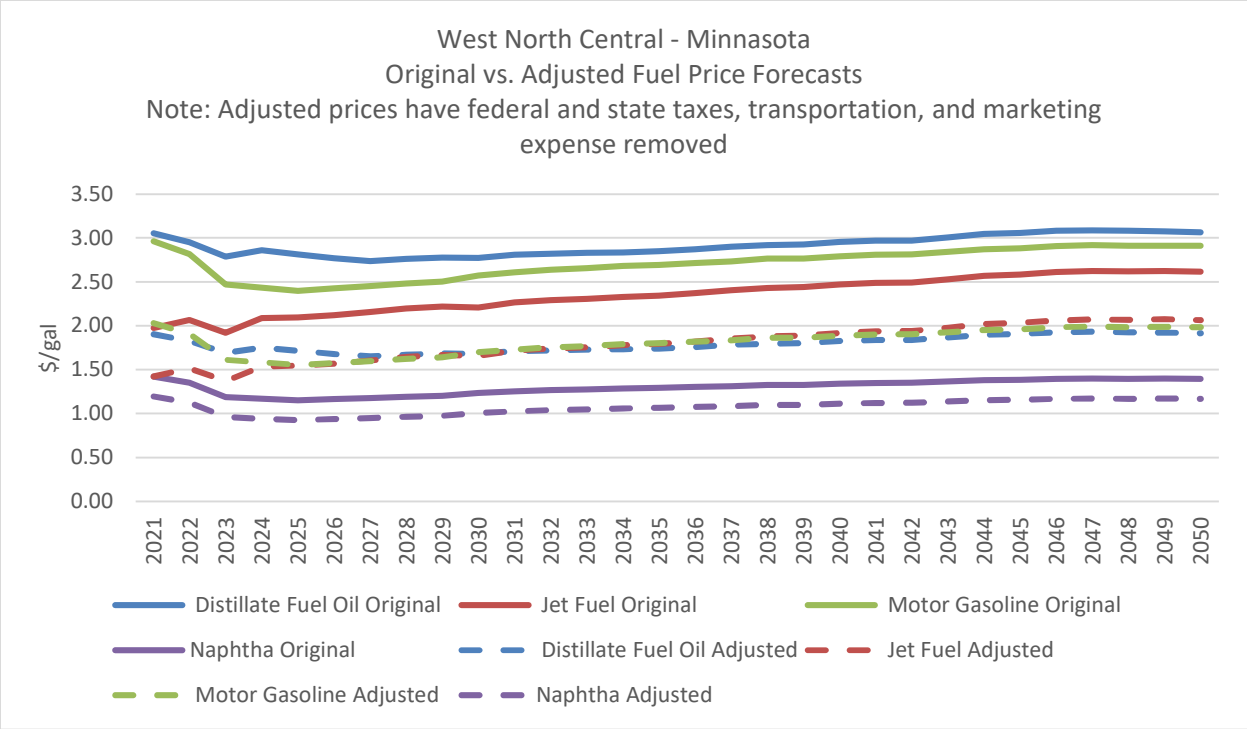
West North Central - Minnasota
Original vs. Adjusted Fuel Price Forecasts
Note: Adjusted prices have federal and state taxes, transportation, and marketing expense removed
$/gal
3.50
3.00
2.50
2.00
1.50
1.00
0.50
0.00
2021 2022 2023 2024 2025 2026 2027 2028 2029 2030 2031 2032 2033 2034 2035 2036 2037 2038 2039 2040 2041 2042 2043 2044 2045 2046 2047 2048 2049 2050
Distillate Fuel Oil Original
Jet Fuel Original
Motor Gasoline Original
Naphtha Original
Distillate Fuel Oil Adjusted
Jet Fuel Adjusted
Motor Gasoline Adjusted
Naphtha Adjusted

(c)

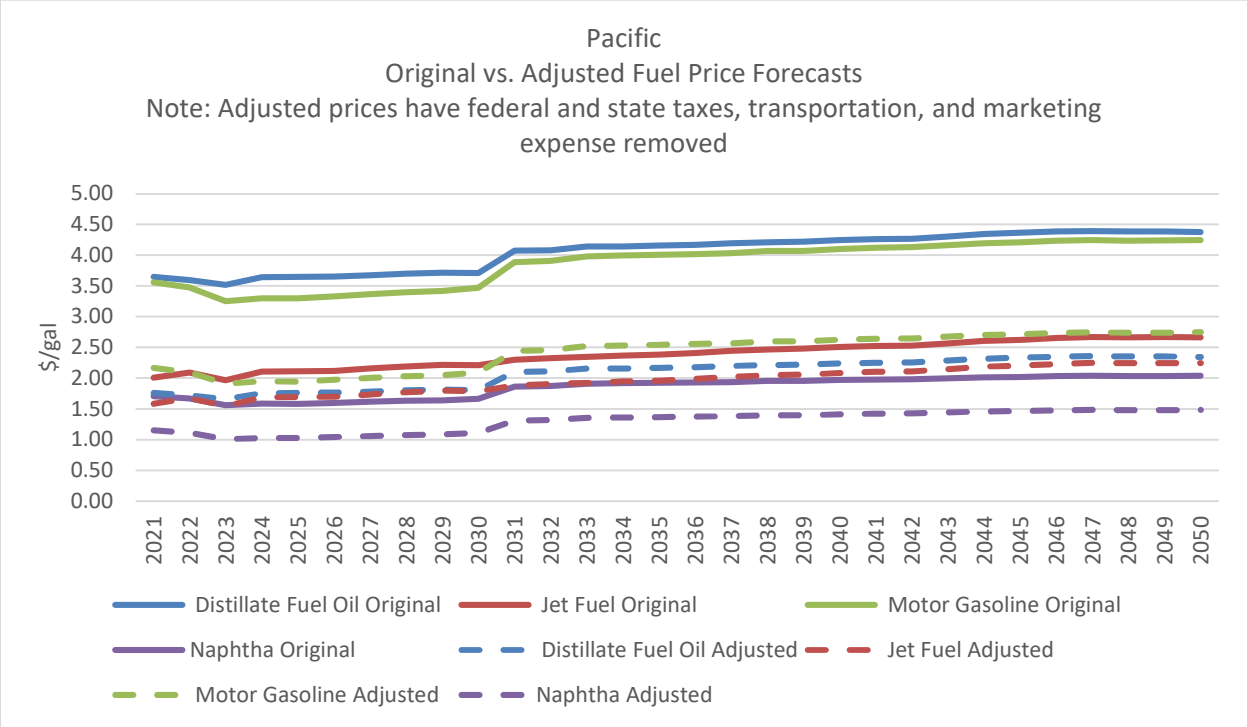
Pacific
Original vs. Adjusted Fuel Price Forecasts
Note: Adjusted prices have federal and state taxes, transportation, and marketing expense removed
$/gal
5.00
4.50
4.00
3.50
3.00
2.50
2.00
1.50
1.00
0.50
0.00
2021 2022 2023 2024 2025 2026 2027 2028 2029 2030 2031 2032 2033 2034 2035 2036 2037 2038 2039 2040 2041 2042 2043 2044 2045 2046 2047 2048 2049 2050
Distillate Fuel Oil Original
Jet Fuel Original
Motor Gasoline Original
Naphtha Original
Distillate Fuel Oil Adjusted
Jet Fuel Adjusted
Motor Gasoline Adjusted
Naphtha Adjusted

(d)

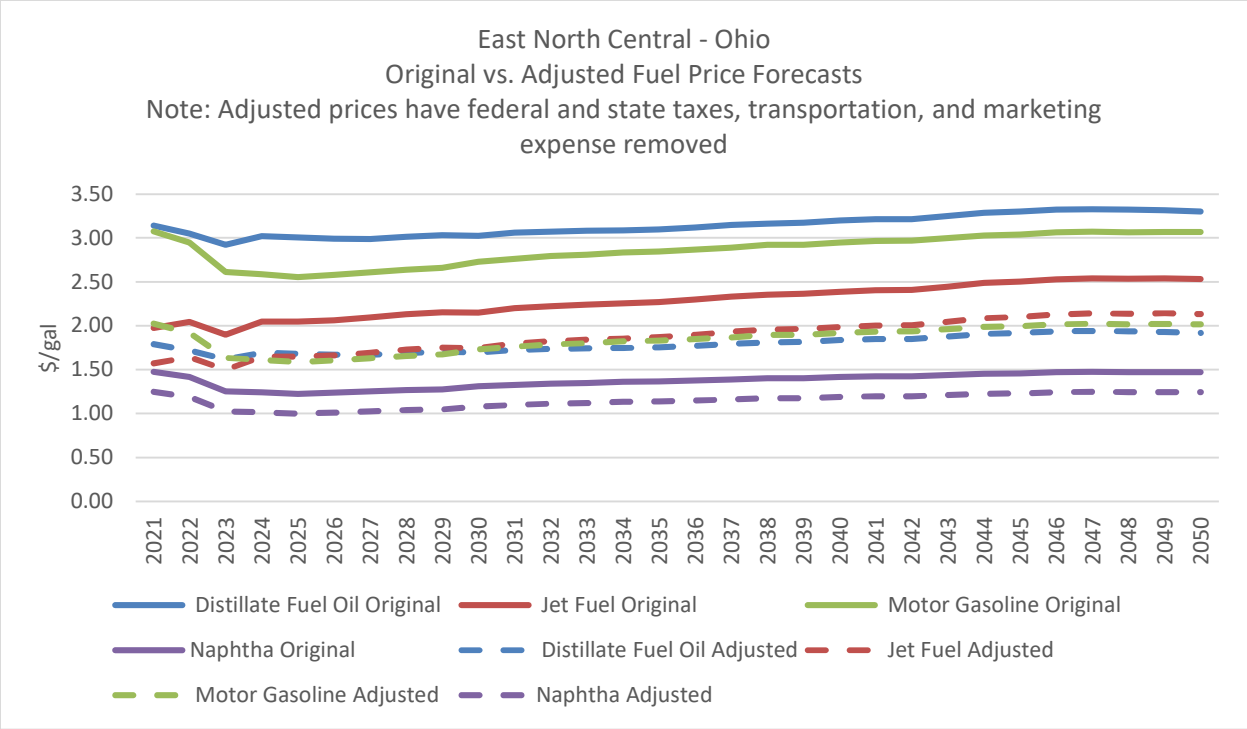

(e)

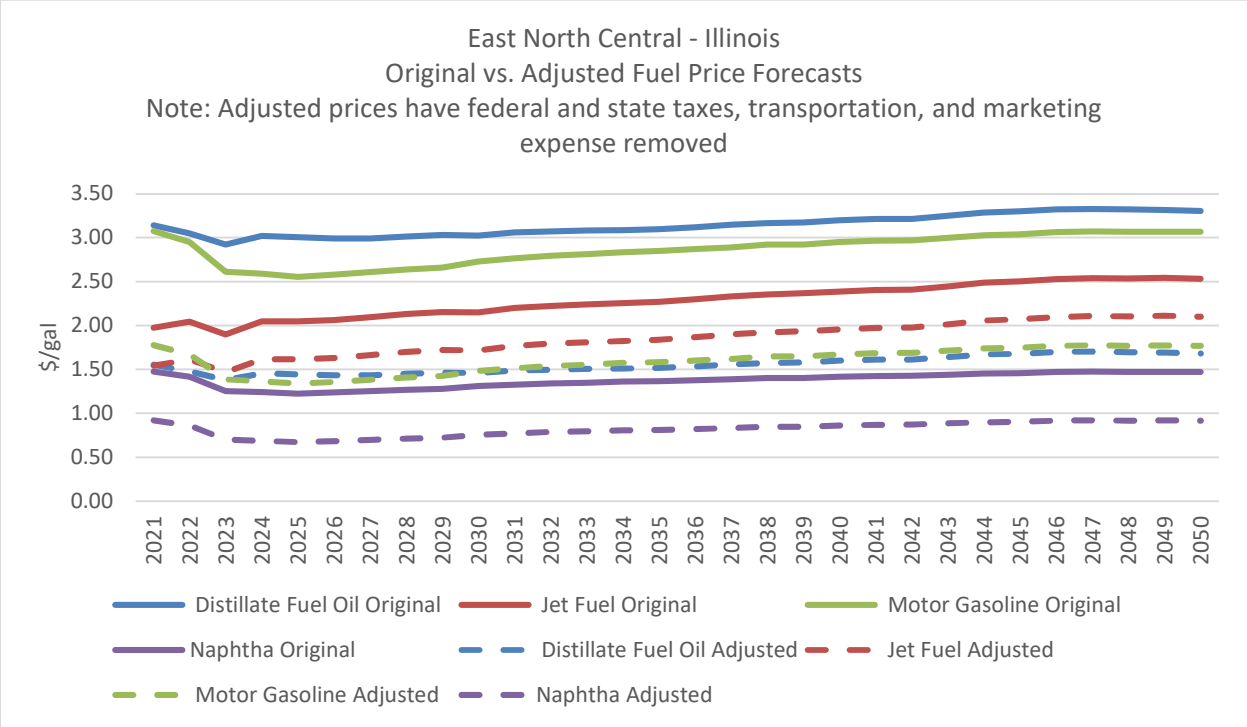

(f)

Figure C-6. Detailed graphical view of how original EIA regional fuel price forecasts compare with adjusted fuel prices once federal and state taxes, transportation, and marketing expenses are removed.

Appendix D

Detailed Data Analysis for Electricity Prices for Each Location

In a previous report, the team did an MSTL data analysis on the electricity prices for Braidwood. At that time, because only two years of data were available, the team only investigated the daily and weekly seasonality of the electricity price data. Since 7–11 years of data for different locations have been collected, this report takes into consideration the yearly seasonality and finds some interesting insights on the evolution of electricity prices for each location studied. The following is a summary of the yearly seasonality conclusions for each location:

- In Cooper, the highest electricity prices take place in February from 2015 to 2021. The peak electricity prices increase consistently from 2015 to 2021. (Figure D-1[b]). This conclusion is not reflected in the monthly average of the electricity prices (Figure D-1[a]), which suggests that the MSTL analysis is helpful in studying the seasonality of the electricity prices.
- In Braidwood, two peaks are identified in the yearly seasonality (Figure D-2[b]). One is in the winter (highest). The other is in the summer (second highest). The peak electricity prices decrease from 2011 to 2021.
- In STP, similar as that in Braidwood, two peaks are identified in the yearly seasonality (Figure D-4[b]). One is in the summer (highest). The other is in the winter (second highest). The peak electricity prices increase from 2011 to 2021.
- Comparing the results between Braidwood and STP, the yearly seasonality indicates a strong correlation with their local weather.
- In Prairie Island, despite the cold weather in winter, the peak electricity price is found in the summer from 2013 to 2021 (Figure D-5[b]). This is because of the reliance on natural gas for housewarming in this area.
- Comparing the 365-day rolling mean and the trend composition obtained by MSTL, the team finds that the trends are consistent with each other for each location. The finding implies the 365-day rolling mean is a good indicator for the general trend of the electricity prices.

In addition, the team shows the daily average, weekly average, monthly average, and 365-day rolling mean for each location in Figure D-1(a) for Cooper, Figure D-2(a) for Braidwood, Figure D-3(a) for Davis-Besse, Figure D-4(a) for STP, and Figure D-5(a) for Prairie Island.

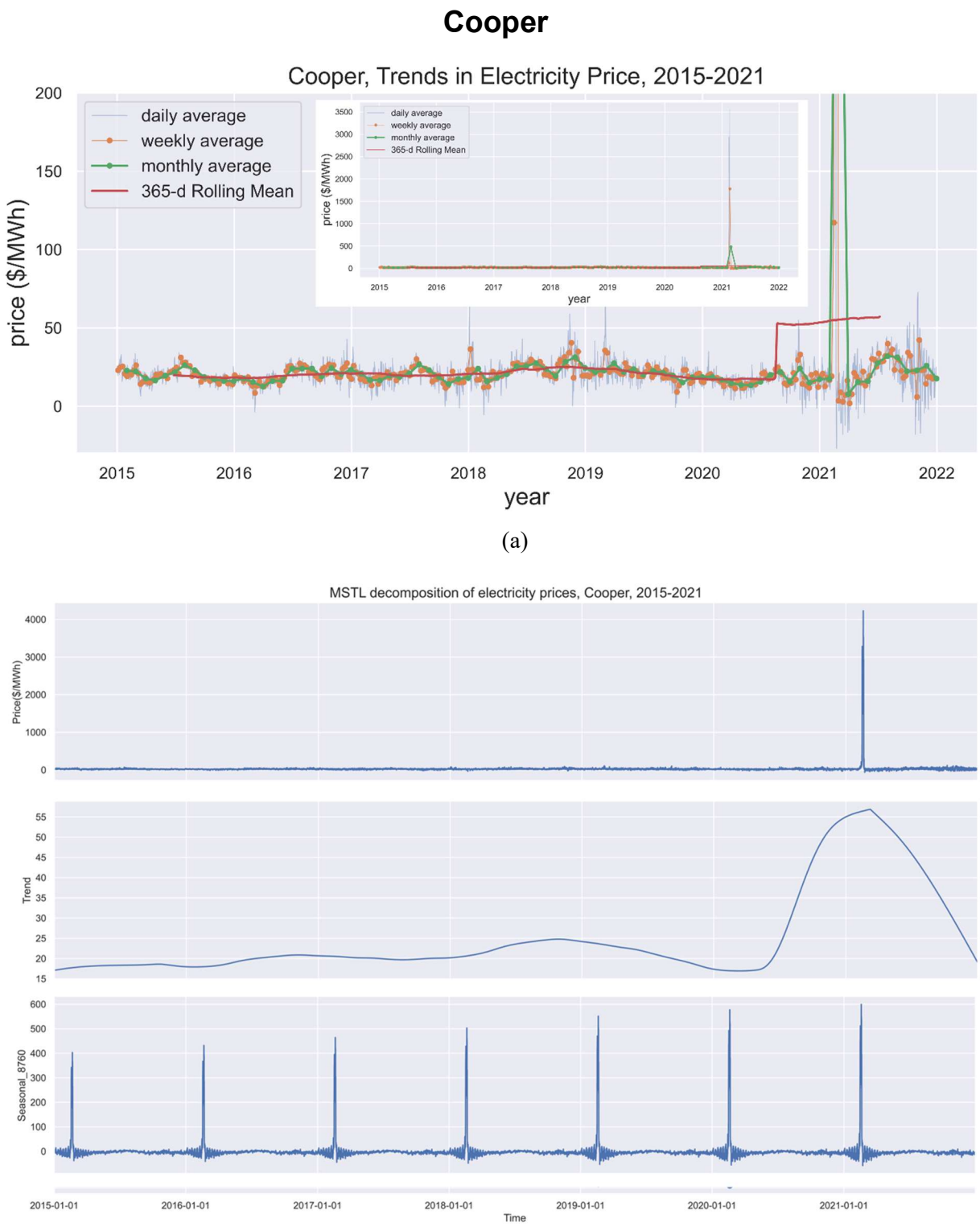

Figure D-1. (a) The daily average, weekly average, monthly average, and 365-days rolling mean in Cooper from 2015 to 2021. (b) The hourly prices and trend and yearly seasonality components obtained from MSTL in Cooper from 2015 to 2021.

Braidwood

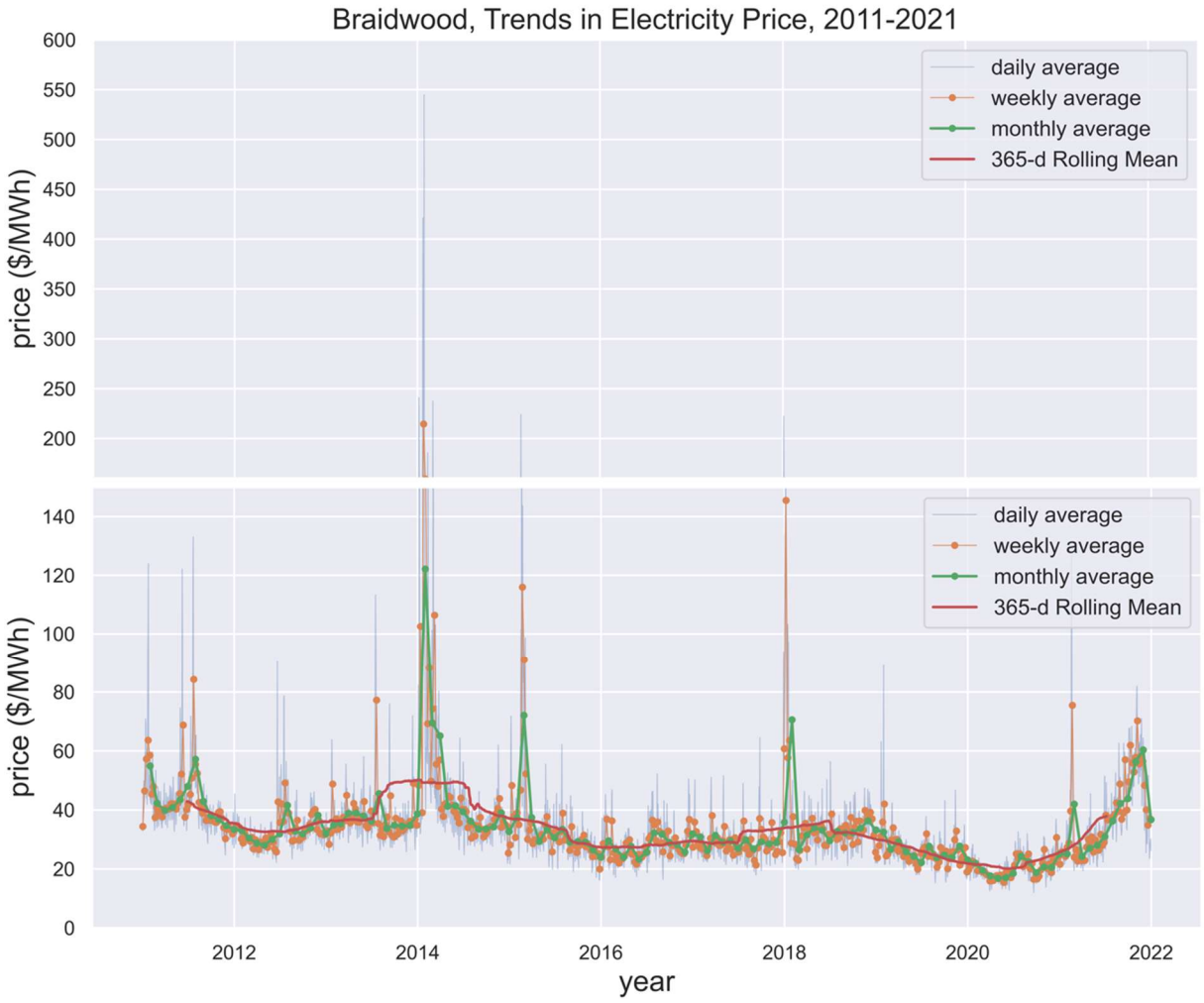
Braidwood, Trends in Electricity Price, 2011-2021
daily average
weekly average
monthly average
365-d Rolling Mean
price ($/MWh)
600
550
500
450
400
350
300
250
200
daily average
weekly average
monthly average
365-d Rolling Mean
price ($/MWh)
140
120
100
80
60
40
20
0
2012
2014
2016
2018
2020
2022
year

(a)

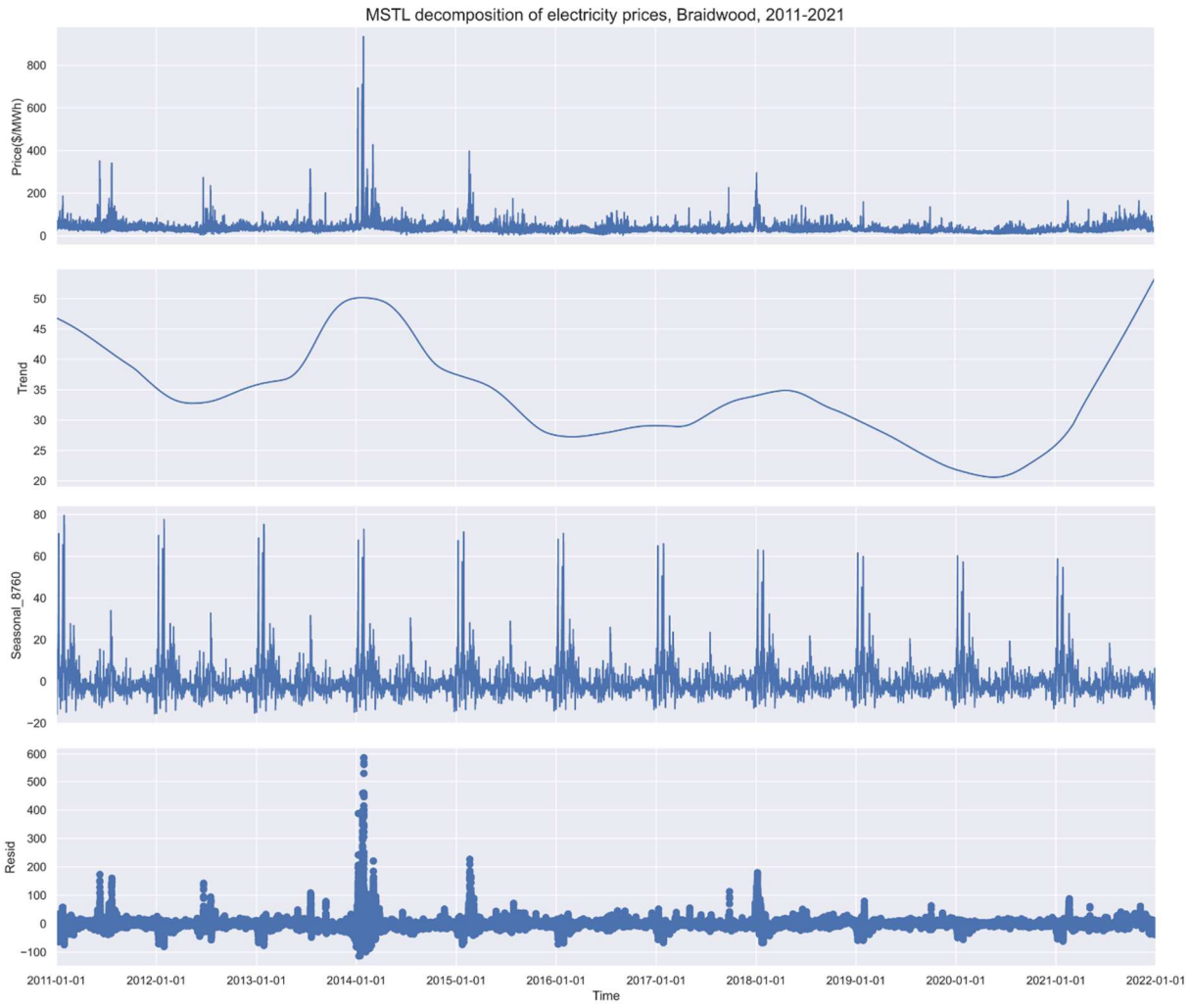

(b)

Figure D-2. (a) The daily average, weekly average, monthly average, and 365-days rolling mean in Braidwood from 2011 to 2021. (b) The hourly prices and trend and yearly seasonality components obtained from MSTL in Braidwood from 2011 to 2021.

Davis-Besse

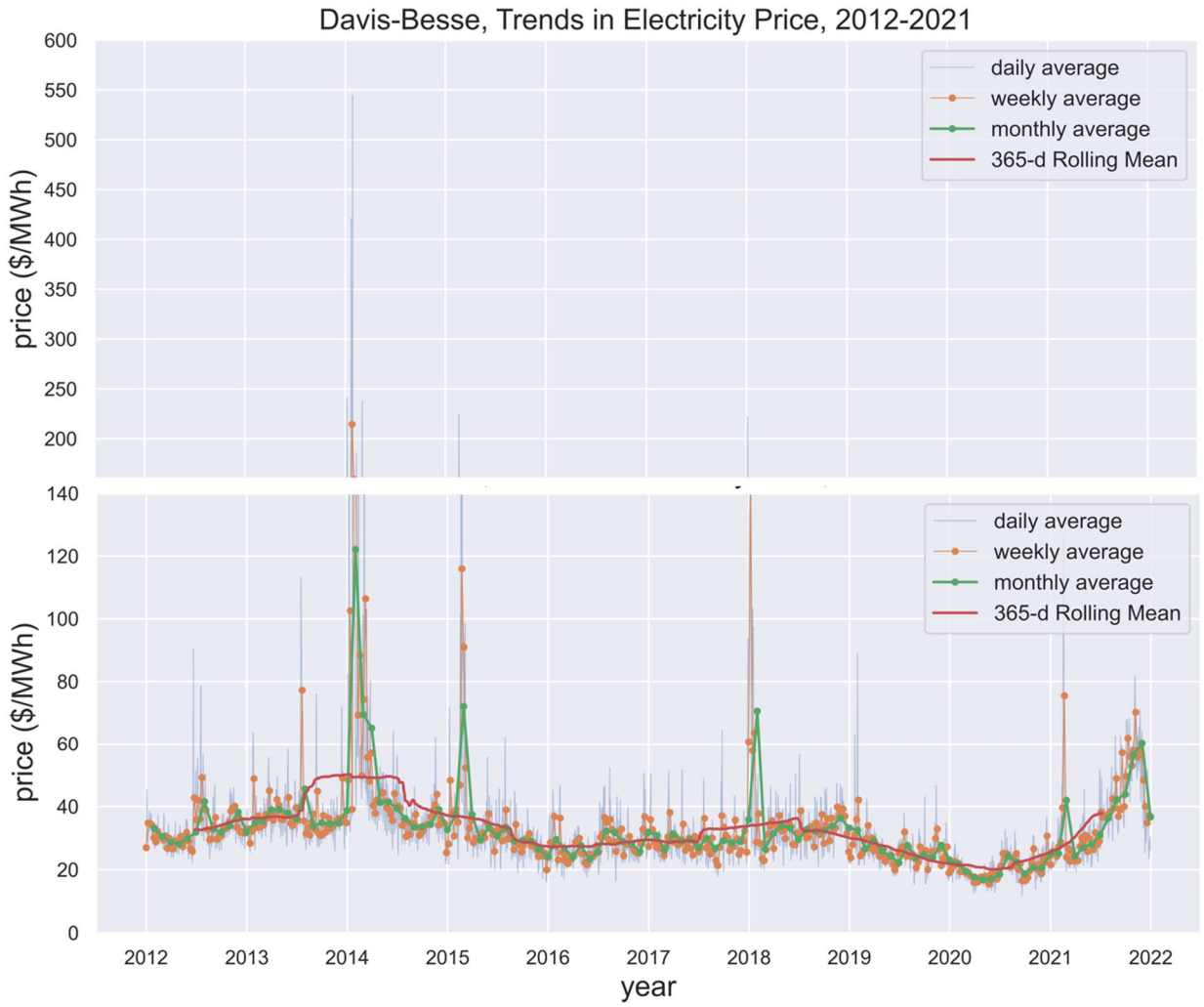

Figure D-3. The daily average, weekly average, monthly average, and 365-days rolling mean in Davis-Besse from 2011 to 2021.

South Texas Project

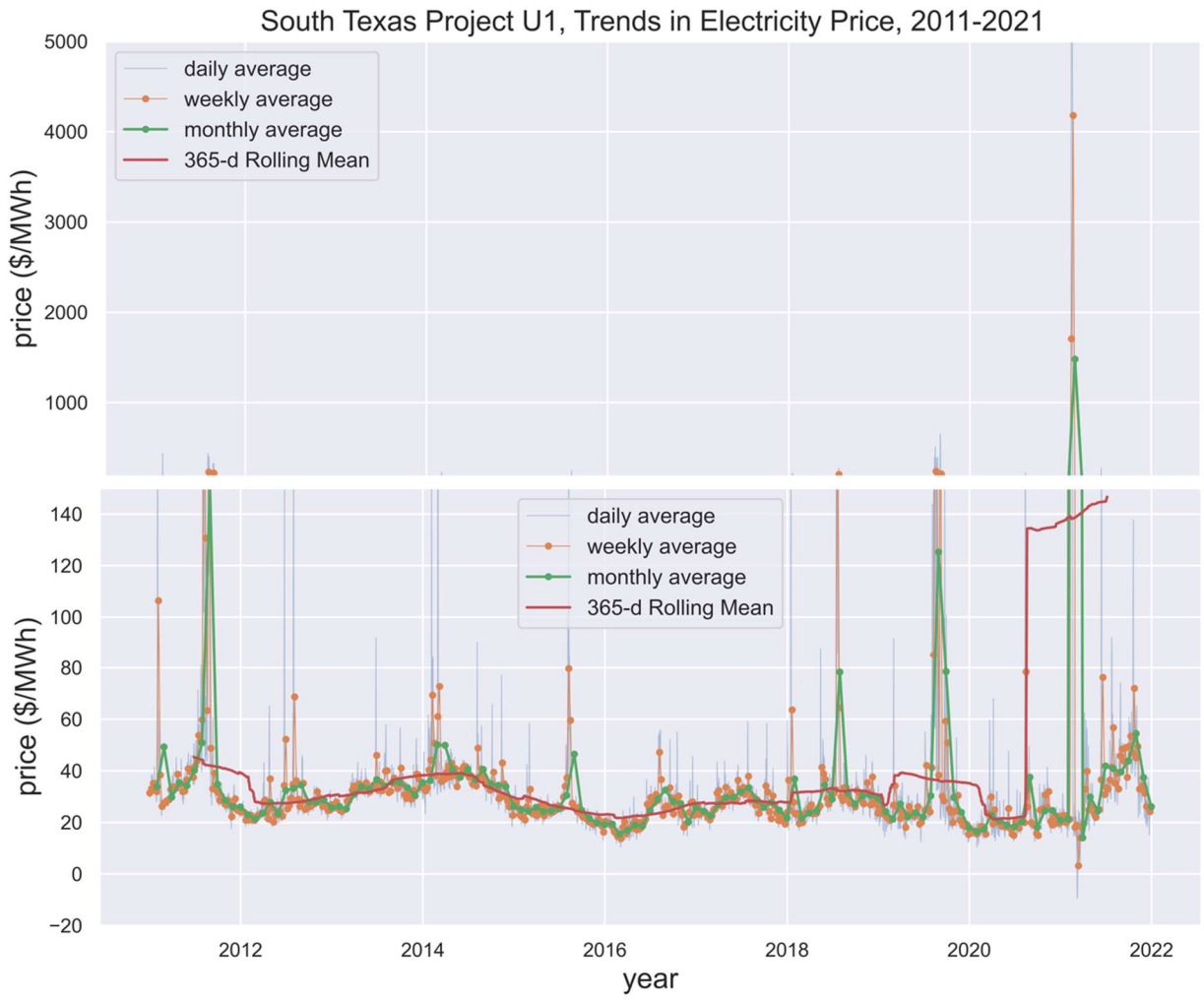

(a)

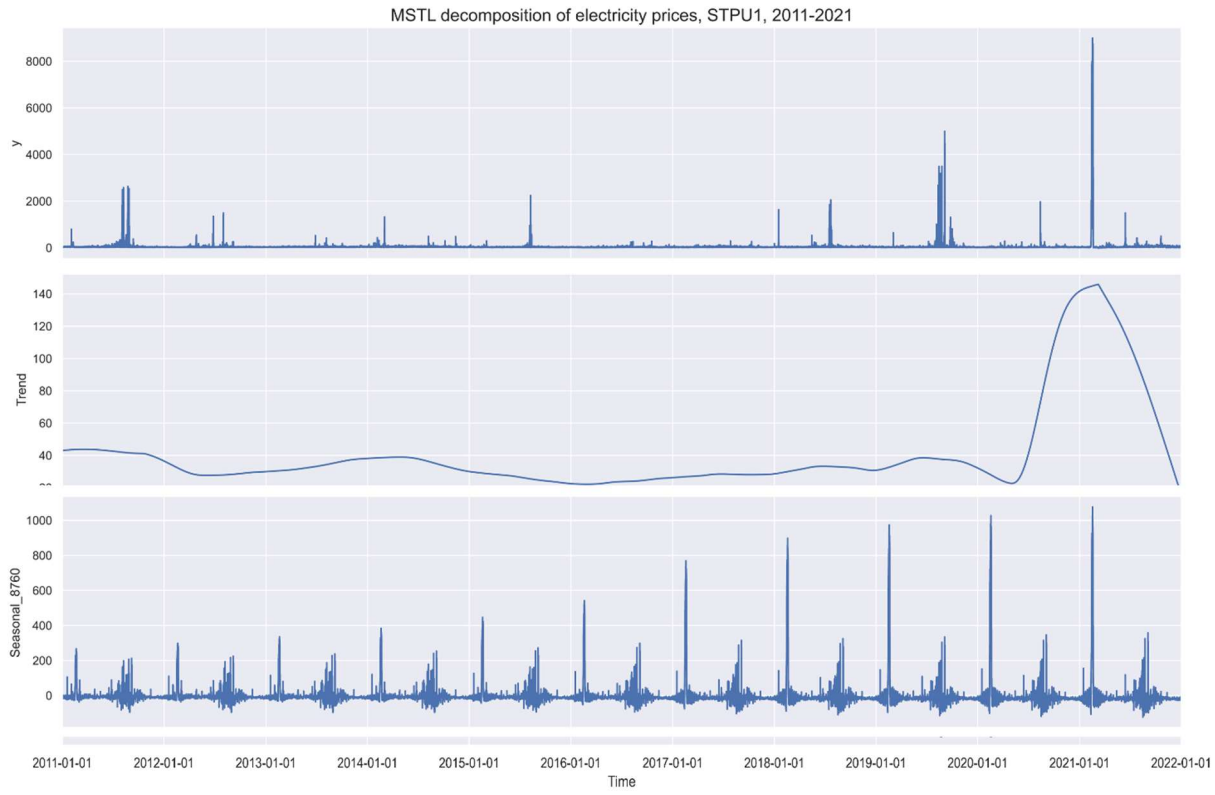

(b)

Figure D-4. (a) The daily average, weekly average, monthly average, and 365-days rolling mean in STP from 2011 to 2021. (b) The hourly prices and trend and yearly seasonality components obtained from MSTL in STP from 2011 to 2021.

Prairie Island

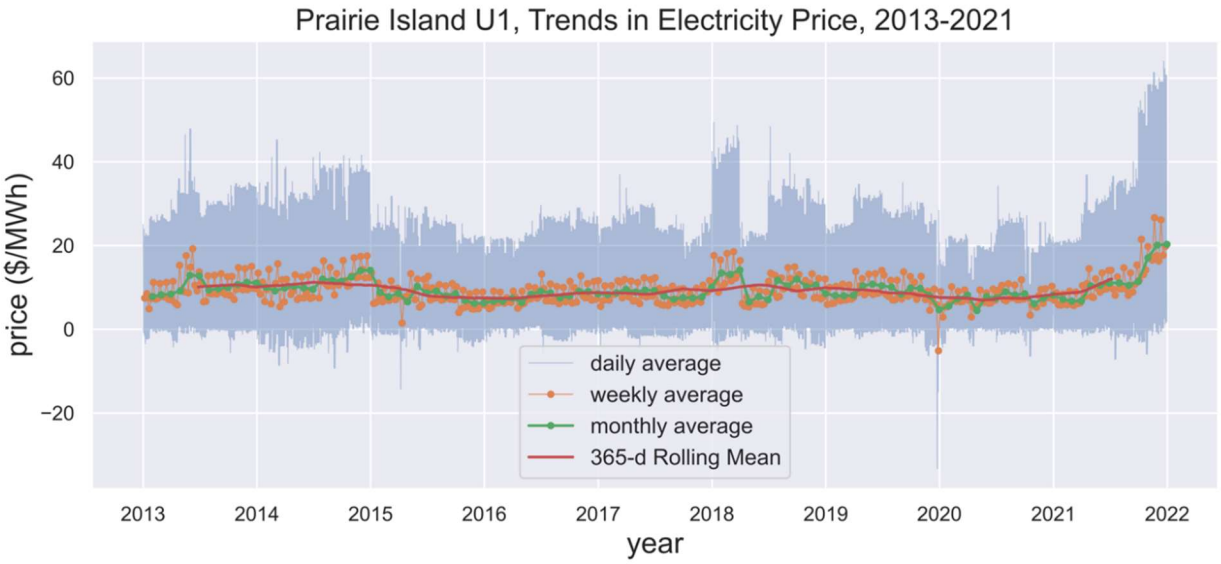

(a)

(b)

Figure D-5. (a) The daily average, weekly average, monthly average, and 365-days rolling mean in Prairie Island from 2013 to 2021. (b) The hourly prices and trend and yearly seasonality components obtained from MSTL in Cooper from 2013 to 2021.

Appendix E

Detailed Supply Curve by Region and Sector

The following figures reveal the individual supply curve for each region and different sources of CO_2.

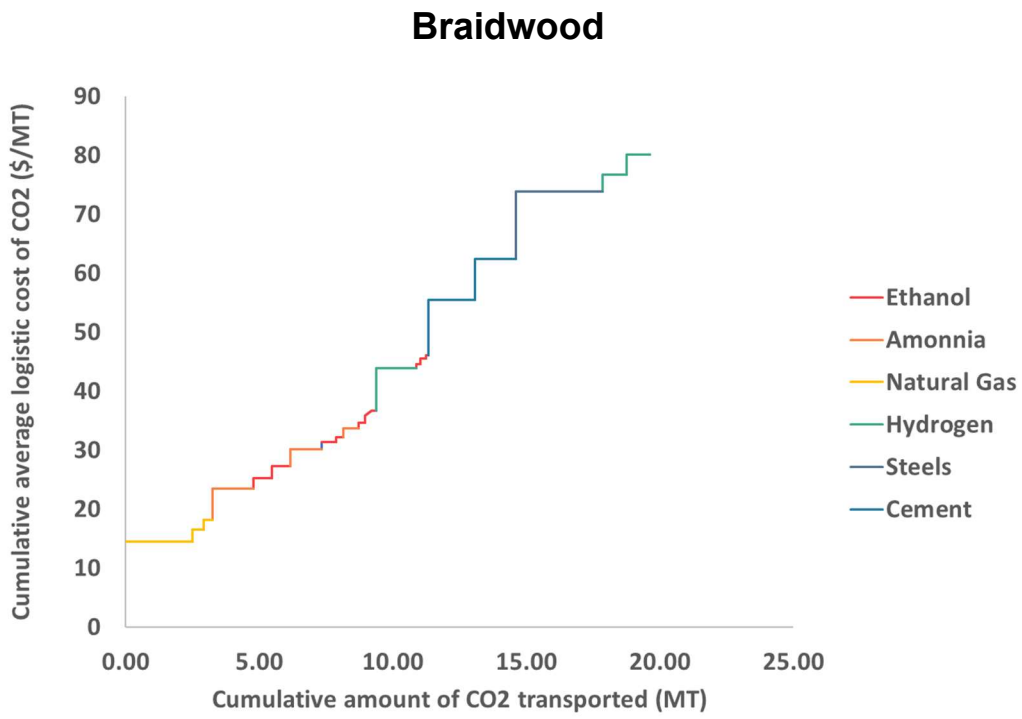

Figure E-1. Supply curve for CO_2 transportation to Braidwood NPP.

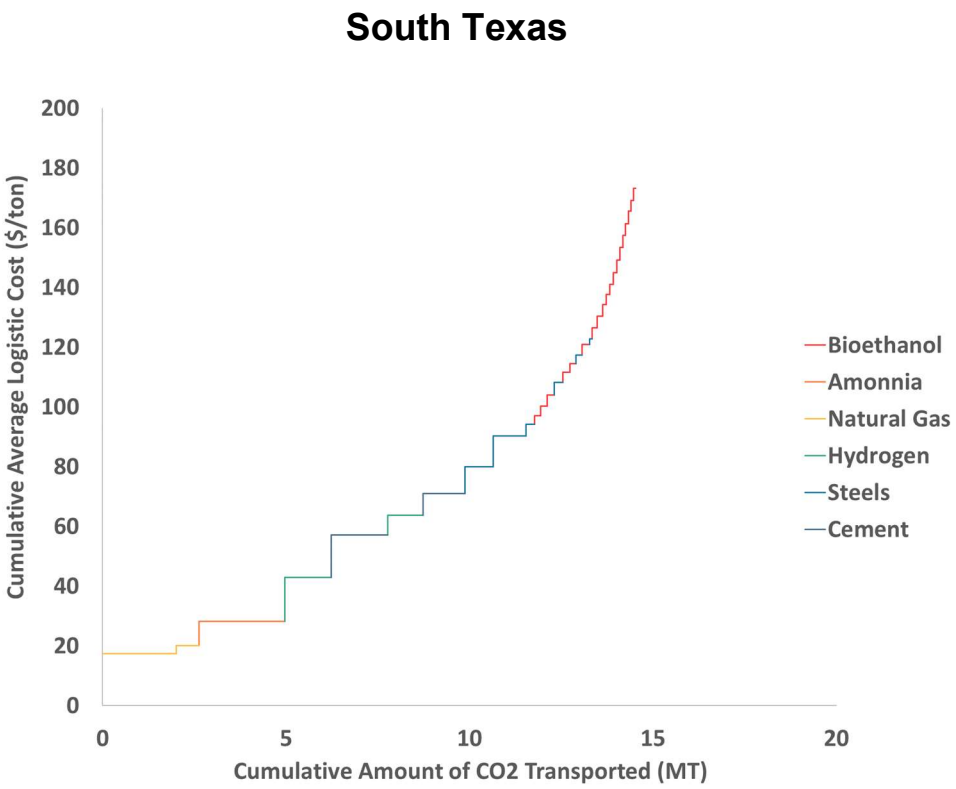

Figure E-2. Supply curve for CO_2 transportation to South Texas NPP.

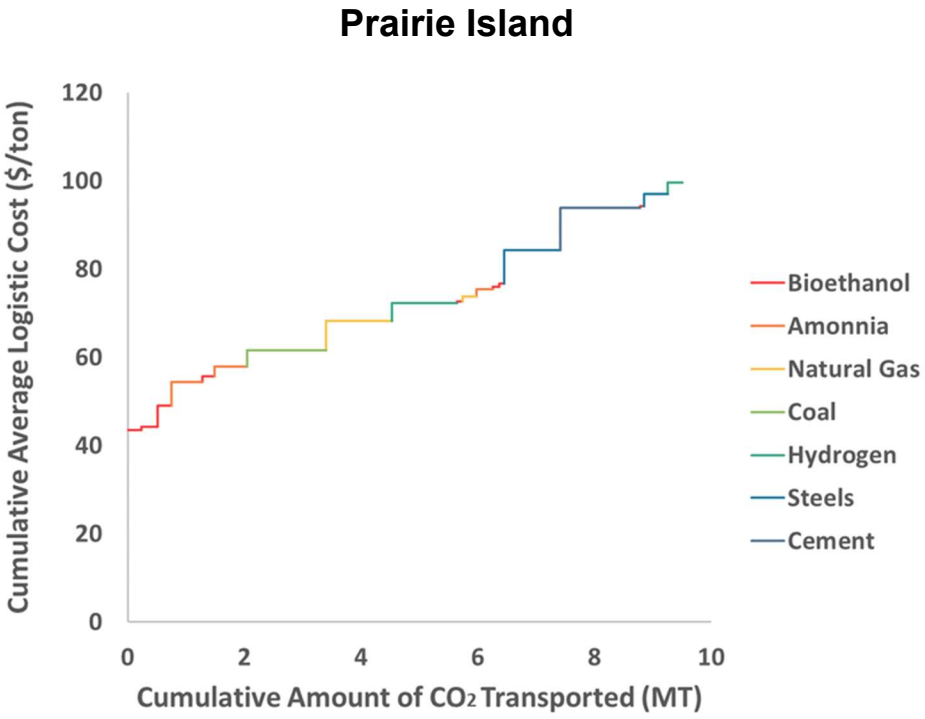

Figure E-3. Supply curve for CO_2 transportation to Prairie Island NPP.

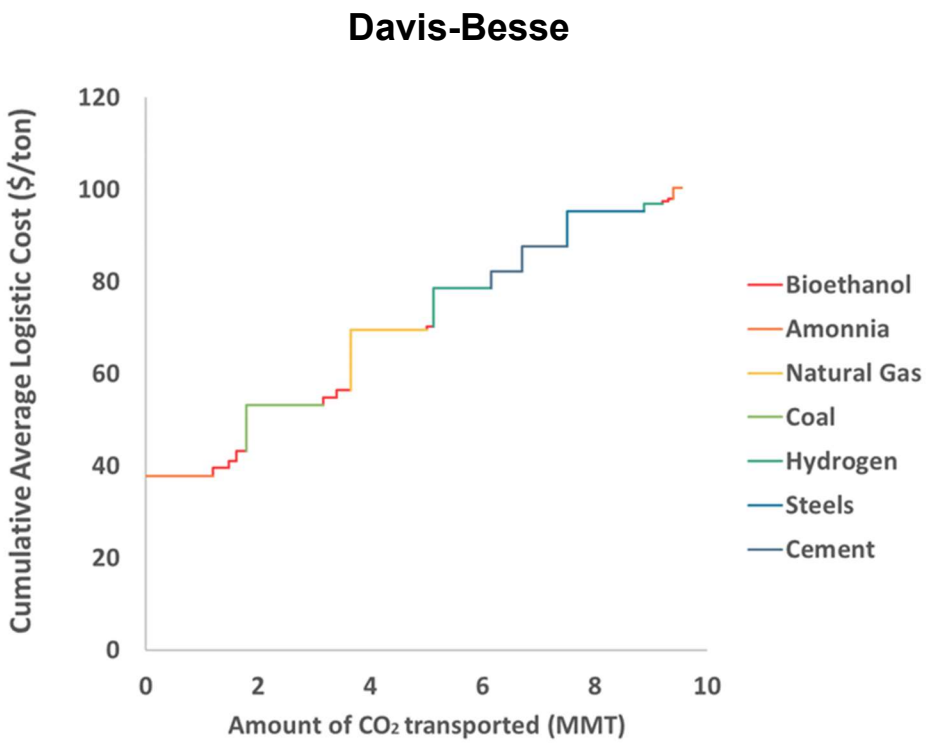

Figure E-4. Supply curve for CO2 transportation to Davis-Besse NPP.

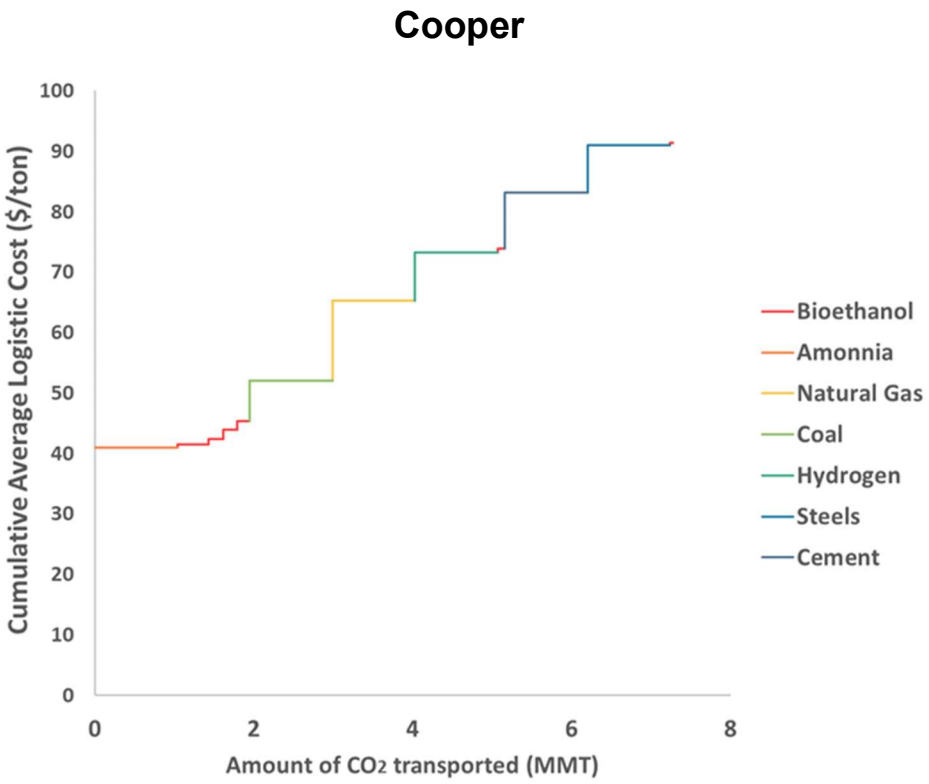

Figure E-5. Supply curve for CO_2 transportation to Cooper NPP.

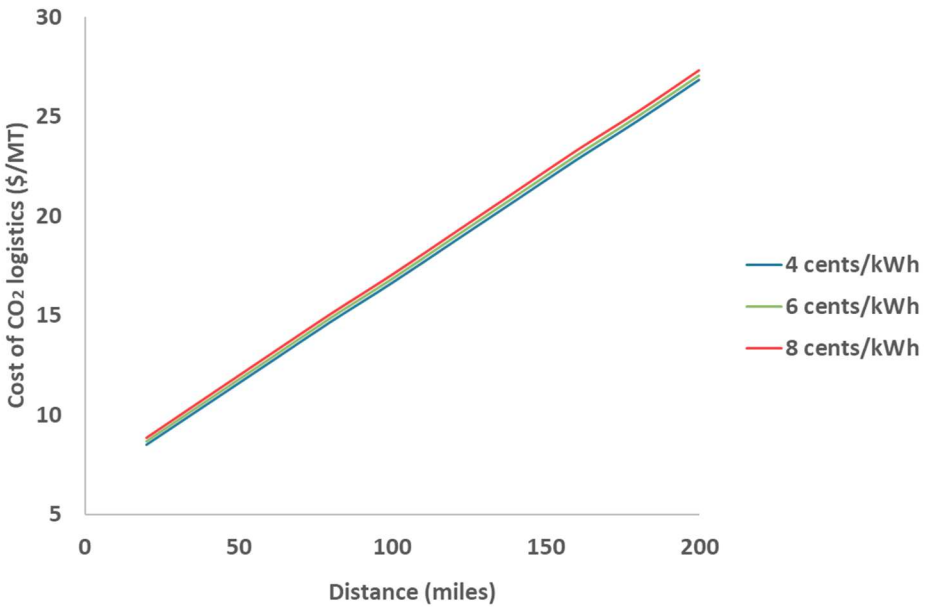

Figure E-6. Variation of cost of CO_2 logistics by distances at different electricity price.

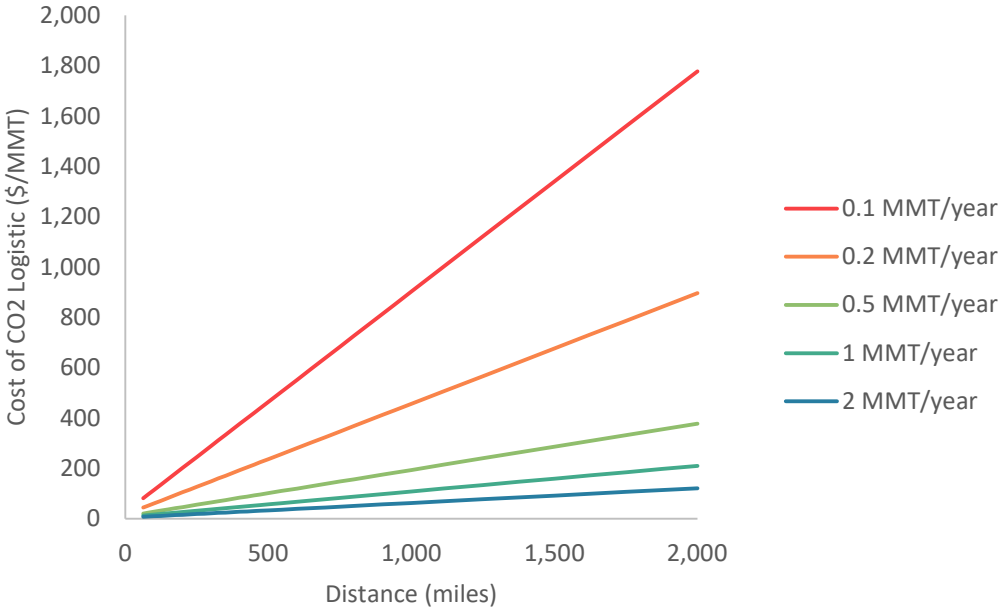

Figure E-7. Variation of cost of CO_2 logistics by distances at different CO_2 rate with grid-supplied electricity price of $0.06/kWh.

Appendix F

Experimental Setup to Evaluate HTSE's Ramping Capabilities

At its most basic, nuclear energy can operate flexibly by ramping power output up or down to match grid demand; however, nuclear energy's services extend beyond just electricity generation. Around the world, research is underway to explore how nuclear systems can use generated thermal energy directly to heat households, drive industrial processes, or produce nonelectric commodities such as purified water. In some instances, hydrogen produced by nuclear systems can be used to store energy for later electricity production or be used as a feedstock to produce a variety of products, from fertilizers and steel to new synthetic fuels ("Flexible Nuclear Energy for Clean Energy Systems," https://www.nrel.gov/docs/fy20osti/77088.pdf).

Due to its ability to produce electricity and high-temperature steam reliably at capacity factors over 90%, nuclear technology is well suited to produce large volumes of low-cost hydrogen at a global market scale. Production from nuclear technology is highly advanced. Decades of research, including whole programs in national laboratories, both with conventional (light water) and advanced reactors, have shown the transformative and near-term potential for low-cost, high volume clean hydrogen production. Recent analyses and planned LWR-generated hydrogen demonstrations in the United States are summarized in the report "Flexible Nuclear Energy for Clean Energy." Along these lines, nuclear energy has attributes well suited to the production of hydrogen. Electricity and heat production at very high-capacity factors enable large-scale production at relatively low-cost with HTSE technology, with zero-CO_2 hydrogen (Boardman et al., "Evaluation of Non-Electric Market Options for a Light Water Reactor in the Midwest," 2019). High power density also enables a relatively tiny environmental footprint. Nuclear production of hydrogen offers additional flexibility in how nuclear energy supports grid demand, assuming that the coupled hydrogen plant can be operated in a flexible manner as well.

Additionally, to the enhanced flexibility and reduced electricity cost to produce hydrogen provided by the fast-ramping rate of HTSE systems, this feature also enables the HTSE-to-grid integration with demand response (DR) bidding opportunities and grid support capabilities, such as voltage and frequency regulation ("Electrolyzers Enhancing Flexibility in Electric Grids," https://www.mdpi.com/1996-1073/10/11/1836). The DR program is a feature in upcoming distribution and transmission grids to connect low-carbon technologies without the need for reinforcement, thus enabling and supporting higher penetration of renewables to the power grid. ("Ramping of Demand Response Event with Deploying Distinct Programs by an Aggregator," https://www.mdpi.com/1996-1073/13/6/1389). As defined by the FERC: "Changes in electric use by demand-side resources from their normal consumption patterns in response to changes in the price of electricity, or to incentive payments designed to induce lower electricity use at times of high wholesale market prices or when system reliability is jeopardized." According to the mentioned definition, DR can be described as the reaction of electricity consumers to the price signals considered as incentives to quickly reduce or modify the electricity use pattern to support grid conditions of grid events, such as transmission lines or step-down transformers overloads.

To validate HTSE's ramping response to provide added flexibility to nuclear integration, revenue optimization with hydrogen production, grid integration support, and DR day-ahead bidding opportunities, INL executed tests with a 100kW HTSE system to verify ramp down time from full power (100% power, 2.7 kg_H_2/h) to Hot Standby (10% power, no hydrogen production) and ramp up time from Hot Standby to Full Power/Full Hydrogen Production.

For the tests, INL provided the test facility, including DC voltage power supply, steam supply, hydrogen gas dilution, and venting. Key features of the system include the following:

- Capacity: The BoP equipment is rated to support hydrogen production at rates up to 3.0 kg an hour, which corresponds to approximately 100 kW of electric DC power consumption.
- Steam supply: The maximum rated steam production rate is 307 lb/hr at 100°C using feedwater at 10°C. The boiler vessel has a pressure rating of 100 psig.
- DC power: Power is supplied by five power converters connected in series. The power converters each have multiple bidirectional ports, including two DC ports and one AC port. The maximum current outputs of each unit are 37 A and 60 A for the AC and DC ports, respectively. The output DC voltage range is 100–1,000 VDC with a 1 A fused ground fault detector/interrupter (GFDI) protection. The maximum rated DC power for the combined system is 150 kW.
- Piping: The piping systems are compliant with ASME B31.3, "Process Piping," ASME B31.12, "Hydrogen Piping," and ASME B31.9, "Building Service Piping," as appropriate. Hydrogen lines and equipment are compliant with NFPA 2 and NFPA 497.

The INL HTSE Support Facility occupies the space inside, adjacent to, and on top of a shipping container located in the north yard outside of INL. The major subsystems include AC and DC electric power delivery, steam supply, nitrogen supply, hydrogen supply, and cooling and venting of exhaust gases, as shown in Figure F-1 through Figure F-3. All major components comprising this system have been obtained from commercial vendors.

Figure F-1. INL's High Temperature Electrolysis (HTE) Support Facility with doors open showing the CE+T power converters and the Chromalox steam generator.

Figure F-2. Photographs of the water seal and condenser, which will be placed outside the shipping container (left) and the distilled water recycle tank (with appropriate insulation and line trace heating) inside the container for freeze protection.

Figure F-3. Photograph of the dilution fan assembly prior to and after installation on the cargo container roof.

Hydrogen is provided by a compressed gas cylinder and regulated to 15 psi. A fail-closed valve shuts off hydrogen supply if an alarm is triggered or electric power is lost. Steam for the tests is provided by a Chromalox CSSB-100 kW electric steam boiler. The steam generator feeds steam into a steam manifold that can provide steam for up to three electrolysis systems simultaneously.

The HTE system does not fully use the supplied steam, so the product gas is a mixture of hydrogen and steam. The product hydrogen and steam are sent to a condenser that condenses most of the steam and allows the wet hydrogen, which is 5–10% water content, to pass through a water seal. The water seal is maintained at the same height as the condenser and is connected to the condenser so that condensed water maintains the fill level of water in the water seal. Excess condensed water is captured in a 70-gallon recycle water tank inside the shipping container. Both the water seal and 70-gallon recycle water tank are shown in Figure F. Cold, wet hydrogen from the condenser bubbles up through the water seal and enters a dilution fan installed above the container. Thermocouples at the duct outlet monitors the temperature of the hydrogen exhaust to identify potential hydrogen combustion. During unattended operation, a FLIR FL500 UV/IR flame detector is used to monitor for hydrogen fires near the exhaust vent. The FL500 has a field of view up to 135 degrees and a range up to 60 ft and response time less than 12 seconds.

The 100 kW HTSE system consists of three modules, including a hot module, a BoP module, and a telemetry cabinet. The modules are installed behind the HTSE Support Facility. The hot module contains the SOEC stacks and heat exchangers, the BoP module contains the necessary electronics, including fans, pumps, and variable DC power supplies, and contains the telemetry cabinet for communications and controls.

Testing the 100 kW HTE system started in May 2022, and the ramp down and ramp up tests were executed in July 2022. The “deload” test was performed after approximately 634 hours of operation to verify the system’s ability to respond to dynamic loading requests as a dispatchable power load. During this test, the system was ramped down from 100–10% power in less than 10 minutes.

Appendix G

HERON Exploration Runs Results

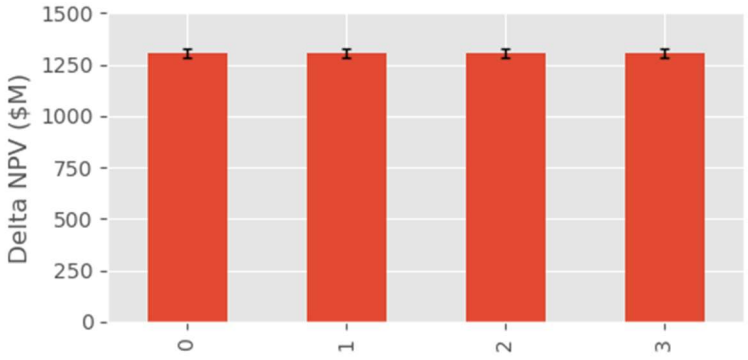

	0	1	2	3
NPP (MW)	1193.0	1193.0	1193.0	1193.0
HTSE (MW)	-1178.0	-1178.0	-1178.0	-1178.0
FT (ton-H2/h)	-29.6	-29.6	-29.6	-29.6
H2 Sto. (ton-H2)	200.0	100.0	10.0	0.0
Delta NPV ($M)	1306.9	1305.9	1305.9	1305.9
2STD Delta NPV ($M)	20.9	20.9	20.9	20.9

Figure G-1. HERON exploration run results, Braidwood location.

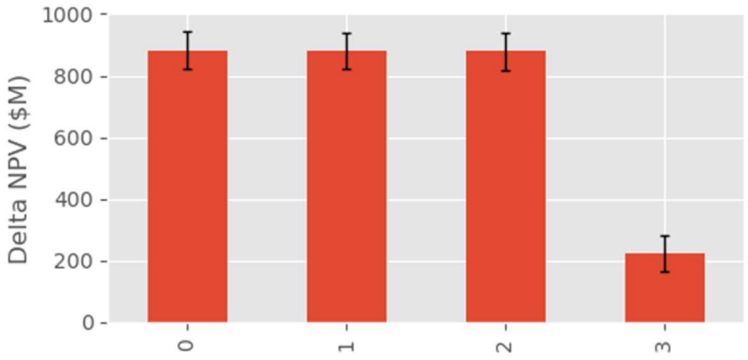

	0	1	2	3
NPP (MW)	769.0	769.0	769.0	769.0
HTSE (MW)	-754.0	-754.0	-754.0	-400.0
FT (ton-H2/h)	-18.9	-18.9	-18.9	-9.0
H2 Sto. (ton-H2)	0.0	40.0	75.8	75.8
Delta NPV ($M)	882.9	880.6	878.9	223.9
2STD Delta NPV ($M)	59.3	59.3	59.3	59.6

Figure G-2. HERON exploration run results, Cooper location.

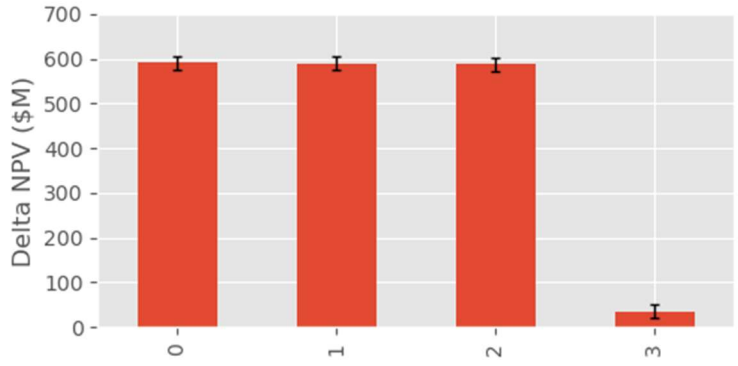

	0	1	2	3
NPP (MW)	894.0	894.0	894.0	894.0
HTSE (MW)	-879.0	-879.0	-879.0	-450.0
FT (ton-H2/h)	-22.1	-22.1	-22.1	-10.0
H2 Sto. (ton-H2)	90.0	45.0	0.0	90.0
Delta NPV ($M)	591.6	590.0	588.1	35.1
2STD Delta NPV ($M)	15.0	15.0	15.0	15.0

Figure G-3. HERON exploration run results, Davis-Besse location.

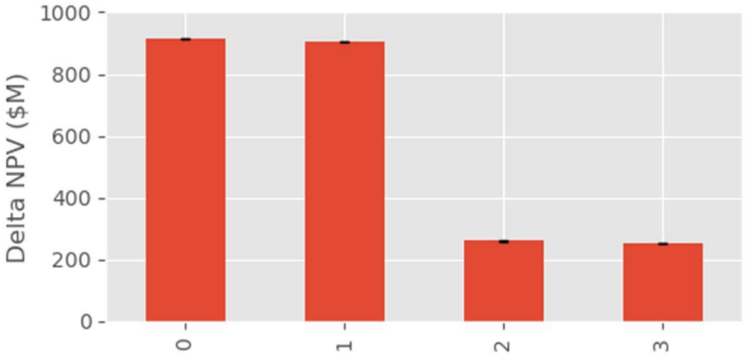

	0	1	2	3
NPP (MW)	522.0	522.0	522.0	522.0
HTSE (MW)	-507.0	-507.0	-250.0	-250.0
FT (ton-H2/h)	-12.7	-12.7	-6.0	-6.0
H2 Sto. (ton-H2)	35.0	70.0	0.0	35.0
Delta NPV ($M)	914.7	905.0	261.0	253.3
2STD Delta NPV ($M)	1.1	1.1	1.3	1.1

Figure G-4. HERON exploration run results, Prairie Island location.

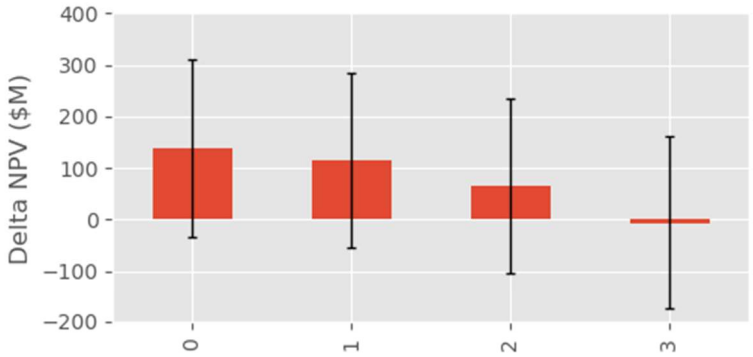

	0	1	2	3
NPP (MW)	1280.0	1280.0	1280.0	1280.0
HTSE (MW)	-1265.0	-1265.0	-1265.0	-1265.0
FT (ton-H2/h)	-31.8	-31.8	-31.8	-31.8
H2 Sto. (ton-H2)	2000.0	1000.0	500.0	0.0
Delta NPV ($M)	138.2	115.7	65.6	-6.7
2STD Delta NPV ($M)	171.8	170.4	168.1	167.8

Figure G-5. HERON exploration run results, STP location.